Dissecting the role of the hippocampal-prefrontal circuit in anxiety

Nancy Padilla Coreano

Submitted in partial fulfillment of the
requirements for the degree of
Doctor of Philosophy
under the Executive Committee
of the Graduate School of Arts and Sciences

COLUMBIA UNIVERSITY

2016

Abstract

Dissecting the role of the hippocampal-prefrontal circuit in anxiety

Nancy Padilla Coreano

The ventral hippocampus (vHPC), medial prefrontal cortex (mPFC), and basolateral amygdala (BLA) are each required for the expression of anxiety-like behavior. Yet the role of each individual element of the circuit is unclear. The projection from the vHPC to the mPFC has been implicated in anxiety-related neural synchrony and spatial representations of aversion. The role of this projection was examined using multi-site neural recordings combined with optogenetic terminal inhibition.

Inhibition of vHPC input to the mPFC disrupted anxiety and mPFC representations of aversion, and reduced theta synchrony in a pathway-, frequency- and task-specific manner. Moreover, bilateral, but not unilateral, inhibition altered physiological correlates of anxiety in the BLA, mimicking a safety-like state. These results reveal a specific role for the vHPC-mPFC projection in anxiety-related behavior and the spatial representation of aversive information within the mPFC. Moreover, these data suggested that theta-frequency input from the vHPC plays a causal role in anxiety-like behavior.

Next, it was investigated whether optogenetic stimulation of the vHPC-mPFC at a theta frequency was sufficient to increase anxiety. Stimulating the vHPC input to the mPFC with a sinusoidal light pattern at 8 Hz significantly increased anxiety behavior. The anxiogenic effect of vHPC terminal stimulation was frequency- (8 Hz but not 20 Hz) and pattern- (sinusoids but not pulses) specific. To understand how pulses and sinusoidal

light modulate mPFC neurons differentially, mPFC pyramidal neurons were recorded both *in vitro* and *in vivo* while stimulating vHPC terminals with the same sinusoidal or pulsatile patterns. *In vitro*, sinusoidal stimulation increased the rate of spontaneous EPSCs, while pulses evoked strong, stimulus-locked EPSCs. Additionally, sinusoidal light resulted in an increase of theta-frequency subthreshold fluctuations in membrane potential of mPFC pyramidal cells. *In vivo*, sinusoidal stimulation of vHPC terminals increased the phase-locking of mPFC single unit spiking to the optical stimulation pattern without changing overall firing rates. Together, these results suggest that sinusoidal stimulation at 8 Hz enhances theta-frequency activity in mPFC neurons as well as anxiety-related behavior. Moreover, they suggest that theta-frequency components of neural activity play a privileged role in vHPC-mPFC communication and hippocampal-dependent forms of anxiety.

TABLE OF CONTENTS

List of Figures

Chapter 1 Introduction

Chapter 2 The role of the hippocampal input to mPFC in anxiety behaviors

Chapter 3 The role of the hippocampal input to mPFC in the representation of aversion in mPFC

Chapter 4 The role of vHPC input to mPFC in theta synchrony in the vHPC-mPFC-amygdala circuit

Chapter 5 Theta frequency oscillatory stimulation of vHPC terminals in mPFC increases anxiety-like behavior

Chapter 6 Discussion

Acknowledgments

The work presented here would have not been possible without the collaboration and support of many people, it takes a village to do science. I would like to thank, first and foremost, my thesis advisor Josh Gordon. Josh has advised me in many ways that have made me a better scientist and a better person. I would like to thank my collaborators: Sarah Canetta, Alvaro Garcia, Bill Hardin, Georgia Pierce, Rick Warren, Scott Bolkan and Dakota Blackman. This thesis wouldn't be the same without their help and collaboration. I would also like to thank the many mentors I've accumulated during the years. You all are great examples to follow. Greg, thanks for believing in my potential. I would also like to thank present and past members of the Gordon lab. All of them have been very helpful and have enhanced my experience in grad school. I would like to especially thank Alex, Scott, Bill, Pia, Avishek and Dakota. Alex's advice, support, company and whistling have been wonderful. Scott's friendship and silliness have been very special to me; he also contributed to much of the work presented here. I would like to thank Bill for his support and disposition with my many experimental endeavors. Pia showed me around the lab and taught me many basic things necessary to succeed in the lab. Avishek's scientific support has been incredible; he was my #1 cheerleader. Dakota, my undergrad, was a great first mentee and a backbone for all my experiments. I would also like to thank my friends for keeping me happy and healthy through grad school especially Jessica, Ale, Sandra, Anita, Sarah, Josh, Conor, Grace, Joe, Pia. Thanks also to Stephen for all the emotional support through the years. Finally, thank you to my dear family and friends back home for making me feel loved despite our distance.

Dedication

A mi querido abuelo Humberto

Chapter 1: Introduction

1.1 What is Anxiety

Anxiety is necessary for survival

Anxiety is a state of increased apprehension that allows avoidance of potential danger. It has been defined as a psychological, physiological and behavioral state induced by a threat, either actual or potential (Steimer 2002). Anxiety results in the expression of defensive behaviors that are necessary for survival. In the wild, a zebra will avoid roaming alone in fear of being the prey of a pack of lions that lives nearby. In this case the zebra acts defensively toward the potential threat (pack of lions), demonstrating how anxiety-related behaviors can increase survival.

Fear versus anxiety

As defined in the DSM-5 manual, fear is the emotional response to real or perceived imminent threat, whereas anxiety is anticipation of future threat (DSM-5, pg 208). These definitions have been expanded by neuroscientists. Fear is defined as an adaptive state of apprehension to an imminent threat, where the state dissipates rapidly once the threat is removed. Threats that evoke fear tend to be a specific stimulus, and those threats can emerge from learning or be innate (McFarland 1986; Steimer 2002). On the other hand, anxiety is a longer state of apprehension elicited by a less predictable threat. Threats that evoke anxiety are physically or psychologically more distant, therefore they are more uncertain (Davis et al. 2010; Steimer 2002). However, fear and anxiety have many features in common. Fear and anxiety both result in the expression of defensive behaviors (freezing, avoidance, attack, etc.) in response to threats. Fear and anxiety trigger activation of the sympathetic nervous system and the hypothalamo-

pituitary-adrenal axis (HPA), which results in secretion of glucocorticoids and preparation to fight or flight (Canon 1915; Steimer 2002). Furthermore, fear and anxiety can even be evoked by the same threat depending on the distance and certitude of the threat. Additionally, in Plutchik's theory of emotions, fear and anxiety are in the same overall category with fear being stronger than anxiety. Anxiety is proposed to be a state of sustained fear by Davis and colleagues. Under this framework some tasks of learned fears evoke anxiety, like contextual fear, since the stimulus is sustained and not very specific (Davis et al. 2010). This definition of anxiety can be conflicting with the clinical definition.

Fear and anxiety are sometimes indistinguishable without confirmation from the subject experiencing the threat. For example, if a predator odor is presented to a rodent, would that be interpreted as an imminent threat or is the odor an indication of a possible threat in the near future? Without asking the rodent, we cannot distinguish these two possibilities. For this reason, most researchers treat fear and anxiety as indistinguishable emotions, unless they are using a task that has been extensively validated for one of these emotions.

Learned vs innate behaviors

Defensive behaviors can be learned or innate. Specifically, fears can be innate or learned (Gross and Canteras 2012). Anxiety assays take advantage of innate fears (or anxieties), like bright spaces, open spaces, or predator smells. Learned fear is most commonly studied using pavlovian fear conditioning in which a neutral unconditioned

stimulus (e.g. tone) is repeated paired with an aversive stimulus (e.g. shock). The neutral stimulus subsequently becomes conditioned and evokes a conditioned response (CR; changes in locomotion, respiration, etc.). This fear memory to the conditioned stimulus (CS) is long lasting has been extensively used to understand the plasticity underlying an aversive memory (Maren and Quirk 2004). One challenge in using learned fears paradigms to elucidate the fear circuitry is dissociating which effect is due to the learning component vs the emotion. It is also possible to study a learned anxiety. Some anxiety assays commonly used required learning (table 1; conditioned responses). One example is active avoidance task in which animals learned that they can avoid a shock that is signaled by a tone (Bravo-Rivera et al. 2014).

1.2 Anxiety in humans

"A thousand miseries at once

Mine heavy heart and soul ensconce,

All my griefs to this are jolly,

None so sour as melancholy."

Dysfunctional anxiety

This poem was written by Robert Burton in *The Anatomy of Melancholy* in 1621. As he described his condition in the preface: "for I had *gravidum cor, foetum caput* [a heavy heart, hatchling in my head], a kind of imposthume in my head, which I was very desirous to be unladen of". What was known as melancholy in 17th century now includes symptoms of both depression and anxiety disorders. In *The Expression of the Emotions in Man and Animals*, Charles Darwin describes a woman who suffers from a strong fear

of death, for herself, her husband and children, and is diagnosed with acute melancholia. This woman would probably be diagnosed with generalized anxiety disorder nowadays. As in the case of the woman described by Darwin, excessive anxiety can be maladaptive. Psychiatric disorders that include pathological anxiety states have been defined and characterized towards the end of the twentieth century. The DSM-5 defines anxiety disorders as those that include features of excessive fear and anxiety and related behavioral disturbances. One example is generalized anxiety, in which people are over-anxious about many different issues. Another example is social anxiety, in which people experience anxiety about interacting with other humans. All anxiety disorders are characterized by increased avoidance behavior, and fear or anxiety to specific objects or situations. It has been estimated that the lifetime prevalence of anxiety disorders in the USA is 28% (Kessler RC et al. 2005), making anxiety disorders a major economic and health problem (Greenberg et al. 1999).

Common treatments for anxiety disorders

The most commonly used treatments for anxiety disorders are pharmacological and behavioral therapy. The best studied behavioral therapy is Cognitive Behavioral Therapy (CBT), which is the most commonly used therapy for patients with anxiety disorders. Pharmacological treatment is commonly combined with behavioral therapy. Common drug groups prescribed include: selective serotonin reuptake inhibitor (SSRIs) or a serotonin-norepinephrine reuptake inhibitor (SNRIs) and benzodiazepines. A major problem in the field of psychiatry is that as many as 40% of patients do not respond to SSRIs or other drug treatment (Kupfer, Frank, and Phillips 2012). Moreover, CBT only

works on 50% of adolescents with anxiety disorders (Walkup et al. 2008). There is some evidence that CBT only significantly works for OCD and PTSD, which correspond to a small subset of anxiety disorders (Hofmann and Smits 2008). The lack of effective treatments for anxiety disorders increases the need to research the neural mechanisms of anxiety behaviors.

Circuits mediating anxiety in humans

Advances in neuroimaging studies have allowed validation of neurobiological network hypotheses for anxiety disorders. In healthy subjects and in patients with anxiety disorders, functional imaging (fMRI) procedures and other imaging techniques have provided evidence of the existence of a complex extended anxiety network. I will discuss some of those findings here.

Insights from imaging patients with anxiety disorders

Many studies have imaged patients with PTSD, phobias, panic disorder and GAD (Shin and Liberzon 2009). Many studies have shown increased fMRI activity in the amygdala of PTSD patients in response to trauma-related imagery or cues (Shin et al. 2001; Bremner et al. 2007). Several studies, however, have found no differential response in the amygdala in PTSD (Lanius et al. 2002). However, the convention is that PTSD patients have increase reactivity in the amygdala. Also, functional neuroimaging studies of PTSD have reported decreased activation or failure to activate the mPFC (including the rACC, medial frontal gyrus, and subcallosal cortex) by the presentation of trauma-related stimuli (Bremner et al. 1999; Yang et al. 2004; Hou et al. 2007). Finally, many

studies have found decreased hippocampal volume in PTSD patients and hippocampal function appears to be abnormal as well. However, a few studies have found no changes on hippocampal volume or function in PTSD patients (reviewed in Shin and Liberzon 2009).

Several studies show that the amygdala and brain stem hyper-responsivity in panic disorder (Van den Heuvel OA et al. 2005; Pillay et al. 2007). Moreover, there is increased Activation in rACC and dACC, and a possible decreased in gray matter volumes. A common limitation in neuroimaging studies of this disorder is the inclusion of participants taking psychiatric medications. Thus, the findings of such studies should be interpreted cautiously (Shin and Liberzon 2009). In the vast majority of the studies the amygdala was hyperactive, with some inconsistencies in panic disorder and GAD. Another common finding is the abnormal activation (compared to healthy controls) in the dorsal and rostral anterior cingulate cortex (ACC), the hippocampus and the insular cortex (Shin and Liberzon 2009). Findings from fMRI imaging of PTSD, panic disorder, social phobia, specific phobia and generalized anxiety patients are summarized in table 1. Functional imaging has helped us identify brain regions dysfunctional in anxiety disorders. One big limitation is the inability to distinguish between these functional abnormalities being signs of the disorder or vulnerability factors. Animal models can be useful to address directionality and causality of the relationship between brain function and behavior.

Insights from trait anxiety studies

Not all humans are alike; the same situation may make one person feel anxious, but not another. Trait anxiety reflects the tendency to respond with anxiety in anticipation of a threat. Healthy individuals can have high trait anxiety, but not pathological anxiety, making them more anxious than the average individual. A recent fMRI study showed that higher levels of trait anxiety during an emotional discrimination task were correlated with increased associated with stronger activation of ACC. Moreover, anxiety was associated with reduced functional connectivity between ACC and lateral prefrontal cortex (LPFC). Suggesting that lack of functional connectivity could be linked to increased risk of anxiety (Comte et al. 2015). Moreover, high trait anxiety healthy subjects had higher amygdala and insula activation during presentation of emotional faces than lower trait anxiety subjects (Stein et al. 2007). Moreover, higher scores on several measures assessing anxiety proneness (e.g., neuroticism, trait anxiety, and

	Amygdala	rACC	dACC	Hippocampus	Insular Cortex
Posttraumatic stress disorder	↑	↓	↑ *	↑ ↓	↑ ↓
Panic Disorder	↑ ↓ *	↑ *	—	↑ ↓	—
Social Phobia	↑	↑ ↓ *	↑ ↓	—	↑
Specific Phobia	↑	↑ ↓ *	↑	—	↑
Generalized anxiety disorder	↑ ↓ *	↑ *	↑ *	—	—

rACC=rostral anterior cingulate cortex; dACC=dorsal anterior cingulate cortex
↑ = increased function in the disorder (relative to control groups)
↓ = decreased function in the disorder (relative to control groups)
↑ ↓ = mixed findings
* = based on a small number of studies
— = not enough information available

Table 1: Summary of direction of functional neuroimaging finding in anxiety disorders (adapted from Shin and Liberzon *Neuropsychopharmacology (2010) 35, 169-191).*

anxiety sensitivity) were associated with greater activation of the amygdala and the anterior insula (Stein et al. 2007). Another fMRI study showed that activity in the basolateral amygdala elicited by unconscious processed fearful faces correlated with individual differences in trait anxiety in healthy subjects using. This correlation neither detected in the dorsal amygdala nor the hippocampus (Etkin et al. 2004). Although Etkin and colleagues did not find a correlation between trait anxiety and hippocampal activity, another study showed that once you divide the hippocampus into the anterior and posterior compartments, then a correlation with trait anxiety emerged. This study found that during a task that alternated threat and safety trials, state anxiety was related to activity in anterior but not posterior hippocampus, whereas trait anxiety showed the opposite pattern. Additionally, fMRI connectivity analysis showed that activity in anterior hippocampus was more strongly related than the posterior hippocampus to activity in ventromedial prefrontal cortex under threat than under safety conditions (Satpute et al. 2012). Together, these studies suggest that differences in amygdala reactivity to emotional cues correlates with individual differences in trait anxiety, and that this might also be the case for the posterior hippocampus.

Insights from imaging healthy humans

Many studies have imaged healthy human subjects to identify which brain regions are involved in processing emotional stimuli. These studies consistently show that the amygdala, the dorsal anterior cingulate cortex (dACC), and the insular cortex are activated by negative stimuli (e.g. photographs) (Shin and Liberzon 2009). A different approached to identify brain regions involved in anxiety has been to induce a high fear

and anxious state in healthy humans with the use of pharmacological agents. These studies show that under a pharmacologically-induced anxious state there is increased activity in the amygdala, insular cortex, claustrum, cerebellum, brain stem, and the ACC (Javanmard et al. 1999; Schunck et al. 2006). This type of study, however, is problematic since it is very difficult to dissociate the effects of the drug from the effect of the fear or anxiety state induced.

Genetic factors in anxiety disorders

Anxiety disorders are heritable, with some of them having up to 40% heritability (Hettema, Neale, and Kendler 2001). Indeed, gene polymorphisms for dopamine receptors, serotonin receptors, GABA receptors and interlukins have been implicated as risk factors for anxiety disorders (Lacerda-Pinheiro et al. 2014). A specific study showed that patients with a genetic polymorphism of the serotonergic system lower activation of the right prefrontal cortex and increased activity of both amygdalae after presentation of faces with emotional expression (Domschke et al. 2006). Another study showed that a common functional variation on the human 5-HT1A gene was associated with decreased threat-related amygdala reactivity (Fakra et al. 2009). This type of study demonstrates a potential link between genetics and the functional role of specific brain regions.

Conclusions and Caveats

Altogether, fMRI imaging studies show a high overlap on the brain regions that process emotional stimuli in healthy subjects and the brain regions that are potentially

dysfunctional in anxiety disorders. These findings suggest that in anxiety disorders the circuitry that mediates emotional stimuli is dysfunctional, and that dysfunctional activity might account for the inappropriate behavioral response.

Imaging techniques provide, perhaps the best, noninvasive way to study the human brain, but fMRI data has multiple problems and caveats. First, the fMRI signal is based on the complex interaction of neuronal activity, metabolism and blood flow. Also, the spatial scale is poor having hundreds of thousands of neurons in each voxel (Bandettini 2009). The temporal scale in fMRI data is also very limited, in the order of seconds, while neuronal changes can occur much faster in the millisecond scale.

1.3 Animal Models of Anxiety-like Behaviors

Research with human subjects faces many challenges, especially when it comes to the manipulation and control of variables. Additionally, studying any mechanisms underlying anxiety in humans poses ethical problems. Animal models of anxiety-like behaviors provide a way to investigate the neural mechanisms that generate non-pathological anxiety.

“In observing animals, we are not so likely to be biased by our imagination; and we may feel safe that their expressions are not conventional.” –Charles Darwin

In *The Expression of the Emotions in Man and Animals*, Charles Darwin sets the foundation for the view of defensive behaviors across species as evolutionary

precursors to human fear and anxiety (Blanchard and Blanchard 1989). There are dozens of anxiety tests used in animal research (table 2). Some of them measure physiological responses, while others measure behavioral responses (Rodgers, Cao, and Holmes 1997). In 1986, Willner proposed three criteria for assessing animal models of human mental disorders: predictive validity, face validity and construct validity. Predictive validity measures if the test predicts the condition being modeled, face validity regards the phenomenological similarity, and construct validity its theoretical rational (Willner 1986). Most of these tests have been validated using pharmacological agents that affect anxiety behavior in humans, thus establishing predictive validity (Rodgers, Cao, and Holmes 1997). Human anxiety includes behavioral disturbances like avoidance, escape and hypervigilance. Therefore, animal anxiety assays that evoke those behaviors have face validity (Rodgers, Cao, and Holmes 1997).

The most commonly used unconditioned behavioral anxiety tests are the elevated plus maze (EPM) and the open field test (OFT). The EPM was developed by Pellow and colleagues in 1985 for rats, and it is based on the natural aversion of rodents to open spaces. In the EPM there are two open arms and two closed arms, and rats and mice display avoidance to the open arms (Pellow et al. 1985; Lister 1987). Lister and colleagues showed that mice behavior in the EPM was consistent with their behavior in other anxiety tests. Moreover, they showed that anxiolytic drugs (benzodiazepines or ethanol) increased exploration and time spent in open arms, while anxiogenic drugs (caffeine or picrotoxin) decreased it. On the other hand, amphetamines and imipramine did not affect avoidance to open arms in the EPM (Lister 1987). In the EPM, time spent

on the open arms and entries into the open arms are the main behavioral variables that have been validated pharmacologically. Additional anxiety behavioral features that can be recorded in the EPM include head-dipping and distance traveled in the open arms (Rodgers, Cao, and Holmes 1997). The OFT is very similar to the EPM, except that instead of avoiding the open arms, rodents avoid the center of the field and instead spend most time in the periphery (Walsh and Cummins 1976). A different unconditioned anxiety test is the potentiated startle response, which takes advantage of rodents' innate aversion to bright light. In the startle paradigm, rodents are presented with an unpredictable burst of noise and in response the display a startle reflex. The amplitude of the startle reflex is enhanced after rats are presented with an innately aversive stimulus, such as a cat (Blundell, Adamec, and Burton 2005) or bright illumination (Davis, Walker, and Lee 1997). This paradigm has been validated pharmacologically similarly to the EPM and OFT (Davis, Walker, and Lee 1997). Using the EPM, OFT and other common anxiety assays, scientists have learned a lot about the circuitry underlying anxiety behavior.

Unconditioned responses	Conditioned responses
Anxiety/defence test battery	Active/passive avoidance
Elevated plus-maze and zero-maze	Conditioned emotional response (CER)
Fear/defence test battery	Conditioned taste aversion
Free exploration	Conflict tests (pigeons and primates)
Holeboard	Defensive burying
Human threat (primates)	dPAG stimulation
Light/dark exploration	Fear potentiated startle
Open field	Four plate test
Social competition	Geller-Seifter conflict
Social interaction	Learned helplessness
Ultrasonic vocalization (pups)	Ultrasonic vocalization (adult)

Table 2: **Some commonly used tests for anxiety behaviors.** From Rodgers 1997

1.4 The extended circuitry of anxiety and fear

There is a large distributed circuit of brain regions involved in anxiety behaviors, which show a high degree of interconnectivity (Figure 1). The majority of these brain regions have been implicated in anxiety behaviors via lesions, pharmacological inactivations and anti-anxiety drug infusions. More recently, the emergence of optogenetics has allowed controlling neuronal activity with more temporal and spatial resolution. Additionally, optogenetics allows inhibiting or exciting specific projection outputs or specific subpopulations within these brain regions.

There is substantial overlap on the circuits mediating fear and anxiety behaviors (Gross and Canteras 2012; Likhtik et al. 2014; Calhoon and Tye 2015). However, some evidence suggests that there are some differences in the circuits of fear and anxiety, specifically the bed nucleus stria terminalis is necessary for anxiety, but not fear behaviors (Davis et al. 2010). In the following section I will discuss the general findings for the circuitry of both fear and anxiety behaviors. Here, I summarize the evidence for some select brain regions' involvement in anxiety and fear behaviors. I will also emphasize if they interact with the ventral hippocampus or the medial prefrontal cortex.

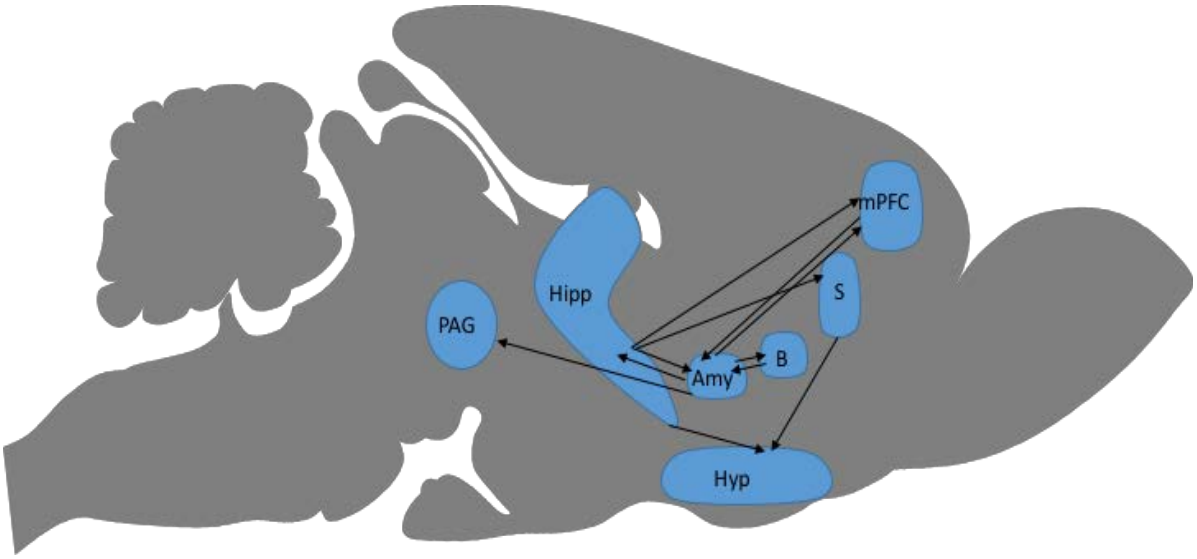

Figure 1: **Distributed circuit involved in anxiety behavior.** S:septum, Hyp: hypothalamus; mPFC: medial prefrontal cortex; Amy: amygdala; B: bed nucleus stria terminalis; Hipp: hippocampus; PAG: periaqueductal gray

As discussed earlier, **the amygdala** is dysfunctional in most anxiety disorders (table 1). In parallel, animal research of learned fear and anxiety shows a major role of the amygdala in mediating these behaviors. Lesioning or silencing the basolateral amygdala (BLA) disrupts the behavioral and autonomic responses to a learned fear stimulus (Davis and Shi 2000; Fendt and Fanselow 1999). Moreover, pharmacological inactivation of the BLA is necessary for the retrieval of a learned fear memory to a tone (Sierra-Mercado, Padilla-Coreano, and Quirk 2011). The BLA projects to the central amygdala (CeA), which is also necessary for the behavioral and autonomic response to a conditioned fear stimulus (Kapp et al. 1979). Lesions or infusion of an anxiolityc drug to the BLA and CeA together, disrupted avoidance behavior to a shock probe (Treit and Menard 1997; Treit, Pesold, and Rotzinger 1993). However, lesioning the BLA alone did not affect avoidance to the open arms in the EPM (K. G. Kjelstrup et al. 2002). Taken together, this data suggests a stronger role of the BLA in learned fear than in anxiety behaviors. However, lesions are problematic to interpret because they can reflect

compensatory mechanisms rather than a functional role. Recent development of optogenetics, a technique that allows to reversible hyperpolarize or depolarize neurons with light, has been used to further clarify the role of the BLA in anxiety behaviors. Optogenetic activation of BLA somatas, using the excitatory opsin channelrhodopsin-2 (ChR2), increases anxiety behavior in the EPM and OFT (Tye et al. 2011). However, ChR2 activation of somas is arguably anti-physiological since normally neurons do not fire simultaneously unless there is a seizure. Experiments using optogenetic inhibition with inhibitory opsins (halorhodopsin, archeorhodopsin, etc.) are easier to interpret. BLA somata inhibition did not affect anxiety behavior. However, inhibition of the BLA projections to the CeA increased avoidance behavior (Tye et al., 2011). On the other hand, inhibition of the BLA projections to the vHPC decreased avoidance behavior (Ada C. Felix-Ortiz et al. 2013). Together these studies demostrate that different outputs of the BLA have opposite roles in the expression of anxiety. This is consistent with recent electrophysiological work that shows that the BLA distinct neuronal populations that encode aversive vs appetitive stimuli and project to different outputs (Beyeler et al. 2016).

The hippocampus is historically known for its role in memory and cognition, and for being part of the limbic system. However, these two roles seem to be anatomically segregated. The idea that the hippocampus has distinct functional domains along the dorsal-ventral axis has been proposed for long based on the anatomical connectivity, and lesion studies of the dorsal vs ventral compartments (Risold and Swanson 1996; Moser and Moser 1998). The ventral compartment of the hippocampus (vHPC) is

necessary for anxiety. Lesioning the vHPC, but not the dorsal compartment (dHPC), decreased anxiety in a variety of tasks (Bannerman et al. 2003; Bannerman et al. 2004). On the other hand, lesions of the dHPC, but not the vHPC, disrupted spatial memory (Moser and Moser 1998).

There is also some evidence for distinct roles of dHPC and vHPC in learned fear using pavlovian fear conditioning paradigms. For cued (e.g. tone) fear conditioning, total or ventral hippocampal lesions produce robust deficits in freezing to auditory stimuli (Maren 1999; Richmond et al. 1999), whereas dorsal hippocampal lesions spare auditory fear conditioning (Kim and Fanselow 1992; Anagnostaras, Maren, and Fanselow 1999; Anagnostaras et al. 2001). Furthermore, muscimol inactivation of the vHPC, but not the dHPC, prior to fear acquisition training prevented the acquisition of a cued fear memory (Maren and Holt 2004). Altogether, this argues that vHPC, and not dHPC, is necessary for acquiring cued fear memories. This role of the vHPC is consistent with the idea that vHPC alters fear conditioning by depriving the amygdala from necessary hippocampal information via the projection of vHPC to BLA.

The role of vHPC in retrieval of cued fear memories is more controversial. One study showed that inactivation of the vHPC prior to a retrieval test had no effect, while vHPC lesions did affect retrieval of cued fear (Maren and Holt 2004). However, other studies showed that inactivating or lesioning the vHPC prior to fear recall impaired retrieval of the cued fear memory (Hunsaker and Kesner 2008; Sierra-Mercado, Padilla-Coreano, and Quirk 2011).

In paradigms of contextual fear, lesion and inactivation studies have implicated both the vHPC and dHPC are necessary for contextual fear expression or acquisition (Maren and Holt 2004; Hunsaker and Kesner 2008). One study showed that inactivating the dHPC or vHPC had no effect on retrieval contextual fear, but inactivating vHPC prior to the training disrupted the acquisition of contextual fear (Maren and Holt 2004). It is important to point out that lesion studies are problematic to interpret because there could be postsurgical recovery or compensatory systems, such as recruitment of another neural system. Optogenetic approaches to excite or inhibit neurons with high temporal control allow to study the role of dHPC in contextual fear. One study used optogenetics to manipulate activity within a specific HPC subregion known as the dentate gyrus. Optogenetic inhibition of the dorsal dentate gyrus, but not the ventral dentate gyrus, blocks acquisition of contextual fear (Kheirbek et al. 2013). Another recent study showed that somatostatin interneurons in the dHPC are necessary for retrieval of a contextual fear memory (Lovett-Barron et al. 2014). These optogenetic studies more clearly implicate the dHPC in contextual fear learning.

Some electrophysiological evidence suggests that the dorsal-ventral axis is more of a gradient than two distinct and independent hippocampal subregions. The representation of spatial information exists throughout the hippocampus although the size of the fields increases dramatically in the vHPC (Kjelstrup et al. 2008; Royer et al. 2010). Considering the electrophysiological and behavioral evidence, the role of the hippocampus in spatial learning and contextual learned fear is consistent with a gradient

model of the dorsal-ventral axis. On the other hand, the role of the hippocampus in fear to a discrete cue, unconditioned fear and anxiety is consistent with a dorsal and ventral dichotomy model. Less work has been done to dissociate the role of the dHPC and vHPC in innate anxiety behavior, but at least one study suggests that activity in the vHPC, and not the dHPC, correlates with levels of anxiety (Adhikari, Topiwala, and Gordon 2010).

The medial prefrontal cortex (mPFC) is an anatomical division of the prefrontal cortex, which is known for its diverse roles from integration of sensory inputs to decision making (Nauta 1971). The medial subdivision of the prefrontal cortex has been long implicated in processing of stress and aversive stimuli (Diorio, Viau, and Meaney 1993). Moreover, a growing body of evidence demonstrates that the mPFC provides top-down control and regulation of fear and anxiety behaviors (Milad and Quirk 2012; Adhikari et al. 2015). The mPFC is necessary for anxiety behaviors, as lesions or pharmacological inactivation of the mPFC result in decreased avoidance behavior in multiple anxiety assays (Shah and Treit 2003). More recently, it has been shown that single units in the mPFC represent aversive features of the environment (Adhikari, Topiwala, and Gordon 2011). The role of the mPFC during learned fear is more complex because of the opposing roles of different subregions of the the mPFC. Mounting evidence shows that the prelimbic (PL) subregion of the mPFC promotes fear, while the infralimbic (IL) subregion promotes extinction of the fear (Burgos-Robles, Vidal-Gonzalez, and Quirk 2009; Burgos-Robles et al. 2007; Milad and Quirk 2012). In humans, the dorsal anterior

cingulate cortex, the homolog of the rodent PL, is consistently abnormal in patients with anxiety disorders as discussed earlier (Milad and Quirk 2012).

There is no clear evidence that this dissociation of the PL and IL exists during innate fear or anxiety behaviors. A recent study showed that optogenetic inhibition of IL somata alone was insufficient to change avoidance behavior in the open field (Adhikari et al. 2015), indicating that PL activity is sufficient to mediate avoidance behavior during the open field. This same study showed that inhibition of outputs of the IL to the basomedial amygdala increased avoidance behavior. This suggests that some IL outputs are anxiolytic, which is consistent with the role of IL promoting extinction of learned fear. This study indirectly demonstrates that PL, more than IL, mediates avoidance behavior. This hypothesis is consistent with electrophysiological work showing that PL firing represents aversive features in the EPM (Adhikari, Topiwala, and Gordon 2011). However, no experiment has yet directly compared the contributions of IL vs PL activity in anxiety-like behaviors.

The bed nucleus stria terminalis (BNST) receives strong projections from the BLA and projects to many hypothalamic and brainstem regions (Dong and Swanson 2004). Therefore, it is anatomically well situated to mediate physiological aspects of anxiety. Additionally, the ventral hippocampus projects to the BNST (Cullinan, Herman, and Watson 1993). The strongest evidence for a role of BNST in anxiety behaviors comes from numerous studies using the light-enhanced startle response test (Davis, Walker, and Lee 1997; Davis et al. 2010). Pharmacological inactivation of the BNST blocks the

potentiation in the fear startle that is normally caused by exposure bright light or injection of corticotropin releasing hormone (Lee and Davis 1997; Walker and Davis 1997). Using the EPM as an anxiety test, there have been conflicting findings on the effect of BNST lesions in avoidance behavior (Treit, Aujla, and Menard 1998; Duvarci, Bauer, and Paré 2009). More recent work that used optogenetics to dissect the role of the BNST and its different outputs in anxiety behavior potentially explains the conflicting lesion findings (Kim et al. 2013). Optogenetic inhibition of the anterodorsal BNST decreased anxiety, while inhibting the oval BNST decreased anxiety behavior. Moreover, specific outputs of the anterodorsal BNST to the lateral hypothalamus, parabrachial nucleus and ventral tegmental area-each implemented an independent feature of anxiolysis: reduced risk-avoidance, reduced respiratory rate, and increased positive valence, respectively (Kim et al. 2013).

> *[Septally lesioned rats] presented a picture of striking alertness with limbs rigidly extended and eyes intently following the movements of the observer approaching the cage. The sudden presentation of almost any auditory stimulus produced an explosive startle reaction. The typical exploratory response of the normal rat to presentation of such an innocuous object as a pencil was replaced by 'freezing'… Rapidly approaching objects were attacked immediately with vigorous biting… - Brady and Nauta, 1953*

The septum has long been implicated in the generation of defensive behaviors that are elicited by feelings of fear or anxiety. Lesioning the septum causes a very strong increase in defensive behaviors, as described in the quote (Gotsick and Marshall 1972;

Brady and Nauta 1953). This increase in defensive behaviors is only seen when the whole septum is lesioning (Gotsick and Marshall 1972). A common interpretation of this rage syndrome is that the septal lesion causes a generalized disinhibition of fear, resulting in an animal that shows exaggerated or inappropriate defensive reactions to nonthreatening environmental stimuli (Sheehan, Chambers, and Russell 2004). The septum is subdivided in the lateral septum (LS) and the medial septum (MS); inactivating independently these subdivisions has different behavioral effects. During fear conditioning paradigms, the subdivisions of the septum might have different roles in the expression of fear. One study suggests a dissociable role for the LS and MS in fear to a conditioned tone and a conditioned context, respectively (Calandreau, Jaffard, and Desmedt 2007), but the results are not very convincing and no other study has reported such dissociation.

The MS projects to the hippocampus (Robinson et al. 2016). A recent study showed that during contextual fear cholinergic inputs from the MS to the dHPC are activated (Lovett-Barron et al. 2014). Furthermore, lesioning or inactivating the MS disrupts local field potential theta-frequency range (4-12 Hz) activity in the hippocampus (Petsche, Stumpf, and Gogolak 1962; Mizumori, Barnes, and McNaughton 1990; Buzsáki 2002). Theta activity in the HPC has been implicated in contextual navigation, suggesting that MS plays a role in contextual fear via its projection to the HPC. The role of MS in hippocampal theta will be further discussed in a later section.

During anxiety assays, lesions of either the LS or MS subdivision decrease avoidance behavior (Menard and Treit 1996). Additionally, pharmacological inactivation of the LS decreases avoidance behaviors (Trent and Menard 2010). However, this study is at odd with the septal rage seen by many labs. The ventral hippocampus (vHPC) strongly projects to the LS (Risold and Swanson 1996). Since early twentieth century it has been proposed that the LS can be a relay station for the hippocampus (Smith 1910). Indeed, pharmacological disconnection of the LS and vHPC decreases avoidance behavior, suggesting that the connection between LS and vHPC is necessary for anxiety behavior (Trent and Menard 2010). A recent study showed that the LS outputs to the anterior hypothalamus are necessary for stress-induce increases on anxiety (Anthony et al. 2014). All of this work together suggests a model in which the vHPC can modulate the hypothalamus via the LS to modulate anxiety, and input from the MS could in turn feedback to the vHPC.

The periaqueductal gray (PAG) is a brainstem region most known for its role in pain. Stimulating certain areas of the PAG causes self-reported fear sensations in humans (Nashold, Wilson, and Slaughter 1969; Jenck, Moreau, and Martin 1995). Specifically, stimulation of the dorsal PAG (dPAG) in humans induces acute signs of autonomic arousal and feelings of subjective anxiety, similar to a panic attack. In animals, dPAG stimulation has a similar effect in autonomic activation and sudden fear behaviors (Jenck, Moreau, and Martin 1995). A body of literature shows that the dorsolateral PAG controls defensive behaviors, like fight or flight, or freeze responses (Bandler and Shipley 1994). Electrical stimulation of the dorsolateral PAG in cats and rats produced

defensive behaviors associated with flight responses. On the other hand, stimulation of the ventrolateral PAG produced freezing responses (Bandler and Carrive 1988). The central amygdala projects strongly to the PAG (Gray and Magnuson 1992). Considering the roles of the amygdala and PAG, the classic model proposed is that dangerous stimuli activate the amygdala which then activates the PAG to evoke defensive behaviors in response (Behbehani 1995). More recent models also acknowledge that the direct projection from the medial prefrontal cortex to the PAG could also be modulating defensive behaviors (Calhoon and Tye 2015; Cheriyan et al. 2016); this hypothesis remains to be tested.

1.5 The tripartite circuit of fear and anxiety

As discussed above, there is a large distributed circuit implicated in anxiety, I will focus on a tripartite circuit within this extended circuit. A growing body of evidence shows that functional connectivity between mPFC, BLA and vHPC are an important feature in fear and anxiety states (Lesting et al. 2011; Sotres-Bayon et al. 2012; Courtin et al. 2014; Likhtik et al. 2014). Some of that evidence comes from recording local oscillations. Brain oscillations are generated from periodic fluctuations in the excitability in a group of neurons. The synchronized changes in membrane potential of neurons create an extracellular current which can be measured by recording the local field potentials (LFP) (Buzsáki and Draguhn 2004; Buzsáki and Watson 2012). In vitro, fluctuations of the extracellular field were sufficient to cause oscillations in the somatic membrane and to entrain spiking activity (Anastassiou et al. 2011). Therefore, it is possible that endogenous brain oscillations can causally affect neural function through field effects

under physiological conditions. Most brain rhythms are paced by inhibition; therefore these oscillations could also provide a mechanism for carrying information in temporal frames (Buzsáki and Watson 2012). The forebrain neuronal networks support different neuronal oscillations that occur at different speeds and frequencies. For fast oscillations the available time is short, so the participating neurons are constrained to a small volume. On the other hand, slower oscillations encompass a larger volume of tissue and more neurons (Buzsáki and Watson 2012).

Theta-range (4-12 Hz) oscillations are one of the slower oscillations. Evidence suggests that theta rhythms are involved in facilitating the transfer of information from one brain region to another during sensory information processing (Colgin 2013). They were first described in the dorsal hippocampus (dHPC) during navigation (Vanderwolf 1969). Theta oscillations were first implicated in anxiety from evidence showing that anxiolytic drugs decreased theta oscillations in the dHPC (McNaughton and Sedgwick 1978). In a mouse genetic model of anxiety, dHPC theta oscillations were stronger during anxiety behaviors (Gordon et al. 2005). Additionally, theta oscillations in the amygdala and dHPC synchronized during retrieval of a fear memory (Seidenbecher, Laxmi, and Pape 2003); suggesting that theta might enhance dHPC and amygdala information transfer during fear recall. In humans with high trait anxiety, electroencephalogram recordings in the temporal lobe showed increase theta activity during presentation of aversive visual stimuli (Aftanas et al. 2003), suggesting that in the human brain theta rhythms are important during threat processing.

As discussed above there is mounting evidence that the vHPC, and not the dHPC, is involved in fear and anxiety behaviors (Kjelstrup et al. 2002; Bannerman et al. 2003; Fanselow and Dong 2010). A study that recorded vHPC, dHPC and mPFC LFPs, showed that only theta in the vHPC increased in relative power during anxiogenic environments (Adhikari, Topiwala, and Gordon 2010). Furthermore, mPFC theta increased relative power with anxiety, and mPFC theta power explained the avoidance behavioral variance (Adhikari, Topiwala, and Gordon 2010). Finally, this same study showed an increase in theta power correlation between the mPFC and vHPC during anxiety behavior. During differential fear conditioning, the BLA, mPFC and vHPC all increased theta during the presentation of conditioned tones. However, only the BLA and mPFC had higher theta during the CS+ compared to a CS- (Lesting et al. 2011; Likhtik et al. 2014). It is important to clarify that in these studies the CS- evoked significant freezing so it was not an absolute safety signal, suggesting that vHPC increases in theta with weaker threats like the CS- and stronger threats like the CS+ alike. Altogether, this work suggests that theta oscillations in BLA, mPFC and vHPC are important for fear and anxiety, although the evidence is of correlative nature.

How are theta oscillations generated? A body of literature shows that theta rhythms in the hippocampus are dependent on input from the diagonal band of the medial septum (MS) (Petsche, Stumpf, and Gogolak 1962; Mizumori, Barnes, and McNaughton 1990). However, a recent study questions this model. In an intact in vitro preparation of the hippocampus, lacking any connections to MS, theta rhythms remained (Goutagny, Jackson, and Williams 2009). Moreover, in this preparation interneuron and pyramidal

synaptic activity was sufficient to elicit theta rhythms in the hippocampus. One possibility to consolidate these findings is that indeed local hippocampal activity is sufficient to generate theta rhythms, but the MS input amplifies and helps maintain the rhythm. However, not all theta oscillations are alike. Theta from the ventral and dorsal HPC can be modulated independently. When theta activity was recorded at two locations in CA1, one dorsal and one ventral, and the regions between were silenced by procaine, both regions continued to oscillate, but the ventral theta was slower than the dorsal theta (Goutagny, Jackson, and Williams 2009). Moreover, theta oscillations in the vHPC and dHPC appear to be functionally distinct, as seen in anxiety-like behaviors (Adhikari, Topiwala, and Gordon 2010).

The amygdala also shows theta rhythms that emerge in vitro in the absence from specific input (Pape et al., 1998). The BLA and mPFC theta also synchronize during fear and anxiety. Fear-induced theta oscillations in mPFC are independent of MS activity (Courtin et al. 2014). This finding provides further evidence that theta oscillations in different regions have different sources. During innate anxiety and retrieval of learned fear, oscillations in the mPFC and BLA increased in synchrony (Lesting et al. 2011; Likhtik et al. 2014). Specifically, mPFC lead BLA theta when animals were in the relative safety of the periphery of the open field or during presentation of a CS-. Conversely, the BLA was more likely to lead the mPFC during the center of the open field or a CS+ (Likhtik et al. 2014). An important observation is that Lihktik et al. mostly recorded in the PL subregion of the mPFC. Recently it was shown that optogenetic inhibition of PL parvalbumin interneurons (PV) caused re-set of mPFC theta and

increases in freezing behavior. Moreover, optogenetic stimulation of PL PV at 4 Hz was sufficient to evoke freezing behavior (Courtin et al 2014). Altogether, suggests that PL theta is strongly linked to fear behavior but it is also necessary for discrimination of fear.

Recent optogenetic work also emphasizes how the vHPC-mPFC-BLA circuits work together during anxiety (Figure 2). Inhibition of the BLA projections to vHPC or to mPFC decreased avoidance behavior, suggesting an anxiogenic role of the BLA-mPFC and BLA-vHPC pathways (Felix-Ortiz et al. 2013; Felix-Ortiz et al. 2016).Interestingly, inhibition of the vHPC projection to the BLA did not affect avoidance behavior, and instead disrupted contextual fear (Jimenez et al. personal communication). Moreover, inhibition of the IL-amygdala projection increased avoidance, suggesting that this subregion of the IL contains anxiolytic neurons (Adhikari et al. 2015).

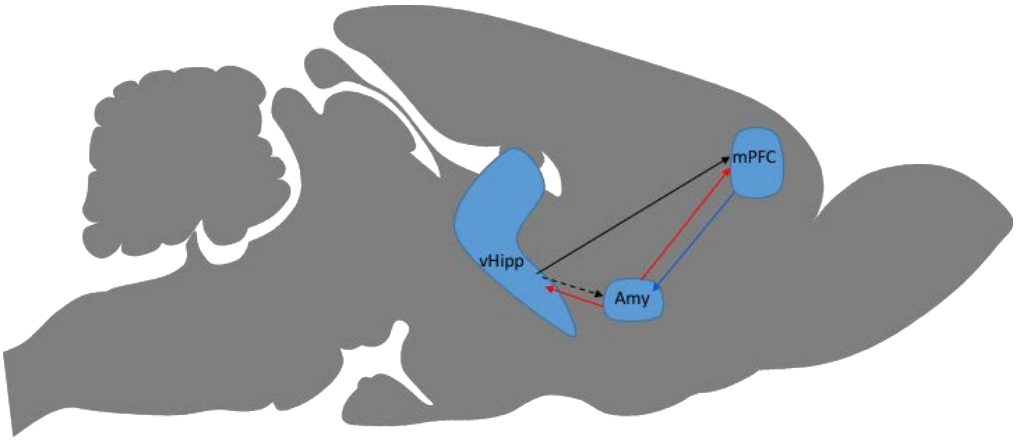

Figure 2: **Projections tested optogenetically within the emotional triad.** Red arrow represents anxiogenic pathways, blue arrow represents anxiolytic pathway and dashed arrow represents no causal role in anxiety.

1.6 Addressing the role of vHPC-mPFC in anxiety behavior

The vHPC serves as the hippocampal output to the mPFC. Theta activity in this pathway increases during anxiety, suggesting it may have a causal role in anxiety behavior. Moreover, single units in the mPFC represent the aversion and safety in the elevated plus maze (Adhikari et al., 2011). That mPFC population of single-units is more phase-locked to vHPC theta; suggesting that these cells could receive projection from the vHPC and that this representation relies on the vHPC projection. To understand the contribution of the direct projection from vHPC to mPFC, I sought to answer the following hypotheses:

Hypothesis 1 The vHPC projection to the mPFC is necessary for avoidance behavior.

Hypothesis 2 The vHPC projection to the mPFC is necessary for the mPFC representation of aversion.

Hypothesis 3 The vHPC projection to the mPFC is necessary for the anxiety-related theta synchrony between vHPC-mPFC.

Hypothesis 4 Activation of the vHPC projection to the mPFC in a theta frequency is sufficient to modulate anxiety behavior.

Optogenetics combined with *in vivo* electrophysiology in behaving mice, provides a tool to address all of these hypotheses with high temporal control. To tests hypotheses 1 through 3, I used archearhodopsin mediated inhibition of the vHPC terminals. The results from these experiments are presented in chapters 2 through 4. To test

hypothesis 4, I used channelrhodopsin mediated excitation of vHPC terminals. The results from these experiments are presented in chapter 5. The implications of the results presented in this thesis are then discussed in chapter 6.

Chapter 2: The role of the ventral hippocampal input to mPFC in anxiety behaviors

The work in this chapter is published
in Padilla-Coreano et al., 2016 *Neuron*

2.1 Introduction

As discussed in the general introduction, anxiety is an adaptive state of increased apprehension that allows avoidance of potential danger. However, inappropriate expression of anxiety is maladaptive and, in humans, can lead to anxiety disorders. In order to develop better treatments for these disorders, we must understand the neural circuits that support normal anxiety behaviors. Studies in rodents have shown that anxiety-like behavior involves the ventral hippocampus (vHPC). Lesioning the vHPC, but not the dorsal compartment of the hippocampus (dHPC), decreased anxiety in a variety of tasks (Bannerman et al. 2003; Trent and Menard 2010). Moreover, the vHPC, and not the dHPC, is anatomically interconnected with the amygdala, therefore well situated to modulate emotional regulation within the amygdala (Pikkarainen et al. 1999).

Besides the vHPC, the medial prefrontal cortex (mPFC), and basolateral amygdala (BLA) have been implicated in anxiety-like behaviors (Shah and Treit 2003; Tye et al. 2011). These three regions share anatomical and functional connectivity (Pikkarainen et al. 1999; Hoover and Vertes 2007; Lesting et al. 2011; Likhtik et al. 2014); suggesting that they function as a distributed network that supports anxiety behavior in an interdependent manner. In particular, the vHPC has a direct monosynaptic excitatory projection to the mPFC (Jay and Witter 1991; Jay et al. 1992). The vHPC neurons that project to the mPFC are located in the intermediate and ventral CA1 pyramidal layer, and the ventral subiculum. These vHPC neurons innervate pyramidal cells and interneurons alike in the mPFC (Carr and Sesack 1996; Gabbott, Headlam, and Busby

2002); therefore vHPC can both excite mPFC and inhibit mPFC activity through feedforward inhibition.

The vHPC–mPFC projection appears to be a key component of this circuit, especially during the expression of innate forms of anxiety-like behavior. In rodents, theta-frequency (4–12 Hz) synchrony emerges between the vHPC and mPFC during exposure to anxiogenic environments such as the elevated plus maze (EPM) (Adhikari et al. 2010). This finding suggests that activity in the vHPC-mPFC pathway is necessary for anxiety-like behaviors; however, the existing evidence is correlative. Theta activity in BLA is also linked to anxiety-like behavior (Likhtik et al. 2014), making the BLA projection to vHPC and mPFC a possible mediator of the increased synchrony in theta between vHPC and mPFC. However, a recent study showed that vHPC units that have task related information in an anxiety-task are more likely to project to the mPFC than to the amygdala (Ciocchi et al. 2015). Altogether, these findings suggest that the direct projection from the vHPC to mPFC is necessary for anxiety-like behavior. To test this hypothesis, we optogenetically inhibited the vHPC terminals in the mPFC during different anxiety assays. Bilateral inhibition of vHPC-mPFC pathway decreased anxiety behavior during the EPM, the open field and the novelty suppressed feeding test. This was not the case during unilateral vHPC-mPFC inhibition or bilateral inhibition of the mediodorsal thalamic input to the mPFC.

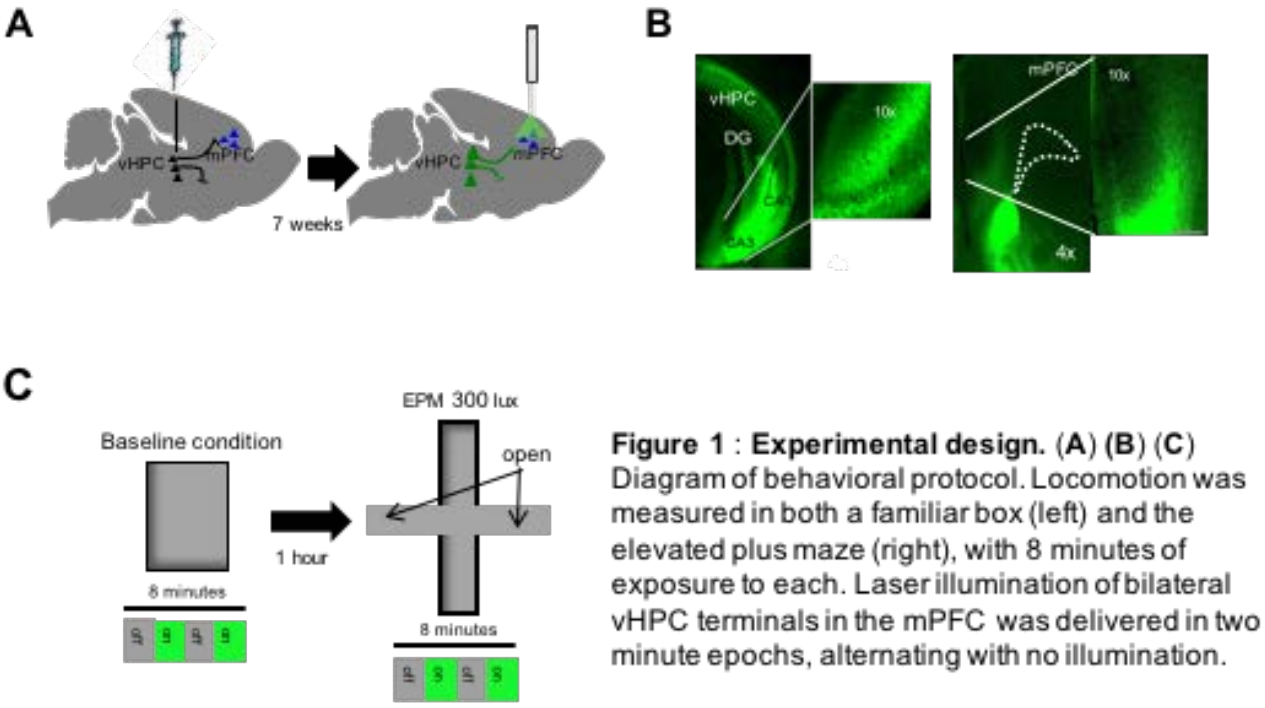

Figure 1 : Experimental design. (**A**) (**B**) (**C**) Diagram of behavioral protocol. Locomotion was measured in both a familiar box (left) and the elevated plus maze (right), with 8 minutes of exposure to each. Laser illumination of bilateral vHPC terminals in the mPFC was delivered in two minute epochs, alternating with no illumination.

2.2 Results

To examine the role of the direct vHPC-to-mPFC pathway during anxiety-like behavior, vHPC terminals in the mPFC were inhibited using an optogenetic approach. An adeno-associated virus (AAV) carrying either the inhibitory opsin, enhanced Archeorhodopsin 3.0 (Arch), or enhanced yellow fluorescent protein (eYFP) under the control of the CamKIIa promoter was injected bilaterally into the vHPC of wild-type mice (Figure 1A). Optical fibers were implanted in the mPFC, along with microelectrodes in the mPFC, vHPC, and BLA. Seven weeks were allowed for viral expression to achieve maximal opsin levels in vHPC terminals within the mPFC (Figure 1B); we have previously shown that this approach results in at least a 40% reduction in effective neurotransmission in vivo (Spellman et al., 2015). Mice were then tested in the EPM for 8 min, with

alternating 2-min periods of no illumination and illumination of the mPFC with green (532 nm) light (Figure1C).

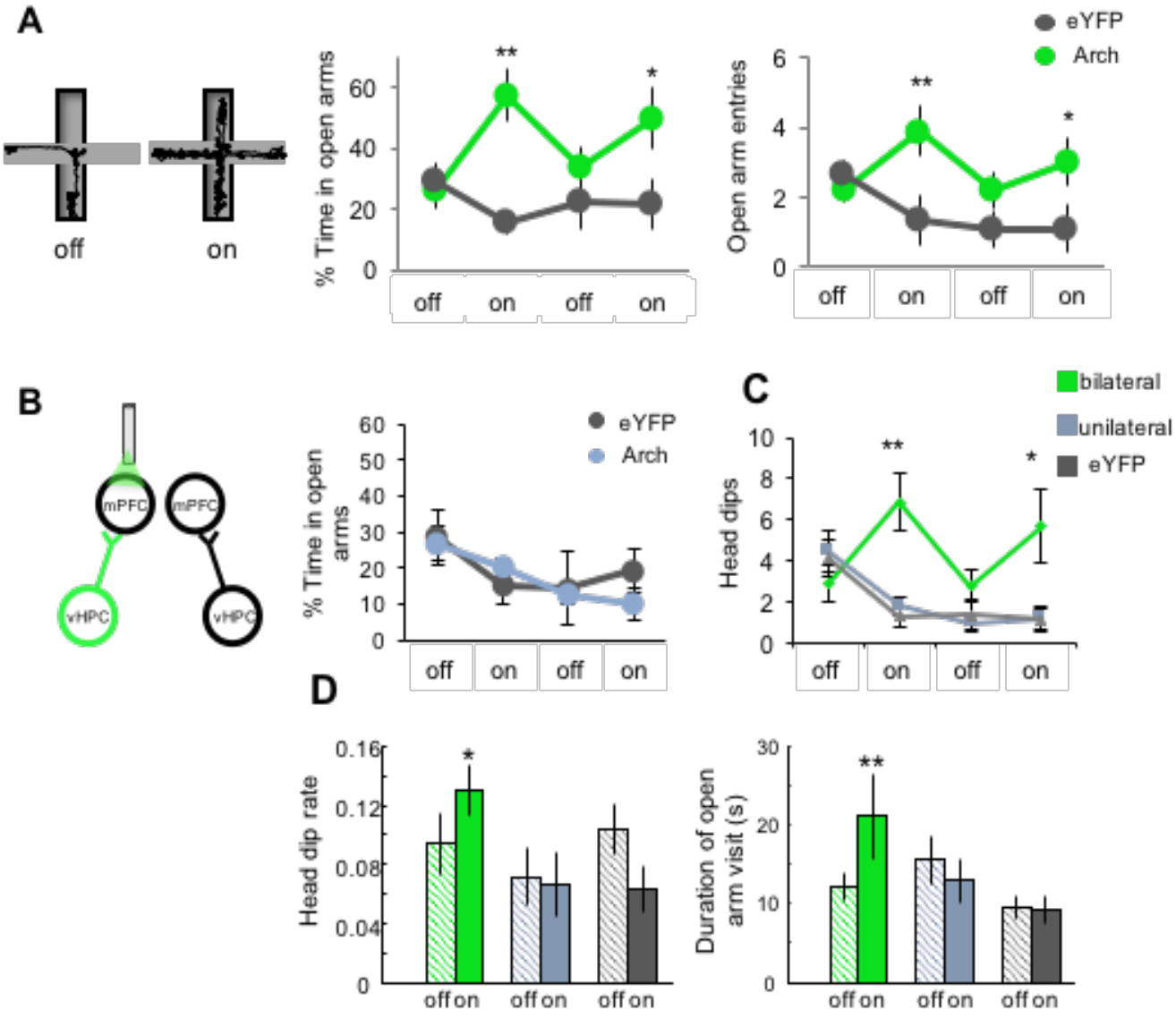

Fig 2: **Selective inhibition of hippocampal-prefrontal input disrupts avoidance behavior in the EPM**. (**A**) Paths for an example mouse during laser off and on in the EPM. Right, Open arm avoidance in vHPC Arch- and eYFP-expressing animals (Arch n=12; eYFP n=12; Two-way ANOVA, interaction of light and virus, $F_{(1,47)}$=9.15 p=0.0043; *p<0.05, **p<0.01 for Arch vs eYFP by post-hoc Bonforeni t-test). (**B**) Avoidance behavior during unilateral inhibition of vHPC-mPFC input. n=XX. **(C)** Head dips during bilateral (green) vs unilateral (blue) inhibition (n=12 per group; Two-way rmANOVA, interaction of light and group, $F_{(4,48)}$=8.74, p<0.001; bilateral vs unilateral inhibition, p<0.01, post-hoc Wilcoxon rank sum). **(D)** Left, frequency of head dips (total head dips/time in open arms) as a function of illumination (effect of light in bilateral group, p=0.03, Wilcoxon paired test). Right, Duration of open arm visits as a function of illumination (effect of light in bilateral group, p=0.0063, Wilcoxon paired test). Duration of open arm visits as a function of illumination (effect of light in bilateral group, p=0.0063, Wilcoxon paired test).

In mice expressing Arch, but not those expressing eYFP alone, bilateral inhibition of vHPC terminals in the mPFC decreased open arm avoidance, as evidenced by both entries into and increased time spent in the open arms (Figure 2A). Locomotion, measured as distance traveled, was not affected by light in neither environment (Figure 3). Moreover, inhibition of vHPC-mPFC did not affect velocity in the EPM (Figure 4).

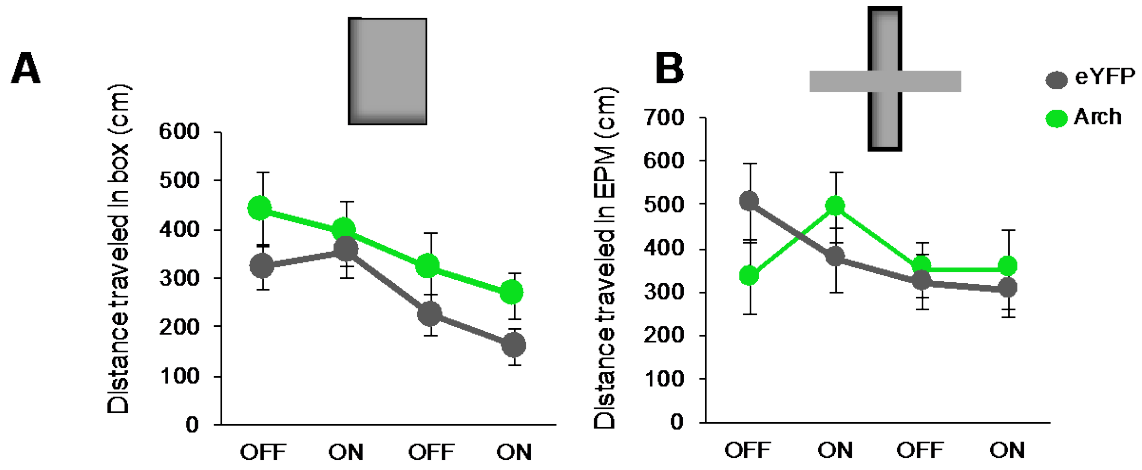

Figure 3 : Inhibition of vHPC input to the mPFC does not affect distance traveled in baseline condition. (**A**) Effects of terminal inhibition on distance traveled in the baseline box (left), and in the EPM (**B**) in Arch- and eYFP-expressing mice (n=10 and n=9, respectively).

Unilateral lesion of vHPC does not affect anxiety behavior (Shah et al., 2003), which suggests that unilateral inhibition of vHPC-mPFC pathway would not affect avoidance behavior in the EPM. To test if unilateral inhibition of vHPC-mPFC is sufficient to disrupt anxiety behavior, a new cohort of wildtype mice were unilaterally injected with Arch under the CamKIIa promoter and an optical fiber was implanted in the ipsilateral mPFC. The same behavioral protocol as in the bilateral inhibition was repeated. As predicted,

unilateral vHPC terminal inhibition did not affect avoidance behavior in the EPM (Figure 2B).

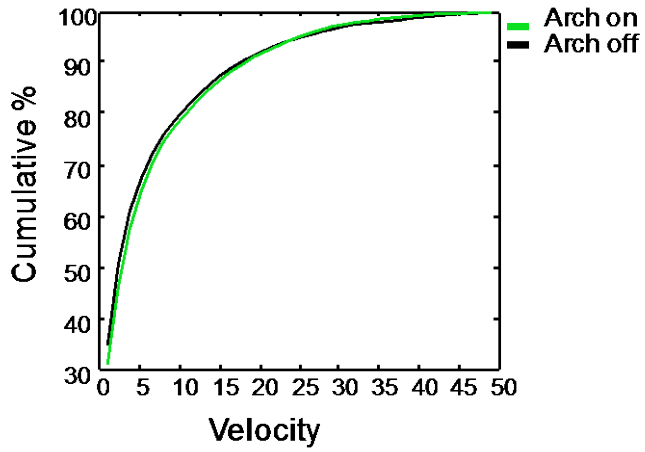

Figure 4 : Inhibition of vHPC input to the mPFC does not affect velocity
Cumulative histogram of average velocity during bilateral terminal inhibition in the EPM for Arch expressing mice (n=10).

Given that vHPC has been implicated in contextual fear (Maren and Holt, 2004), one potential caveat of these results is that the reduced open arm time is a consequence of disrupted contextual/spatial integration rather than a decreased in anxiety behavior.

To address this potential caveat, we measured additional behavioral variables that indicate changes in anxiety-like behavior. We examined head dips in the open arms and the duration of open arm visits. The number of head dips over the open arm edge is

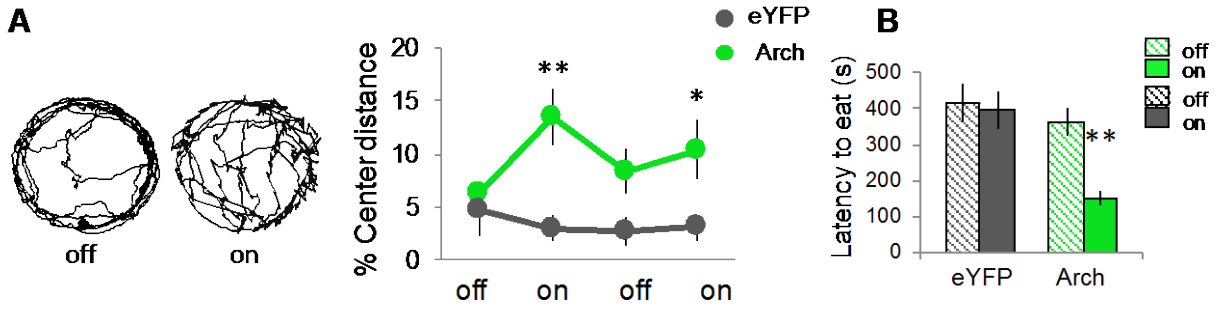

Figure 5 Selective inhibition of hippocampal-prefrontal input disrupts avoidance behavior in the OF and NSF: (**A**) Paths for an example mouse during laser off and on in the open field (Arch n=10; eYFP n=10; Two-way ANOVA interaction of light and virus $F_{(1,39)}$=5.84 p<0.05 ; T-test **p<0.01*p<0.05). (**B**) Latency to eat pellet in novelty suppression feeding test (Arch n=8; eYFP n=9; Two-way ANOVA interaction of light and virus $F_{(1,33)}$=4.66 p<0.05, Paired & unpaired t-test **p<0.01

associated with anxiety behavior in the EPM (Rodgers and Johnson, 1995). We reasoned that if spatial representations alone were disrupted, without altering anxiety per se, the mice would continue to avoid head dips and make rapid exits from the open arms, despite bilateral inhibition of the vHPC-mPFC pathway. However, bilateral inhibition of the vHPC-mPFC pathway increased both the total number of head dips and the frequency of head dips per unit time spent in the open arms; unilateral inhibition had no effect on these measures, as expected (Figure 2C-D). Similarly, bilateral, but not unilateral, inhibition increased the duration of open arm visits (Figure 2C-D). Terminal illumination in eYFP-expressing mice had no effect on either behavior. These findings suggest that with bilateral (but not unilateral) terminal inhibition, mice fail to treat the open arms as aversive. In addition, bilateral inhibition of vHPC terminals in the mPFC also decreased center avoidance in the open field test (Figure 5A) and decreased latency to eat in the novelty suppression feeding test (Figure 5B), only in the Arch group.

To control for the non-specific effects of decreased excitation in the mPFC, Arch was used to inhibit inputs from the mediodorsal nucleus of the thalamus (MD) (Figure 6A). The strength of MD inputs onto mPFC neurons approximates that of vHPC inputs (Little and Carter, 2012). Bilateral inhibition of MD inputs to the mPFC had no effect on open arm avoidance (Figure 6B), suggesting that the behavioral effects of vHPC terminal inhibition are not solely due to a non-specific decrease in excitatory input.

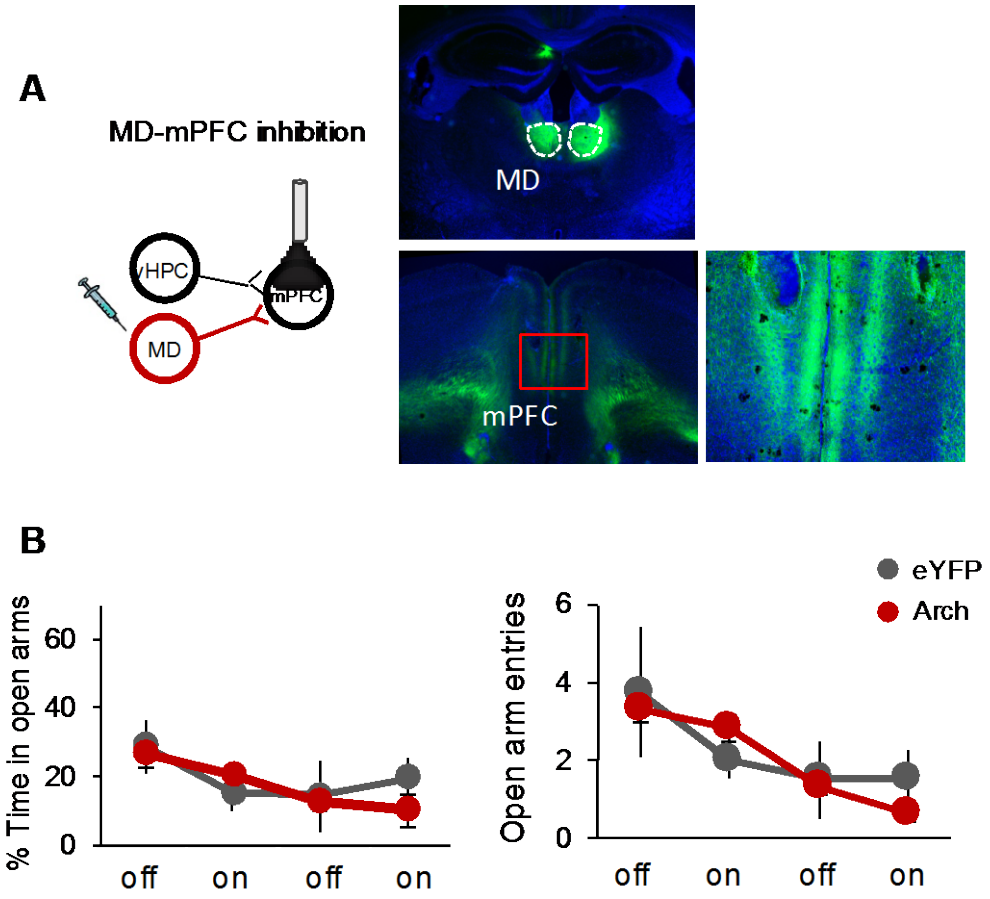

Fig 6: Selective inhibition of MD thalamic-prefrontal input does not affect avoidance behavior. (A) Left, schematic of bilateral inhibition of the mediodorsal thalamus (MD). Right, example expression of eYFP-tagged Arch flourescence in cells in the mediodorsal thalamus (MD, top) and terminals in the mPFC (bottom), after MD viral infection. Red square in bottom left indicates region shown magnified in bottom right. White scale bar is 1 mm. (B) Right, time spent in open arm, and (left) Open arm entries in MD Arch- and eYFP-expressing animals (Arch n=7; eYFP n=4; p=0.90). Error bars, +/- s.e.m. throughout.

2.3 Discussion

The findings described here demonstrate that the direct vHPC-to-mPFC pathway is necessary for anxiety-related behavior. The implications of these findings, particularly in terms of the extended BLA-vHPC-mPFC circuit, are discussed below.

The experiments reported here demonstrate that the direct vHPC-mPFC pathway is necessary for anxiety-like behavior as measured in the EPM, OF and NSF anxiety assays. These behavioral effects were not due to non-specific decreased of excitatory input to mPFC, as inhibiting the MD input did not affect anxiety. This work is consistent with a recent study demonstrating that blocking neuronal gap junctions between vHPC and mPFC decreased anxiety-like behavior (Shoenfeld et al., 2014). Interestingly, unilateral inhibition of vHPC-mPFC pathway did not affect avoidance behavior, suggesting that one functional hemisphere is sufficient to carry out the role of vHPC-mPFC during anxiety. Disruption of the the BLA-to-vHPC pathway also results in decreased anxiety-like behavior (Felix-Ortiz, et al., 2013). This suggests that aversive task-relevant information could be indeed upstream of vHPC and might go from the BLA to vHPC to the mPFC.

vHPC-mPFC pathway beyond innate anxiety

In addition to innate forms of anxiety, such as those tested in the EPM and OF, learned fear also engages the vHPC-mPFC circuit. In learned fear paradigms, silencing the vHPC, similar to the BLA, disrupts both the expression (during fear recall) and suppression (during extinction recall) of fear (Maren and Holt 2004; Sierra-Mercado et al., 2011). These reports suggest that the role of the vHPC during learned fear may be more complex than during innate anxiety, as it is pro-fear during fear recall, but anti-fear after extinction has occurred (Sotres-Bayon et al. 2012).

The role of vHPC-mPFC pathway is not exclusively aversive processing. Our group has recently reported that inhibiting of vHPC-mPFC during a spatial working memory task results in decreased performance. This indicates that this pathway carries information that is relevant for both emotional and cognitive processing. It remains to be determine if distinct subsets of vHPC mPFC-projecting neurons mediate the effects of the pathway in emotional and cognitive processing. Discussion in chapters 2-3 will expand more on the type of information that vHPC-mPFC carries during a working memory task vs the EPM.

Finally, it can be concluded that, as hypothesized, the direct hippocampal projection to the mPFC is necessary for anxiety-like behavior. The subsequent chapters discuss physiological changes that could explain the change in anxiety behavior.

2.4 Methods

Surgical Procedures: For the EPM experiments, mice were unilaterally or bilaterally infected (n = 29 and 23, unilateral and bilateral, respectively) with either AAV5 CamKIIa-eArch3.0-eYFP or AAV5 CamKIIa–eYFP into the vHPC under isoflurane anesthesia. 200 nl of 10 12 vg/ml virus was pressure-injected through a glass micropipette. In each hemisphere, six injections were done at -3.10 and at -3.30 AP levels for a total of 12 injections per hemisphere. At each AP level, the six injection sites were ±2.90, -4.0; ±2.90, -1.65; ±3.30, -3.60; ±3.30 -1.7; ±3.70, -3.2; ±3.70, -2.5 (ML and DV, respectively). Coordinates are in mm relative to Bregma (AP, ML) or brain surface (DV). All viruses were obtained from the University of North Carolina Vector core. Virus was infused at a

rate of 100 nl/min. Using this protocol, we have recently demonstrated that vHPC terminal inhibition in the mPFC decreases vHPC stimulation-evoked firing rates by approximately 40% in vivo (Spellman et al., 2015). 6–8 weeks after viral infection, mice for the EPM experiment, were implanted with electrodes and optical fibers in a second surgery, also under isoflurane anesthesia. Stereo-optrodes were implanted in the mPFC (AP -1.60 ML ±0.4 DV -1.25). Each stereo-optrode was comprised of a 230 um optical fiber glued to a bundle of 14 tungsten wire (13 mM diameter) stereotrodes placed 400–500 mm below the end of the optical fiber. 75 mM diameter tungsten wire LFP electrodes were implanted in the BLA (AP -1.80, ML ±3.16, DV -4.10) and the CA1 region of the vHPC (AP -3.30, ML ±3.30, DV -3.60). A reference screw was implanted in the skull over the frontal cortex and a ground screw in the skull over the cerebellum.

For the MD experiments, AAV5-hSyn-eArch3.0-eYFP or AAV5-hSyn-eYFP was used. 200 nl volume of [10 12 vg/ml] virus was injected into the MD of 15 mice (AP -1.2, ML ± 0.35, DV -3.2). Eleven mice were used to determine the effects of bilateral MD-mPFC inhibition on avoidance behavior (Figure 6).

EPM behavioral protocol: Behavior 5–7 days after electrode microdrive implantation, mice were food restricted to 80% of pre-operative weight and habituated to the opto/electrical tether in a small dark wooden box (20x3x30 cm) as they foraged for food pellets. On the fifth day of habituation, after 1 hr rest, mice were placed in the EPM under 300 lux illumination. Five mice were excluded from behavioral analysis for having less than 3 s of exploration in the open arms throughout the duration of the experiment. Behavior in the EPM was hand scored to ensure consistency of analysis. A mouse was

said to be inside an open or closed arm if all four paws were inside the arm. Head dips were defined as the full head of mouse coming out of open arm borders; this head-dipping behavior is quantified and described in Rodgers and Johnson (1995). The laser output was controlled using Neuralynx Trial Control (Neuralynx) to deliver constant 532 nm light at 10 mW (measured at the tip of the optical fiber) every 2 min.

To test additional anxiety assays a cohort of 17 mice was injected with AAV5 CamKIIa-eArch3.0-eYFP or AAV5 CamKIIa-eYFP and implanted with bilateral optical fibers in mPFC (see Surgical Procedures for coordinates). After 7 to 8 weeks of viral expression, the mice were tested in the open field (25 cm radius, 40 cm high) under 80 lux illumination for 8 min with the same laser protocol as the EPM. For the novelty-suppressed feeding test, animals were food restricted for 24 hours and were place in a 40×60 cm brightly lit arena (200-250 lux) with a food pellet in a diameter filter paper placed in the center. The trial was terminated either when an animal began chewing or 600 seconds transpired. Immediately after terminating the trial, animals were then placed in their home cage and the amount of food consumed in 5 minutes was measured (home cage consumption), followed by an assessment of post-restriction weight. Percentage body weight lost during food deprivation prior to the testing was assessed to ensure both groups lost similar amounts of weight, and home cage consumption immediately after testing was assessed as a relative measure of hunger (mg pellet consume/mouse weight). The task was repeated twice on different days for each mouse, counterbalanced for light stimulation (ON) or no stimulation (OFF). Percentage body weight lost during food deprivation prior to the testing was assessed to

ensure both groups lost similar amounts of weight, and home cage consumption immediately after testing was assessed as a relative measure of hunger (mg pellet consume/mouse weight). Neither variable was affected by illumination in either eYFP or Arch animals.

Statistics: To test significance of behavioral changes, two-way repeated-measures ANOVAs with post hoc, Bonferroni-corrected t tests were used.

Chapter 3: The role of the vHPC input to mPFC in the representation of aversion in mPFC

The work in this chapter is published in Padilla-Coreano et al., 2016 *Neuron*

3.1 Introduction

In the previous chapter I presented evidence that ventral hippocampus (vHPC) input to medial prefrontal cortex (mPFC) is necessary for anxiety behavior. What necessary information may the vHPC input be relaying to the mPFC? The hippocampus (HPC) is well known for having a spatial representation of the environment, specifically “place cells” in the dorsal HPC fire when animals are in a specific field location. The representation of spatial information exists throughout the HPC, although the size of the fields increases dramatically in the vHPC and the place cells are weaker (Kjelstrup et al. 2009; Royer et al. 2010). Evidence from human hippocampal imaging suggests that the anterior hippocampus (the human homolog of the vHPC) responds to negative valence more than positive valence (Gerdes et al. 2010; Sterpenich et al. 2014). A recent publication showed that vHPC units that fire to specific arm-types (open vs closed arms) during the EPM are more likely to project to the mPFC than other brain regions (Ciocchi et al. 2015). These units in the vHPC are said to represent arm-type during the EPM.

The mPFC is known for being involved in cognition and top-down regulation of emotions. In many types of behavioral paradigms there is task-relevant information represented by mPFC (Burgos-Robles, Vidal-Gonzalez, and Quirk 2009; Jones and Wilson 2005). Neurons in mPFC indeed show task-modulation tasks ranging from fear learning, working memory and appetitive and addiction related tasks (Jones and Wilson 2005; Peters, Kalivas, and Quirk 2009; Sotres-Bayon and Quirk 2010). During fear conditioning, mPFC neurons increase firing to the conditioned stimulus, that mPFC response is dependent on BLA activity (Sotres-Bayon et al. 2012). Similarly, the input

from BLA to mPFC is necessary for anxiety-like behaviors (Felix-Ortiz et al. 2016). Lesioning or inactivating the mPFC decreases anxiety-like behavior in rodents (Shah et al. 2003; Shah et al. 2004). These results suggest that mPFC neurons encode important aversive information that mediates anxiety responses.

Single units in the mPFC represent spatial aversion in the elevated plus maze (EPM), some cells fire in open/aversive arms while others fire in closed/safe arms. This representation of aversion correlates with the animal's anxious behavior suggesting that the representation is important for the behavior (Adhikari et al, 2011). Both the BLA and vHPC are possible inputs that could contribute to this representation in the mPFC.

Interestingly, mPFC units that are synchronized with vHPC theta (4-12 Hz) preferentially represent arm-type in the EPM (Adhikari et al. 2011); suggesting that vHPC input, directly or indirectly, is necessary for this aversive representation. Given the high degree of interconnectivity in the vHPC-mPFC-BLA circuit complicate the picture, as BLA input to both mPFC and vHPC could contribute information for the arm-type representation. Is the direct vHPC-to-mPFC pathway required for this arm-type representation? Here, we specifically test the role of the direct projection from the vHPC in the mPFC representation of valence in the EPM by inhibiting the vHPC terminals while assaying mPFC activity during the EPM. We found that the spatial representation of aversion in mPFC is abolished during inhibition of vHPC.

3.2 Results

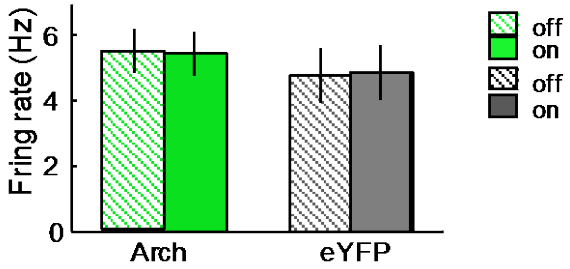

Figure 1: Inhibition of hippocampal-prefrontal input does not change overall firing rate. Overall firing rate in the EPM during light on or off epochs (Arch: n=82 and eYFP: n=46).

To address the role of vHPC input in mPFC single-unit activity, we turned to unilateral inhibition. Aversion in the EPM is determined by arm-type; the strength of mPFC representations of arm-type varies with avoidance behavior (Adhikari et al. 2011). The behavioral effects of the bilateral inhibition could confound physiological findings. To eliminate this confound, mPFC single-unit activity was recorded during unilateral inhibition of the vHPC-to-mPFC pathway in an additional cohort. As shown in the previous chapter, unilateral vHPC terminal inhibition did not affect avoidance behavior. Thus, unilateral inhibition has the potential to separate the physiological and behavioral effects of disrupting the vHPC-mPFC circuit.

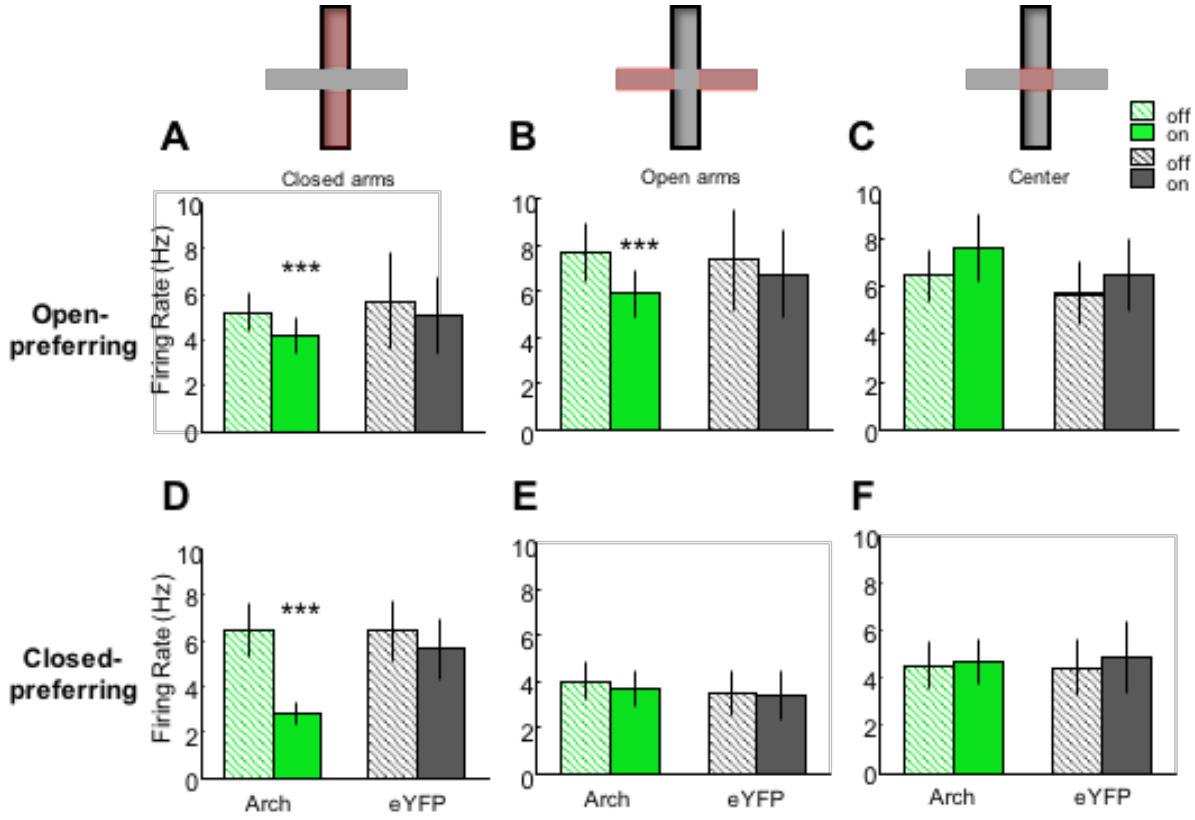

Fig 2: **Inhibition of hippocampal-prefrontal input decreases mPFC neuronal firing rates in the preferred arms.** Open arm preferring cell firing in closed arms(Arch: n=42, p<0.001; eYFP: n=26, p=0.46; Wilcoxon sign rank paired test), in open arms (**B**) (Arch: n=42, p<0.001; eYFP: n=20, p=0.55; Wilcoxon sign rank paired test), and center (**C**). (**D-F**) Firing rate for closed-preferring units in the closed arms (**D**) (Arch: n=40, p<0.001; eYFP: n=20, p=0.12), open arms (**E**) and center (**F**).

Inhibition of vHPC-mPFC pathway did not change overall firing rate of mPFC singe-units (Figure 1) or for putative interneurons or pyramidal neurons (data not shown).

To further examine the contribution of vHPC input toward mPFC unit activity during EPM exploration, task-related firing rates were examined. Each unit was classified as open- or closed-arm preferring, depending on where the firing rate was highest for that unit. Although net firing rate did not change, firing rates in the preferred arm type decreased with vHPC inhibition for both open- and closed-preferring units (Figure 2), suggesting that the net effect of vHPC input during the EPM is excitatory.

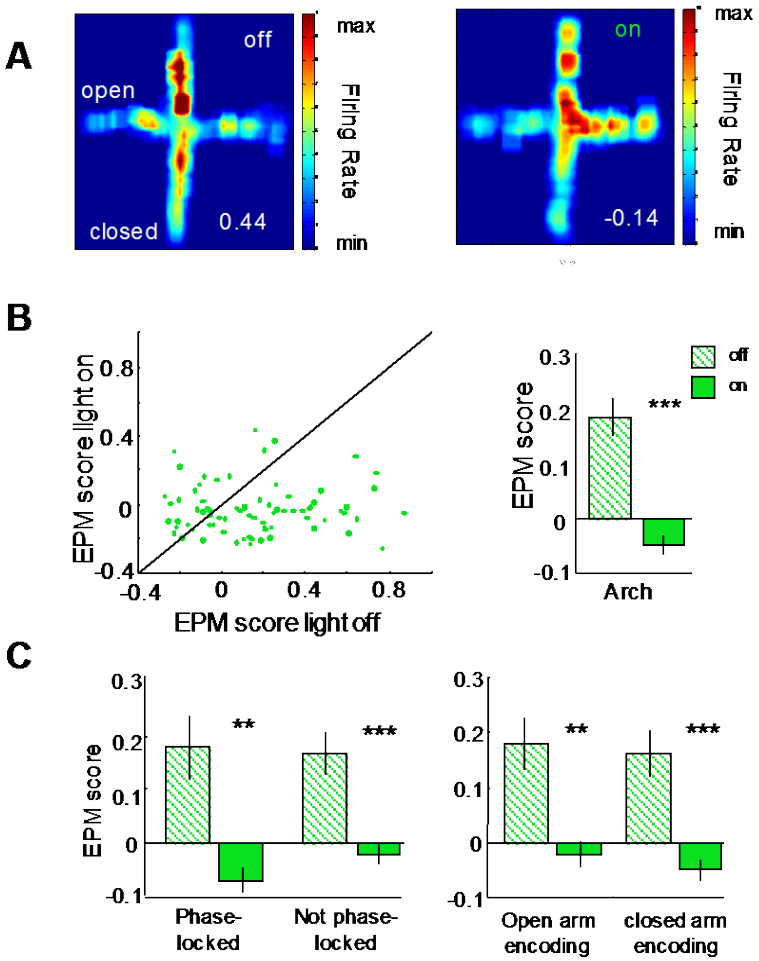

Fig 3: Unilateral inhibition of hippocampal-prefrontal input disrupts single unit representations of arm type in the mPFC. (**A**) Firing rate map as a function of light for an example mPFC single unit. Top, light off; Bottom, light on. (**B**) Strength of representation of arm type (EPM Score, see text) during light on vs light off epochs, for all mPFC single units from Arch mice. Right, mean EPM score as a function of light for units from Arch mice (n=82, p=4.1e-07, Wilcoxon sign rank. (**C**) Mean EPM score as a function of light for units characterized by significant phase-locking to vHPC theta (left) or by preferred arm type (right). **p<0.01, ***p<0.001; Wilcoxon sign rank paired test.

To address if vHPC input is necessary for spatial representations of aversion, we also turned to unilateral inhibition. Aversion in the EPM is determined by arm-type (Adhikari et al. 2011). Unilateral inhibition of vHPC-mPFC inputs abolished the representation of aversion in mPFC single units, as measured by the EPM score, which reflects arm-type selectivity (see Experimental Procedures; Figures 3A-B). Mean EPM score was decreased regardless of whether the units were significantly phase-locked to vHPC theta or whether they fired preferentially in the open or closed arms (Figure 3C). Terminal illumination in mice expressing eYFP only did not affect EPM scores (Figure 4A). Moreover, the decrease in arm-type representation was not simply due to a non-

specific loss of excitation, since inhibiting the MD-mPFC pathway did not affect EPM scores (Figure 4B). Altogether, these findings suggest that direct vHPC inputs provide patterned excitation that is required for mPFC spatial representations of aversiveness in the EPM.

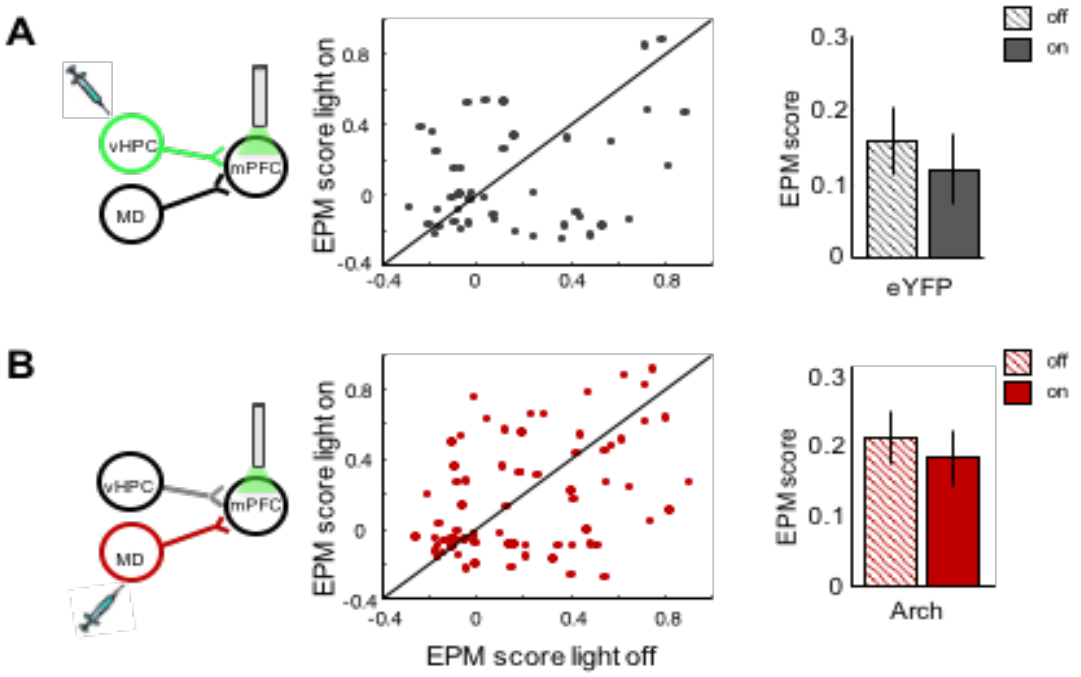

Fig 4: Disruption of arm-type representations requires active inhibition and is input specific. (**A**) Effect of unilateral mPFC illumination on EPM scores in mice expressing eYFP in vHPC (n=48, p=0.44, Wilcoxon sign rank paired test), or Arch in MD. (**B**) (n=74, p=0.68; Wilcoxon sign rank paired test).

However, mPFC neurons can represent task-relevant information in a variety of tasks. To determine whether vHPC input is important for mPFC representations of a similar, but non-aversive context, a modified neutral plus maze was created. In this maze, all four arms were fully enclosed, and the two types of arms were marked by different visual patterns (see Methods). An additional cohort of mice was injected in vHPC and

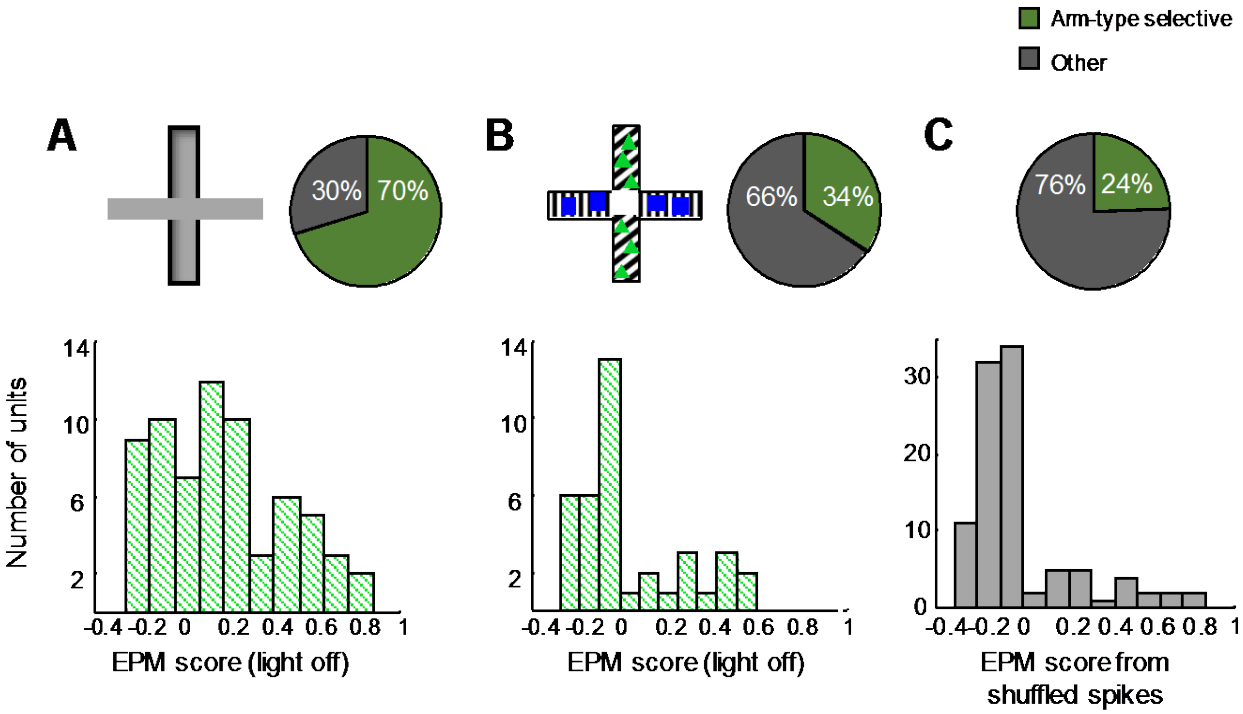

Fig 5: Arm-type representations in an aversive vs. non-aversive environment . (A-C) Distribution of arm-type representation in the standard EPM (**A**), a modified, non-aversive maze (**B**), and 100 EPM scores generated from randomly shuffled spikes from the standard EPM data (**C**). Top, schematics of mazes, and percentage of cells with EPM scores > 0 ("arm-type selective," orange). Bottom, full distribution of EPM scores for each condition. The distributions in **A** and **B** are significantly different from each other (Standard EPM, n=64; non-aversive, n=40; Kolmogorov-Smirnov test p=0.002). The distribution in **B** and **C** are not significantly different from each other (Kolmogorov-Smirnov test p=0.63).

implanted with optrodes in mPFC and recorded during exploration of this neutral maze. Mice did not display a preference for either arm type (58% ± 12% and 42% ± 12% time spent in each arm type, respectively; p = 0.40). Importantly, mPFC units only weakly represented arm-type in this neutral maze compared to the the EPM (Figure 5A-B). Moreover, the EPM scores in the neutral maze were not statistically different from EPM scores generated from shuffled spikes (Figure 5C), suggesting that mPFC representations of arm-type in this neutral maze are minimal. Even so the representation in this non-avesive maze is minimal, inhibition of the vHPC-to-mPFC pathway decreased the mean EPM scores significantly (Figures 6).

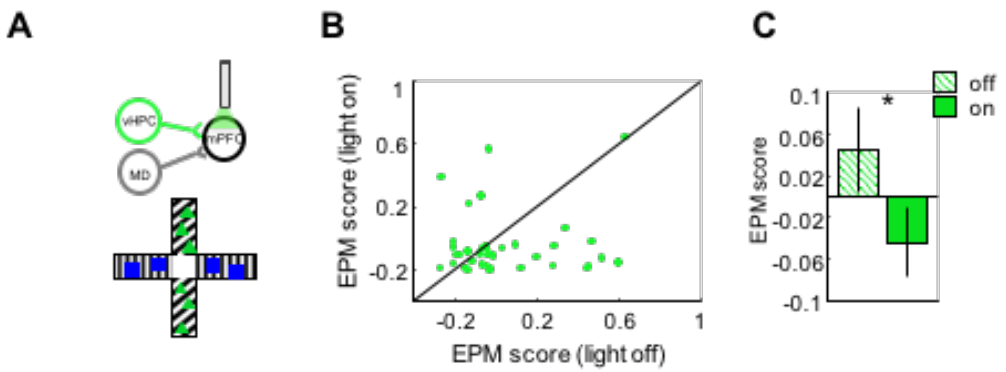

Figure 6: **Inhibition of vHPC-mPFC input in a non aversive environment.** (**A**) Schematic of unilateral vHPC-mPFC inhibition in the modified maze. (**B**) Scatter plot of EPM scores for individual single units with and without illumination in the neutral maze. (**C**) Mean EPM score of mPFC units with and without unilateral inhibition of vHPC-mPFC (Arch n=40 units, sign rank *p<0.05).

This result suggested the possibility that the EPM score effects seen in the standard EPM are due to overall lost of spatial information rather than lost of aversive information. To test if vHPC input disrupted overall spatial information in mPFC single units, we computed the spatial information for each unit. This computation is standard in the field of place cells, and it measures how much firing is explained by location, thus how much spatial information a cell contains (Markus et al. 1994). Inhibition of the vHPC-to-mPFC pathway during the EPM did not affect spatial information in mPFC single units (Figure 7). Altogether, these results suggest that spatial information in mPFC does not rely in vHPC input unless it is aversive related information (like arm-type in the EPM).

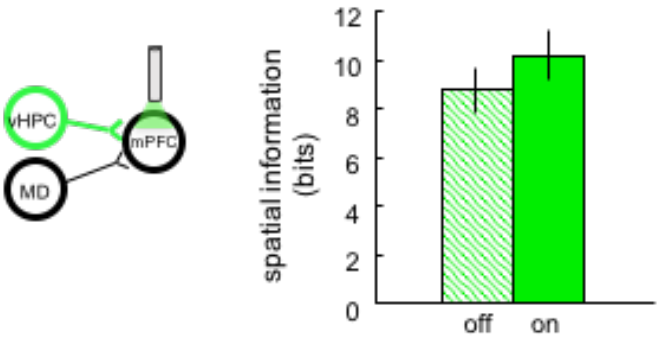

Figure 7 Inhibition of vHPC-mPFC does not disrupt overall spatial information in an aversive environment. Spatial information during EPM for the Arch group (n=64; sign rank p>0.05)

3.3 Discussion:

The experiments reported here show that inhibition of the direct vHPC input ablated the representation of aversive and non-aversive context within the mPFC. However, mPFC units encode negative valence; neurons that fire in response to bright, enclosed arms also fire in response to open arms in the dark (Adhikari et al. 2011). Moreover, terminal inhibition altered additional behavioral measures of valence, independent of arm choice (see Chapter 1), suggesting that vHPC inputs are crucial not just for spatial representations but also for the anxiety valence. This result is consistent with recent findings during a working memory task, in which the representation of goal location was disrupted by the same manipulation (Spellman et al. 2015). It is possible that in the working memory task the representation of goal location is positive valence, while in the EPM the arm-type representation consists of negative valence. Thus, the vHPC input to mPFC could convey necessary task-related valence information.

Whether this valence is constructed in the mPFC with the help of vHPC input or is present in the vHPC itself is unclear. A recent report demonstrates that mPFC-projecting vHPC neurons preferentially encode arm type in the EPM, while very few have well-defined place fields (Ciocchi et al. 2015). However, this study did not test if

the arm-type encoding at the level of vHPC represented valence or contextual differences of the closed vs open arms. On the other hand, evidence from human fMRI imaging suggests that the anterior hippocampus (the human homolog of the vHPC) responds to negative valence (Gerdes et al. 2010; Sterpenich et al. 2014). These findings suggest the possibility that vHPC inputs indeed convey valence information to the mPFC. Where might the vHPC get information about valence? It could come from the BLA, given the demonstration that optogenetic inhibition of BLA terminals within the vHPC also disrupts anxiety-like avoidance behavior (Felix-Ortiz et al. 2013).

As discussed in the previous chapter, in addition to innate forms of anxiety, learned fear also engages the vHPC-mPFC circuit. However, it is possible that the influence of vHPC input on mPFC unit activity may differ across anxiety and learned fear paradigms. Silencing the vHPC during learned fear recall results in increased mPFC single-unit responses to the conditioned stimulus (Sotres-Bayon et al. 2012), suggesting an inhibitory role for the vHPC projection. Here, inhibiting vHPC input resulted in decreased neuronal activity within a neuron's preferred arm, suggesting an excitatory role (Figure 2). These opposite results may be due to differences in experimental methods—Sotres-Bayon et al. (2012) used muscimol in the vHPC, which silences all projections, while here only those projections to the mPFC are inhibited. Alternatively, they may be genuine, task-related differences between learned and innate forms of anxiety. At least for innate anxiety, as demonstrated here, it does appear that the predominant effects of vHPC input are excitatory and, in particular, that this excitation boosts firing rates specifically in each neuron's preferred arm. These data are consistent with findings

during a spatial working memory task, which indicate that inhibiting vHPC terminals eliminates the boost in firing that occurs in mPFC neurons in their preferred goal locations (Spellman et al. 2015).

3.4 Methods:

For general surgical procedures and behavioral protocol please see methods listed in Chapter 1. For the MD experiments, AAV5-hSyn-eArch3.0-eYFP or AAV5-hSyn-eYFP was used. 200 nl volume of [10 12 vg/ml] virus was injected into the MD of 15 mice (AP -1.2, ML ± 0.35, DV -3.2). Four of those mice were used to determine the effects of unilateral inhibition on arm type representations in mPFC neurons (Figure 4B). The mice utilized in the unilateral experiment underwent training and testing in a spatial working memory task 4 weeks prior to the exposure to the EPM. For the non-aversive maze experiment (Figures 5-6), an EPM under 100 lux illumination was modified such that all arms were closed. The walls of two arms were covered with vertical stripes and blue squares while the walls of the other two arms were covered with diagonal stripes and green triangles (58% ± 12% and 42% ± 12% time spent in each arm type, respectively; $p = 0.40$).

Data Acquisition: Electrophysiological data were acquired using a Digital Lynx system (Neuralynx). LFPs were referenced to a screw located in the skull over the frontal cortex/olfactory bulb, band-pass filtered (1–1,000 Hz), and acquired at 2 kHz. Unit recordings were band-pass filtered at 600–6,000 Hz and acquired at 32 kHz; spikes were detected by thresholding and sorted off-line. Initial automated spike sorting was done based on peak, energy and principal component analysis, using Klustakwik (Ken

Harris, UCL) instantiated in SpikeSort3D (Neuralynx); clusters were subsequently manually confirmed. Isolation distance and L-ratio were computed as described in Schmitzer-Torbert et al. (2005). The median Isolation distance for the single-unit clusters was 26, and the median L-ratio was 0.08.

Single-Unit Analysis: Only units with at least 100 spikes for each light condition were included. Firing rate analysis was also conducted for putative interneurons versus pyramidal neurons, separated as previously described (Spellman et al. 2015). The EPM score was calculated for each single-unit as previously described in Adhikari et al. (2011) (EPM Score = (A -B)/(A + B); where A = 0.25x(|FL-FU| + |FL- FD| + |FR –FU| + |FR –FD|) and B = 0.5x(|FL-FR| + |FU-FD|). FL, FR, FU, and FD are the percentage difference from mean firing rate in left, right, up and down arms, respectively). Only mice that explored each of the four arms on both light conditions for at least 4 s were included in the EPM score analyses. Firing rates for different compartments of the EPM was calculated as total spikes in that compartment divided by the time mouse spent in the compartment. To test the significance of phase-locking strength, EPM score, and firing rate analyses, the non-parametric Wilcoxon sign rank or rank-sum tests were used. To calculate information content (Figure 7), the EPM was divided into 9 bins. Time spent in each bin was calculated for each animal and the following equation was computed for each single unit:

$$\Sigma P_i(R_i/R)\log_2(R_i/R)$$

Where Pi is the probability of being in bin i, Ri is firing rate in bin I and R is mean firing rate for that single unit.

Statistics: To determine light effects on power correlations, cross-correlations, firing rate, MRL, EPM score, PPC, and gamma power, Wilcoxon (sign rank) paired tests were performed. The sign rank test does not assume normality in the data and is meant for paired samples. To determine fold changes or percentage changes in PPC and Granger lead strength, Wilcoxon one-sample tests were performed. To determine if the distributions of EPM scores (Figure 5) were different from each other, Kolmogorov-Smirnov tests were performed. Finally, to determine light effects on the behavioral results, repeated-measures two-way ANOVAs were performed along with post hoc Bonferroni corrected t tests.

Histology: Recording sites were histologically confirmed by visual examination of electrolytic lesions. Lesions were induced immediately before perfusions by passing current through an electrode at each implanted site (50 mA, 20 s). Perfused and fixed tissue was then sectioned and mounted with DAPI Fluoromount-G mounting medium (Southern Biotech). Native fluorescence of Arch and eYFP was imaged using an epifluorescence microscope.

Chapter 4: The role of the vHPC input to mPFC in theta synchrony in the vHPC-mPFC-Amygdala circuit

The work in this chapter is published
in Padilla-Coreano et al., 2016 *Neuron*

4.1 Introduction:

A growing body of evidence shows that functional connectivity between mPFC, BLA and vHPC are an important feature in fear and anxiety states (Lesting et al. 2011; Likhtik et al. 2014; Courtin et al. 2014). Some of that evidence comes from recording local oscillations. Brain oscillations are generated from periodic fluctuations in the excitability of a group of neurons. The synchronized changes in membrane potential create an extracellular current which can be measured by recording the local field potential (LFP) (Buzsáki 2002; Buzsáki and Watson 2012). Theta-frequency oscillations (4-12 Hz) in the local field potential were first described in the dorsal hippocampus (dHPC) during navigation (Vanderwolf 1969), and have been more recently implicated in anxiety behaviors.

Anxiety states are distinguished in particular by an increase in theta-frequency (4-12 Hz) synchrony in the amygdala-hippocampal-prefrontal circuit. Theta oscillations in the vHPC, and not the dHPC, increase in relative power during anxiogenic environments (Adhikari et al. 2010). Moreover, the relative power of theta in increases during anxiety and the strength of theta explained the avoidance behavioral variance (Adhikari et al. 2010). Theta power in the vHPC and mPFC correlate stronger during anxiety compared to a baseline non-aversive environment. The vHPC has a direct projection to the mPFC that could potentially mediate the increase in theta power correlation seen during anxiety.

The high degree of interconnectivity in the vHPC-mPFC-BLA circuit and presence of multiple interacting oscillatory activity patterns complicate the picture. Theta-frequency

synchrony between the vHPC-BLA and BLA-mPFC is also enhanced during innate forms of anxiety (Lesting et al. 2011; Likhtik et al. 2014; Stujenske et al. 2014). Moreover, optogenetic inhibition of the projection from the BLA to the vHPC is anxiolytic (Felix-Ortiz et al. 2013). While theta power is increased with anxiety, fast gamma power is decreased, both in the BLA and mPFC (Stujenske et al. 2014). Even so, coupling between theta and gamma oscillations within the BLA is enhanced by anxiety (Stujenske et al. 2014). Finally, anxiety state modulates the directionality of oscillatory interactions between the mPFC and BLA, such that relative safety is associated with a shift toward enhanced mPFC influence over the BLA in both theta- and gamma-frequency ranges (Likhtik et al. 2014; Stujenske et al. 2014). These findings emphasize the degree to which each of these three structures functions within an interconnected, interacting circuit. What then might be the role of an individual element within such an interactive circuit? We sought out to test the hypothesis that the direct ventral hippocampal projection to mPFC is necessary for the anxiety-related theta synchrony. To do so, we optogenetically inhibited the vHPC-mPFC pathway while simultaneously recording LFPs from the mPFC,vHPC and BLA during a safe environment and during exposure to the elevated plus maze (EPM). Inhibition of vHPC terminals decreased theta synchrony in a task-, frequency- and pathway-dependent manner.

4.2 Results:

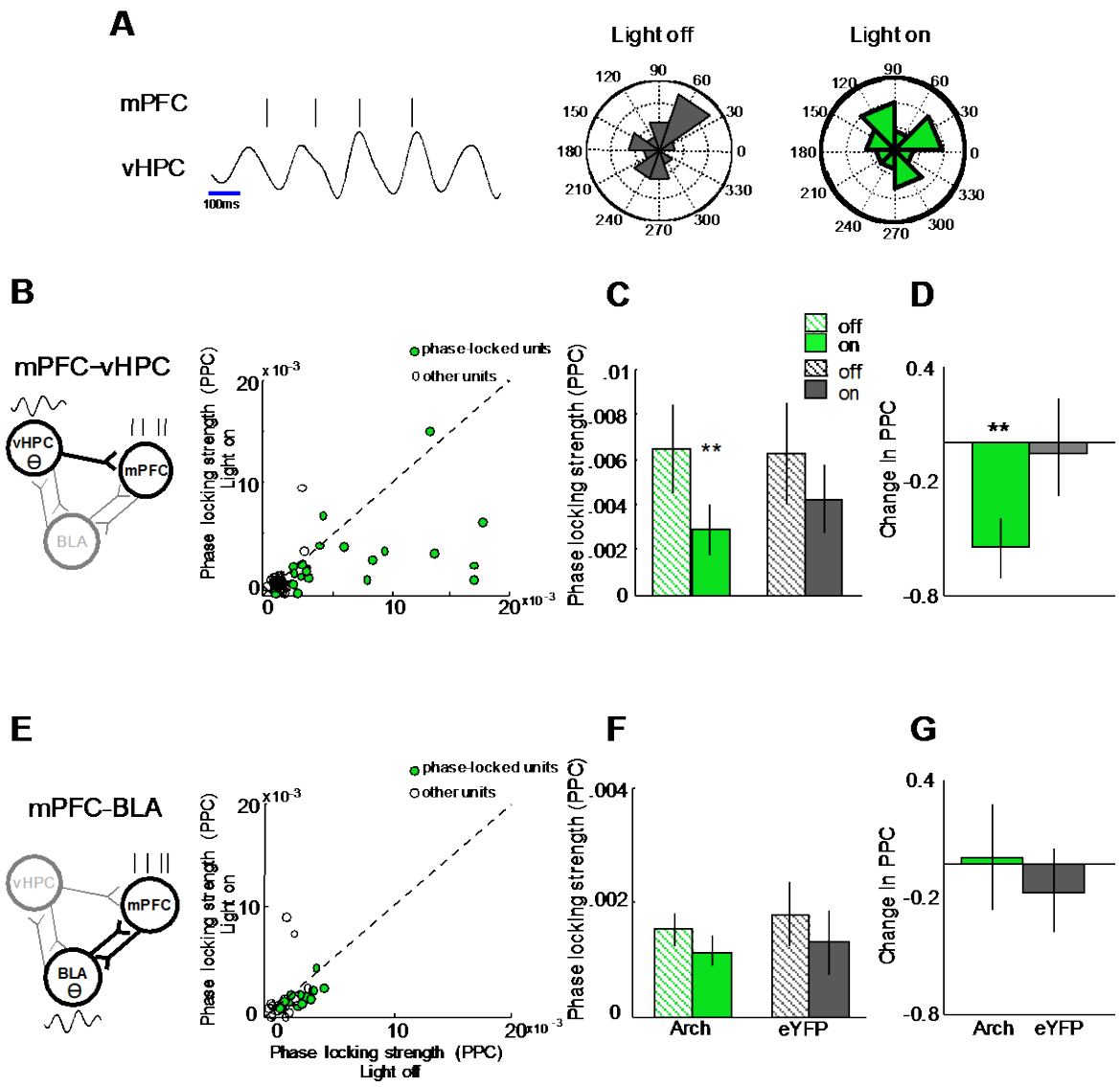

Fig 1: Inhibition of hippocampal-prefrontal input disrupts synchrony of mPFC units to vHPC but not BLA theta (**A**) (Left) Representative raster plot of mPFC unit spiking in phase with simultaneously recorded vHPC theta oscillation; (Right) Distribution of vHPC theta phases on which this unit spiked during light off and light on epochs. Outer ring indicates 30% of spikes. (**B**) Strength of phase locking (pairwise phase consistency; PPC) of mPFC units to vHPC theta with light on and light off; Arch animals only; n=76. Green circles, significantly phase-locked units ($p<0.05$, Rayleigh's test). (**C**) Phase locking strength as a function of light for significantly phase-locked Arch and eYFP units (**$p=0.007$, Wilcoxon sign rank test; total recorded Arch: n=76; eYFP: n=75). (**D**) Normalized change in phase locking with illumination (significantly different from zero Arch $p=0.0015$, eYFP $p=0.97$, Wilcoxon sign rank). (**E-G**) As in **B-D**, for phase-locking of mPFC units to BLA theta (total recorded Arch: n=44; eYFP: n=22).

The effects of bilateral vHPC-mPFC terminal inhibition on activity and synchrony within the extended vHPC-BLA-mPFC circuit were examined by recording single units in the mPFC and local field potentials (LFPs) in the mPFC, BLA, and vHPC. LFPs predominantly reflect summed synaptic activity within a brain region (Buzsaki et al., 2012). The temporal relationship between spikes and/or LFP activity in one region and LFPs in another can be used as a measure of synchrony (Siapas, Lubenov, and Wilson 2005; Harris and Gordon 2015).

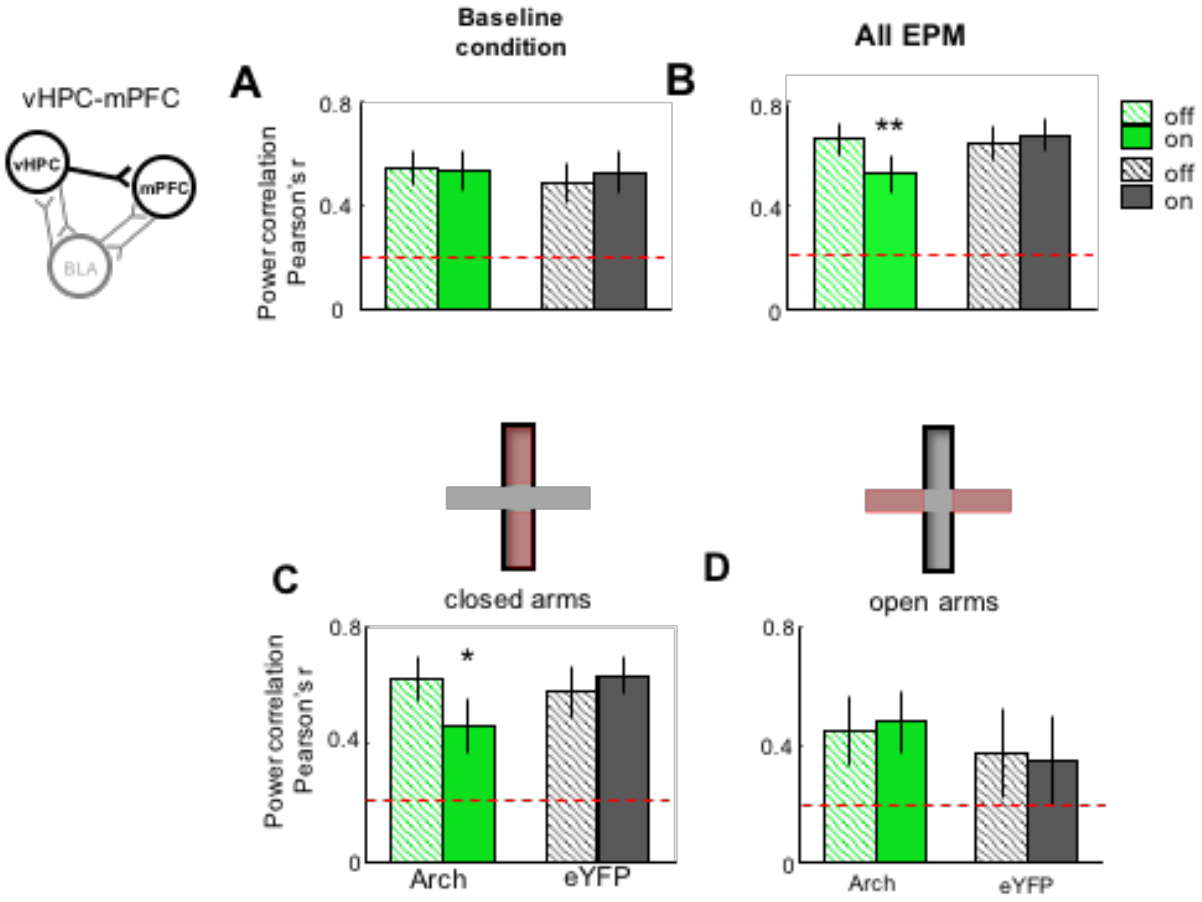

Fig 2: Terminal inhibition decreased theta power correlation in the EPM. (A) Power correlation in the theta-Frequency range between vHPC and mPFC in the baseline condition (n=10 for Arch p=0.84 and n=12 for eYFP; p = 0.27, sign rank test). Theta power correlations during EPM (**B-D**) (Arch n=10, p<0.01 Wilcoxon sign rank test & eYFP n=11); Theta power correlation calculated separately for data from the closed arms (C) and open arms (D).

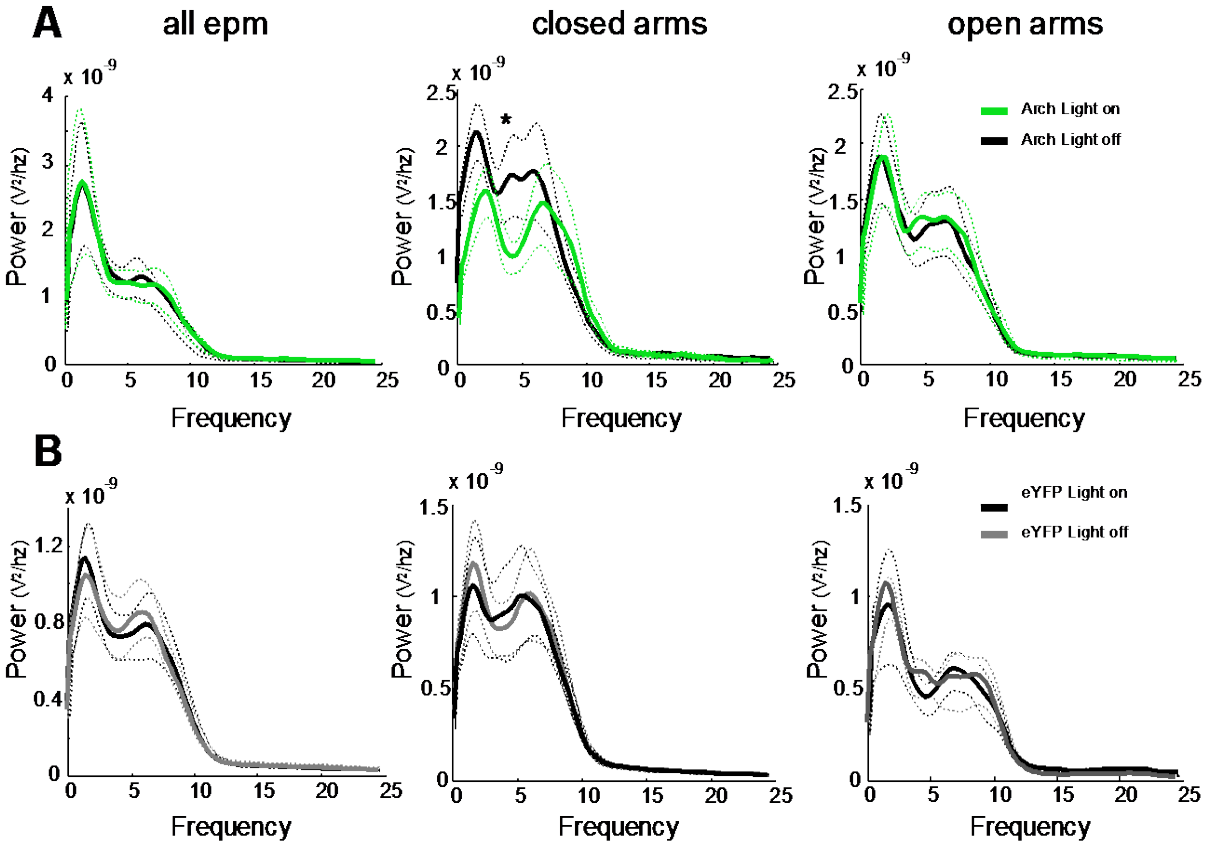

Fig 3: **vHPC Terminal illumination effects on oscillatory LFP Power in the mPFC. (A)** mPFC Power spectra by light condition for the Arch group (n=10) for active movement times (mean±sem). Power spectra were computed from the entire EPM session (left), as well as separately for time spent in the closed (middle) and open (right) arms. For the closed arm data only, Two way repeated measures ANOVA on the 0-12 hz frequency range revealed a main effect of light ($F= 6.2381_{(1,7)}$ $p<0.05$). Wilcoxon post hoc tests revealed an effect on 0-5 Hz Power ($p=0.03$) but not on 4-12 Hz Power ($p=0.37$). **(B)** As in (A), but for the eYFP (n=9) group.

Terminal inhibition in the EPM decreased synchrony in the theta-frequency range between the vHPC and mPFC, as measured by the strength of phase locking of mPFC spikes to theta oscillations in the vHPC LFP (Figures 2B-D). Phase locking of mPFC spikes to BLA theta was unaffected by terminal inhibition (Figures 2E-G), demonstrating pathway specificity of the vHPC terminal inhibition. However, phase-locking to BLA was considerably weaker than to vHPC, allowing for a possible floor effect. Unilateral

inhibition of vHPC-mPFC decreased phase locking of mPFC spikes to vHPC theta to a similar degree (Arch n = 16, p < 0.01; eYFP n = 11, p = 0.4258; Wilcoxon one-sample test).

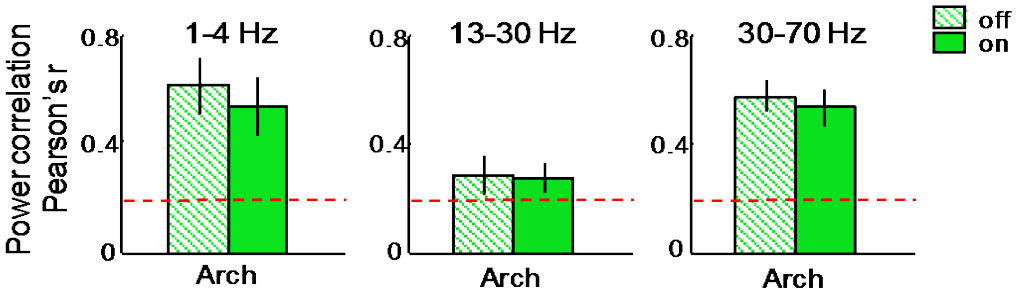

Figure 4: Inhibition of vHPC-mPFC pathway disrupts power synchrony in a frequency dependent manner Power correlations for vHPC and mPFC LFPs in the delta (1-4 Hz; Wilcoxon sign rank test p=0.13), beta (13-20 Hz) and slow gamma (30-70 Hz) frequency ranges during the EPM. Red line indicates critical value (p<0.05) for power correlations generated with shuffled data.

Synchrony was further examined using the LFPs recorded from each brain region. Consistent with decreased phase locking of mPFC spikes to vHPC theta, terminal inhibition decreased the correlation of theta power between the mPFC and vHPC (Figure 2B). This effect was specific to the closed arms of the EPM (Figure 2C-D), consistent with previous reports showing that theta power correlation is higher in the safe compartments of the task (Adhikari et al., 2010; Likhtik et al., 2014). Terminal inhibition had no effect on overall power in mPFC (Figure 3); therefore, this decrease in theta power correlation was not due to a decrease on theta power. Terminal inhibition had no effect on vHPC-mPFC theta power correlations in a familiar, non-aversive environment (Figure 2A), demonstrating task specificity. Terminal inhibition had no effect on coherence between vHPC and mPFC (data not shown). Interestingly, unilateral inhibition of vHPC did not result in decreased theta power correlation between vHPC and mPFC. Considering that phase locking to theta was decreased with

unilateral inhibition, this suggests that phase locking measurements are more sensitive than power correlation measurements.

The disruption in vHPC-mPFC theta power correlation was also frequency and pathway

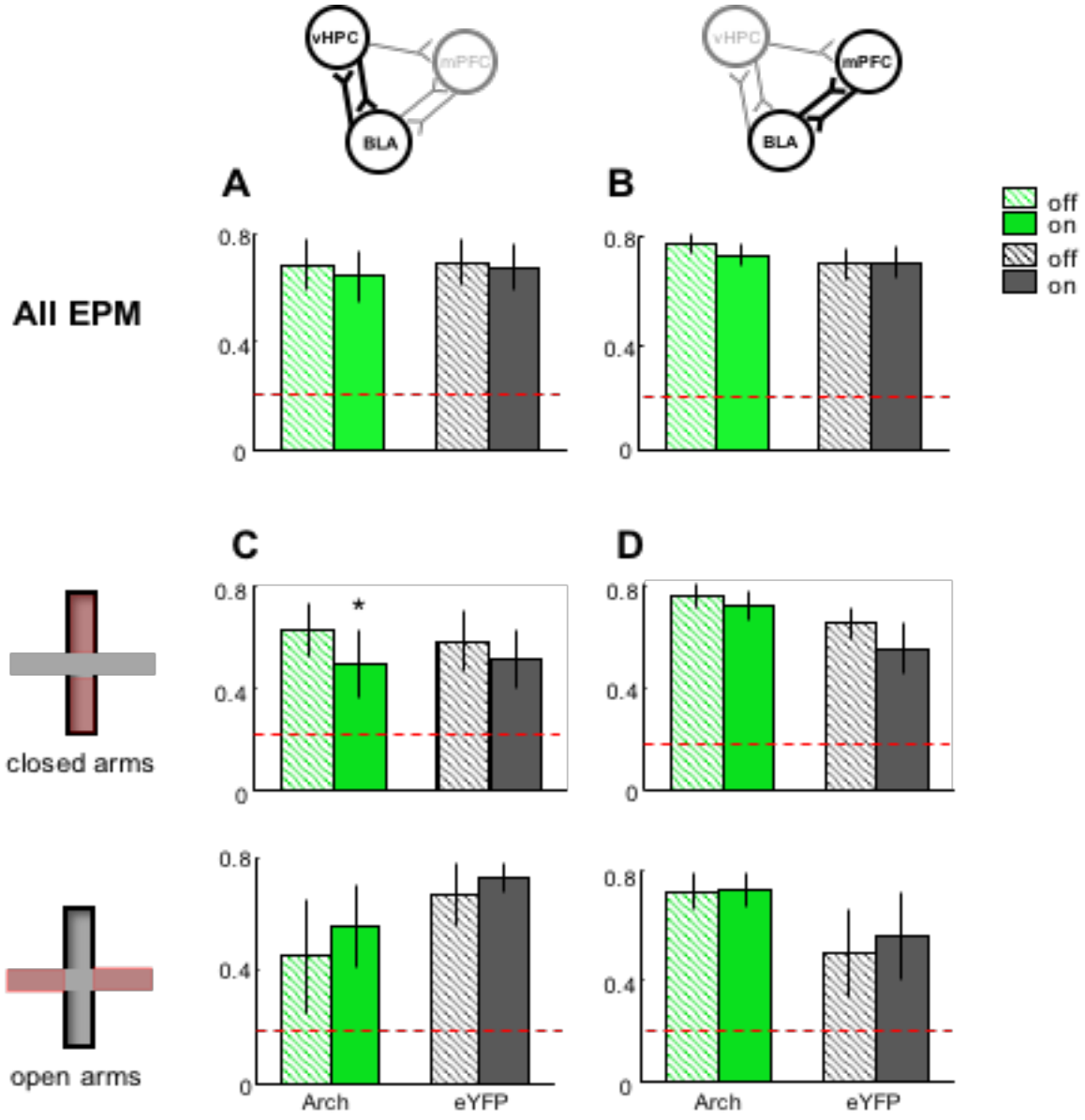

Figure 5: Inhibition of hippocampal-prefrontal input disrupts theta power correlation in a pathway-specific manner (**A-B**) Theta power correlation during the EPM for vHPC-BLA (**A**) (n=7 per group); and mPFC-BLA (**B**) (Arch n=7; eYFP n=6). (**C-D**) Theta power correlation calculated separately for data from the closed arms (top) and open arms (bottom) for the vHPC-BLA (**C**) (for closed arms p=0.0413 Wilcoxon sign rank test) and the mPFC-BLA (**D**). Red line indicates critical value (p<0.05) for power correlations generated with shuffled data.

specific. Inhibiting vHPC terminals did not affect mPFC-vHPC power correlations in the delta (1–4 Hz), beta (13–30 Hz), or slow gamma (30–70 Hz) frequency ranges (Figure 4). This frequency specificity is consistent with previous reports showing that anxiety does not modulate vHPC-mPFC synchrony in frequency ranges other than theta (Adhikari et al., 2010).

Overall mPFC-BLA theta power correlations were unaffected by vHPC-mPFC terminal inhibition (Figures 5B,D). Similarly, there was no overall effect on vHPC-BLA theta power correlations (Figure 5A), though a decrease in theta power correlation could be detected when analysis was restricted to data from the closed arms (Figure 5C). These findings reinforce the pathway specificity of the manipulation.

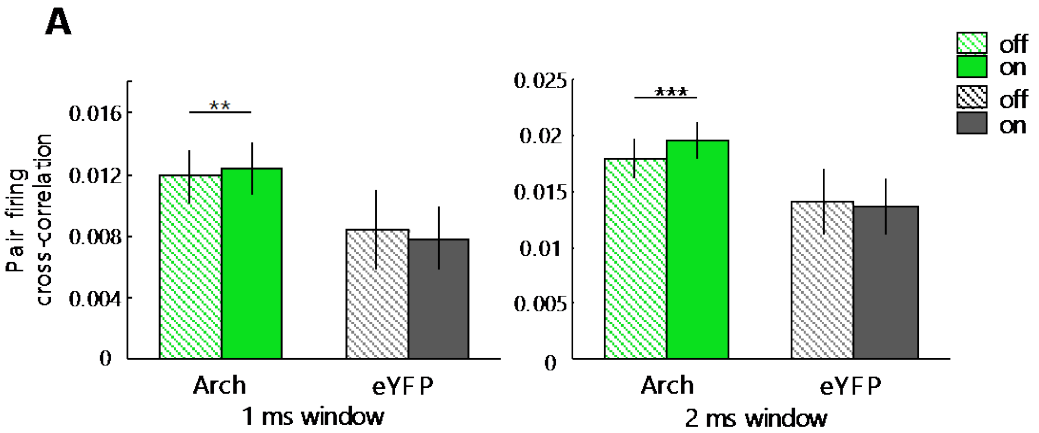

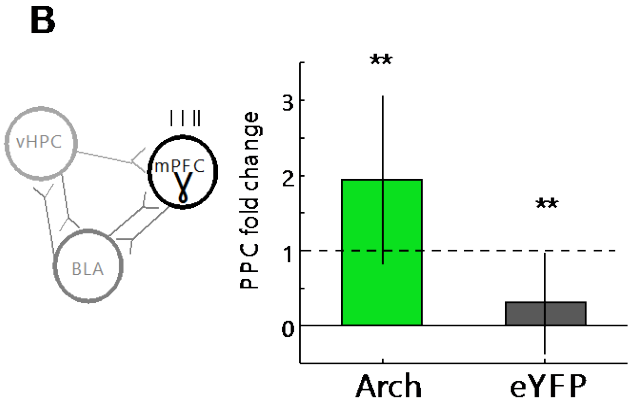

Figure 6: Inhibition of vHPC-mPFC pathway increases synchrony within the mPFC. (A) Cross-correlation of spikes during 1 ms window for mPFC simultaneously recorded single units pairs during the EPM (Arch n=842 p<0.01; eYFP n=416 p=0.26; Wilcoxon paired test). Cross-correlation of spikes during 2 ms window for mPFC simultaneously recorded single units during the EPM (Arch n=842 p<0.001; eYFP n=416 p=0.10; Wilcoxon paired test). **(B)** Fold change (ON/OFF) for phase locking strength to local fast gamma (Arch n=79 p<0.01; eYFP n=46 p<0.01; Wilcoxon one sample test).

Together, these findings demonstrate that terminal inhibition functionally disconnects the mPFC from the vHPC during anxiety-like behavior, particularly disrupting communication in the theta-frequency range. Interestingly, two measures of local synchrony within the mPFC were increased by terminal inhibition. Both correlated firing of simultaneously recorded mPFC single units (Figure 6A) and phase-locking of mPFC single units to mPFC fast gamma (70–120 Hz) (Figure 6B) were increased by illumination in Arch- but not eYFP-expressing animals. These findings raise the

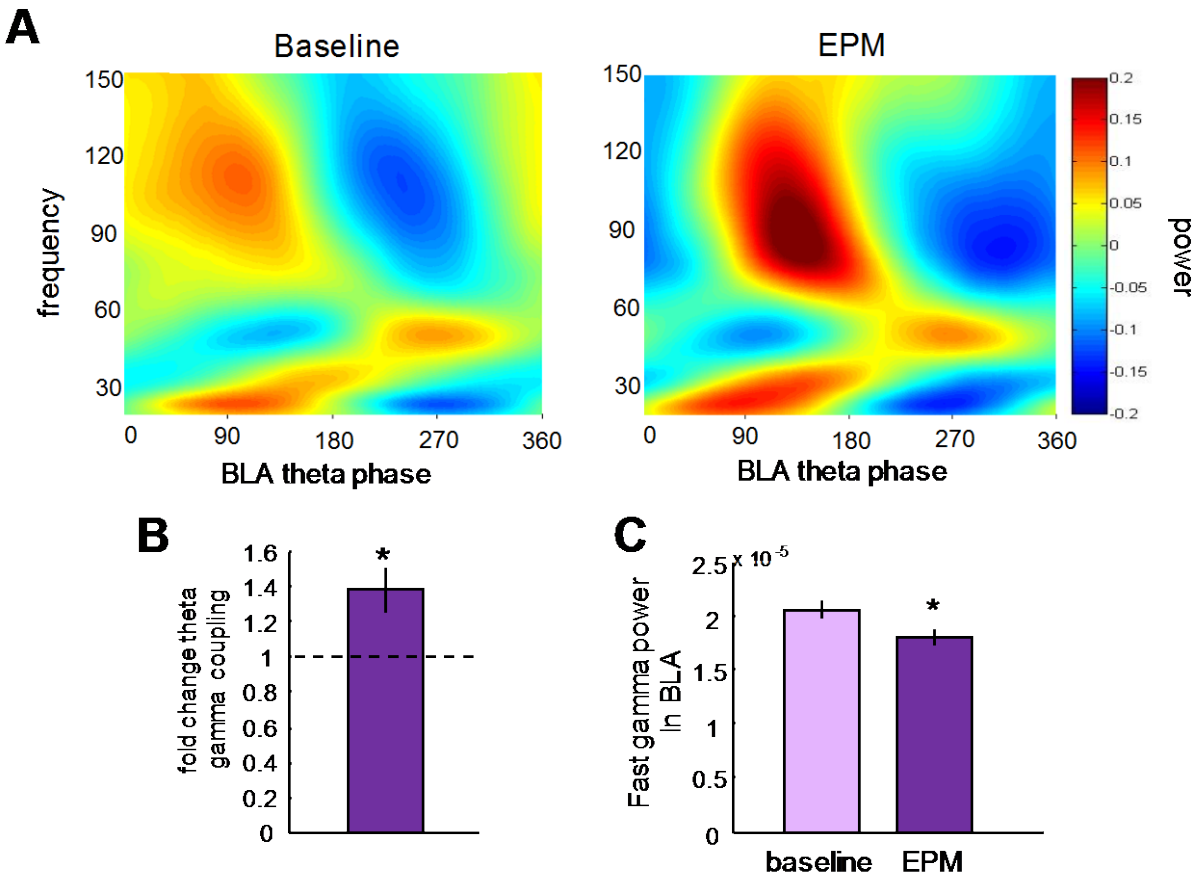

Figure 7: Theta-gamma coupling and fast gamma power are modulated during anxiety. (A) Example comodulogram of gamma power across theta phases in the BLA. **(B)** BLA theta and fast gamma (70-120 Hz) coupling fold change in EPM from baseline during light off condition (combined groups n=22; Wilcoxon paired test *p<0.05). **(C)** Fast gamma power in BLA during baseline and EPM light off (combined groups n=22; Wilcoxon paired test *p<0.05)

possibility that when decoupled from vHPC inputs, mPFC neuronal spiking synchronizes more strongly with local inputs.

We explored the effect of inhibiting vHPC-mPFC pathway on previously established markers of anxiety in the amygdala and mPFC LFPs. Fear conditioning and open field exposure induce characteristic patterns of neural activity in the BLA and mPFC (Lesting et al., 2011; Likhtik et al., 2014; Stujenske et al., 2014). Specifically, in addition to the increased theta activity and synchrony discussed above, the strength (power) of fast gamma-frequency (70–120 Hz) oscillations in the BLA and mPFC decrease during anxiety and increase during relative safety (Stujenske et al., 2014). Within the BLA, the strength of the relationship between theta- and gamma-frequency oscillations is increased with anxiety and decreased with relative safety (Stujenske et al., 2014). Accordingly, exposure to the EPM decreased fast gamma power and increased theta-gamma coupling compared to a baseline safe condition (Figure 7A-C). If inhibition of the vHPC-mPFC pathway is truly anxiolytic, we would expect that bilateral inhibition would reduce these physiological markers of anxiety. Indeed, bilateral terminal inhibition mimicked the effects of relative safety on each of these parameters. Bilateral inhibition increased the strength of gamma oscillations in the BLA and mPFC (Figure 8), inducing a shift in the directionality of gamma synchrony toward increased mPFC lead (Figure 8D). Bilateral inhibition also reduced the strength of coupling between theta and gamma oscillations within the BLA (Figure 8E). Unilateral inhibition, however, did not alter any of these parameters in the inhibited hemisphere (Figures 8F–H), nor did illumination in eYFP-expressing mice (data not shown).

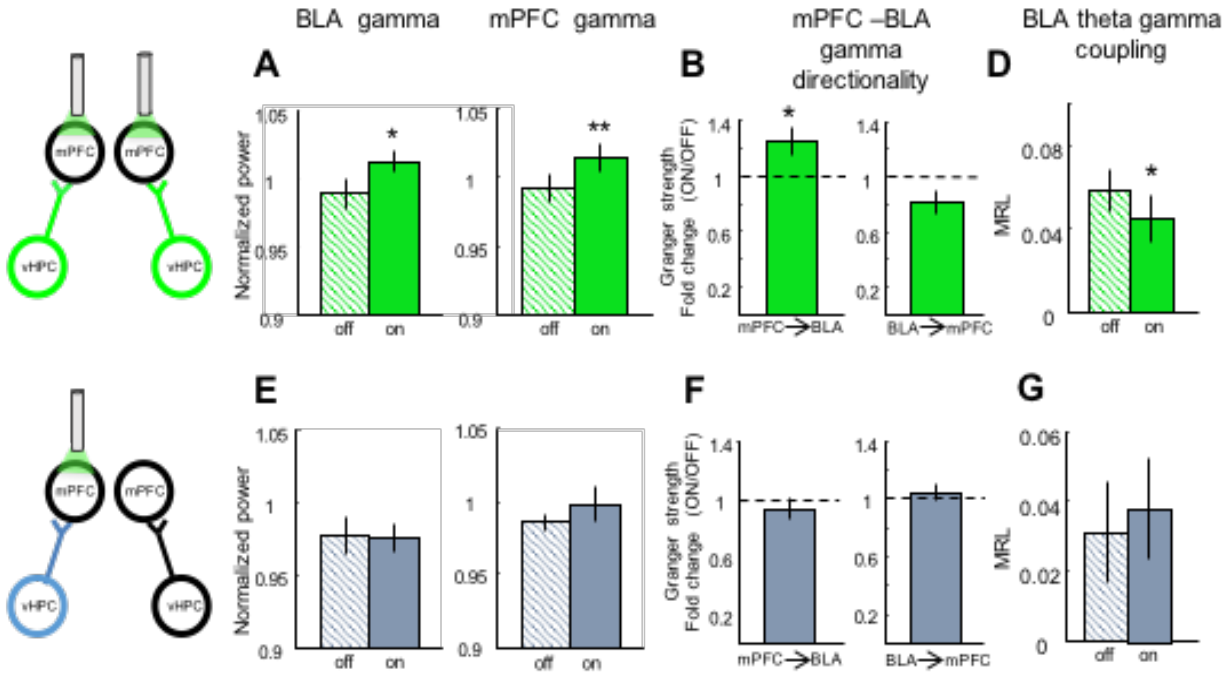

Fig 8: Physiological evidence of decreased anxiety during bilateral, but not unilateral, vHPC-mPFC inhibition. (A-C) Effect of bilateral (green, **C-E**) vs. unilateral (blue, **E-G**) terminal inhibition on fast gamma power in the BLA and mPFC (**A,E**) (*n=8, p=0.04; **n=10, p=0.009; Wilcoxon paired test) , Granger causality (*n=8, p=0.039, Wilcoxon one sample test) (**B,F**) and BLA theta/gamma coupling (**D,G**). (*n=8, p=0.01, Wilcoxon paired test).

4.3 Discussion:

The BLA, vHPC, and mPFC comprise a tripartite circuit in which each element is important for anxiety-like behavior. Silencing or lesioning any of these three structures alters avoidance behavior in tests such as the EPM (Jinks and McGregor 1997; K. G. Kjelstrup et al. 2002; Shah and Treit 2003; Bannerman et al. 2003). Similarly, optogenetically manipulating BLA inputs into the vHPC (Felix-Ortiz et al. 2013) or the mPFC (Felix-Ortiz et al. 2016) alters anxiety. However, these structures are intimately interconnected (Hoover and Vertes 2007; Pikkarainen et al. 1999), as evidenced by the remarkable degree of synchrony that arises during fear and anxiety behaviors (Adhikari et al. 2010; Lesting et al. 2011; Likhtik et al. 2014; Seidenbecher et al. 2003; Stujenske et al. 2014). Thus, manipulations of any one structure could alter activity patterns in any

other within the circuit; the specificity of such manipulations is questionable. Here we attempt to address this caveat by recording simultaneously from the three structures. Inhibition of the vHPC terminals within the mPFC was relatively specific, disrupting synchrony in the theta frequency range between the vHPC and the mPFC with minimal effects on theta synchrony between the BLA and either structure. Importantly, phase-locking of mPFC units to vHPC theta was reduced in both unilateral and bilateral silencing experiments, demonstrating that reduced theta synchrony is a primary effect of inhibiting vHPC input. By contrast, only bilateral inhibition had effects on BLA and mPFC gamma strength and synchrony, suggesting that these measures may be read-outs of the anxiety state rather than being causally involved in generating it.

The effects of terminal inhibition on vHPC-mPFC interactions were remarkably specific. Theta- synchrony was unaffected in a familiar, non-aversive environment, arguing that vHPC input is required for the increase in synchrony seen in the EPM; indeed, terminal inhibition completely wipes out the fold increase in power correlation from the familiar environment to the EPM (compare Figure S4BtoFigure S3). The effects of LFP synchrony were confined to the closed arms, consistent with our prior findings (Adhikari et al. 2010), suggesting that vHPC-mPFC interactions are particularly engaged during periods of active inhibition of exploration. We also found deficits in LFP synchrony were limited to effects on power correlations, without any effects on coherence. The phase-locking data presented here are therefore particularly important in demonstrating effective disruption of connectivity.

The experiments reported here also demonstrate that bilateral inhibition of vHPC-mPFC pathway decreased gamma power and theta-gamma coupling within the BLA. These two BLA physiological measurements correlate with defensive behavior in the OF and learned fear (Stujenske et al. 2014). Our experiments show that gamma power and theta-gamma coupling in the BLA are also modulated by exposure to the EPM. Unilateral inhibition of vHPC-mPFC did not affect gamma power and theta-gamma coupling in the ipsilateral BLA. This suggests that vHPC-mPFC activity is not necessary for this anxiety-related BLA gamma patterns, or that these BLA gamma patterns are upstream of the vHPC-mPFC activity. Interestingly, disruption of the the BLA-to-vHPC pathway also results in decreased anxiety-like behavior (Felix-Ortiz, et al. 2013). This suggests that aversive task-relevant information could be indeed upstream of vHPC and might go from the BLA to vHPC to the mPFC.

Conclusion:

A long literature links theta-frequency synchrony between the vHPC, mPFC, and BLA to both learned fear and innate anxiety (Adhikari et al. 2011; Lesting et al. 2011; Likhtik et al., 2014; Seidenbecher et al. 2003; Stujenske et al. 2014). Indeed, directly manipulating theta-frequency oscillations within the mPFC induces freezing, suggesting a causal relationship between theta and fear (Courtin et al. 2014). Here, inhibition of the vHPC-to-mPFC pathway disrupted theta-frequency synchrony between the two structures without affecting synchrony at other frequencies. This specificity is consistent with the frequency-specific increases in synchrony seen during anxiety (Lesting et al. 2011; Likhtik et al. 2014; Seidenbecher et al. 2003; Stujenske et al. 2014). Interestingly,

inhibition of this same vHPC-to- mPFC pathway during a working memory task had no effect on theta-frequency synchrony (Spellman et al. 2015); instead, low gamma (30–70 Hz) synchrony was specifically disrupted. These contrasting findings demonstrate the surprising result that a specific anatomical pathway can mediate synchrony at different frequencies depending on behavioral state.

4.4 Methods:

For surgical procedures please see methods in chapter 2.

Data Acquisition: Electrophysiological data were acquired using a Digital Lynx system (Neuralynx). LFPs were referenced to a screw located in the skull over the frontal cortex/olfactory bulb, band-pass filtered (1–1,000 Hz), and acquired at 2 kHz. Unit recordings were band-pass filtered at 600–6,000 Hz and acquired at 32 kHz; spikes were detected by thresholding and sorted off-line. Initial automated spike sorting was done based on peak, energy and principal component analysis, using Klustakwik (Ken Harris, UCL) instantiated in SpikeSort3D (Neuralynx); clusters were subsequently manually confirmed. Isolation distance and L-ratio were computed as described in Schmitzer-Torbert et al. (2005). The median Isolation distance for the single-unit clusters was 26, and the median L-ratio was 0.08.

Single-Unit Analysis: Only units with at least 100 spikes for each light condition were included. A given unit was said to be significantly phase locked if the distribution of the LFP phases where the spikes occurred was not uniform as assessed with Rayleigh's test for non-uniformity of circular data. Zero phase corresponds to the peak of the signal. Phase locking strength was quantified using pairwise phase consistency (PPC)

(Vinck et al., 2010). To calculate the power envelope and phase of ongoing theta and gamma oscillations, a band-pass filter for 4–12 Hz was used using a zero-phase-delay FIR filter with Hamming window (filter0, provided by K. Harris and G. Buzsaki, New York University, USA), the phase component was calculated by a Hilbert transform, and a corresponding phase was assigned to each spike.

LFP analysis: All data were analyzed using custom-written scripts in MATLAB (MathWorks). Power correlations were computed as previously described (Adhikari et al. 2010). Briefly, we determined power as a function of time using the multitaper method, with window sizes customized for each frequency range. Window sizes for the power correlation were 2.5, 1, and 0.125 s for theta (4–12 Hz), beta (13–20 Hz), and gamma (30–70 Hz) frequencies, respectively. Pearson's correlation was then used to measure the association between power across regions. Although power measurements are not normally distributed, power across vHPC and mPFC meets the criteria for multivariate normality (significant skewness and kurtosis); therefore, a pearson's correlation provides a complete description of the association. To determine the strength of power correlations that would be expected by chance, we randomly shuffled the time windows in one brain region 2,000 times, calculating a Pearson's correlation each time. From these random distributions, we identified the 95% critical value for each frequency range; these were remarkably consistent at r = 0.142 to 0.150 for each frequency,

averaging at 0.146 for theta, beta, slow, and fast gamma, and 0.147 for delta ranges. For open versus closed arm power correlation analysis, only mice that spent at least 3 s in each arm type during each light condition were included. Coherence of mPFC and

vHPC LFPs was estimated using the Welch method (mscohere function in MATLAB) with the same parameters used as for the power spectra. Fast gamma power was calculated for times the animal was in the closed arms of the EPM. LFPs from times spent in the closed arms of the EPM were filtered for 70–120 Hz, and power was calculated using a Hilbert transformation and normalized to fast gamma power throughout the session. To quantify theta-gamma coupling, we computed the mean resultant length (MRL) of fast gamma power as a function of theta phase for times spent in the closed arms of the EPM. Theta phase and gamma power were both calculated using the Hilbert transform. The MRL was chosen because of the observed unimodal relationship of theta phase-gamma amplitude coupling in gamma ranges and its higher statistical power compared to the non-parametric modulation index (Tort et al., 2009).

Granger causality analysis was performed as described in Stujenske et al. (2014) using arfit toolbox for Matlab. The strength of mPFC granger lead was calculated as GCImPFC/BLA=GCImPFC/BLA + GCIBLA/mPFC for each animal, and the strength of BLA granger lead was calculated as GCIBLA/mPFC= GCImPFC/BLA+GCIBLA/mPFC.

Histology: Recording sites were histologically confirmed by visual examination of electrolytic lesions. Lesions were induced immediately before perfusions by passing current through an electrode at each implanted site (50 mA, 20 s). Perfused and fixed tissue was then sectioned and mounted with DAPI Fluoromount-G mounting medium (Southern Biotech). Native fluorescence of Arch and eYFP was imaged using an epifluorescence microscope.

Chapter 5: Theta frequency oscillatory stimulation of vHPC terminals in mPFC increases anxiety-like behavior

The in-vitro physiology in this chapter was collected in collaboration by Sarah Canetta

5.1 Introduction

A growing body of evidence suggests that functional connectivity between the mPFC, BLA and vHPC plays an important role in fear and anxiety states (Lesting et al. 2011; Sotres-Bayon et al. 2012; Courtin et al. 2013; Likhtik et al. 2014). In particular, studies have seen increases in synchrony between local field potential oscillations recorded from these regions during fear and anxiety. These local oscillations (referred to as the local field potential or LFP) reflect an extracellular current which results from synchronized changes in the membrane potentials of local neurons (Buzsáki and Draguhn 2004; Buzsáki and Watson 2012).

Anxiety states are distinguished in particular by an increase in theta-frequency (4-12 Hz) synchrony in the amygdala-hippocampal-prefrontal circuit. In the elevated plus maze, a test of innate anxiety, mPFC and vHPC theta oscillations increase in power, and mPFC theta power correlates with avoidance behavior (Adhikari et al. 2010). Moreover, theta power correlations between the mPFC and vHPC increase during anxiety (Adhikari et al. 2010). During innate anxiety and retrieval of learned fear, oscillations in the mPFC and BLA increased in synchrony in the theta- and gamma-frequency ranges (Lesting et al. 2011; Likhtik et al. 2014; Stujenske et al. 2014; Karalis et al. 2016). Recently, we demonstrated that optogenetically inhibiting the ventral hippocampal (vHPC) input to the medial prefrontal cortex (mPFC) decreases anxiety-like behavior and theta synchrony between the mPFC and vHPC, without affecting other frequencies (Padilla-Coreano et al. 2016). While these data suggest that the theta-frequency may play a unique and specific role in relaying anxiety-related input between

the vHPC and mPFC, the evidence to support this hypothesis remains merely correlative.

To determine whether vHPC-mPFC activity, specifically in the theta frequency, plays a causal role in anxiety-like behavior, we tested whether optogenetically stimulating the vHPC terminals at a theta frequency was sufficient to increase avoidance behavior in the elevated plus maze (EPM). Moreover, we tested whether any such effects might be frequency-specific. To potentially mimic naturally occurring oscillations, we stimulated ChR2 with a sinusoidal waveform at 8 or 20 Hz, as well as with more typical 8 or 20 Hz pulsatile stimulation parameters. We found that stimulation of vHPC terminals increased avoidance behavior in a frequency- and pattern-specific manner.

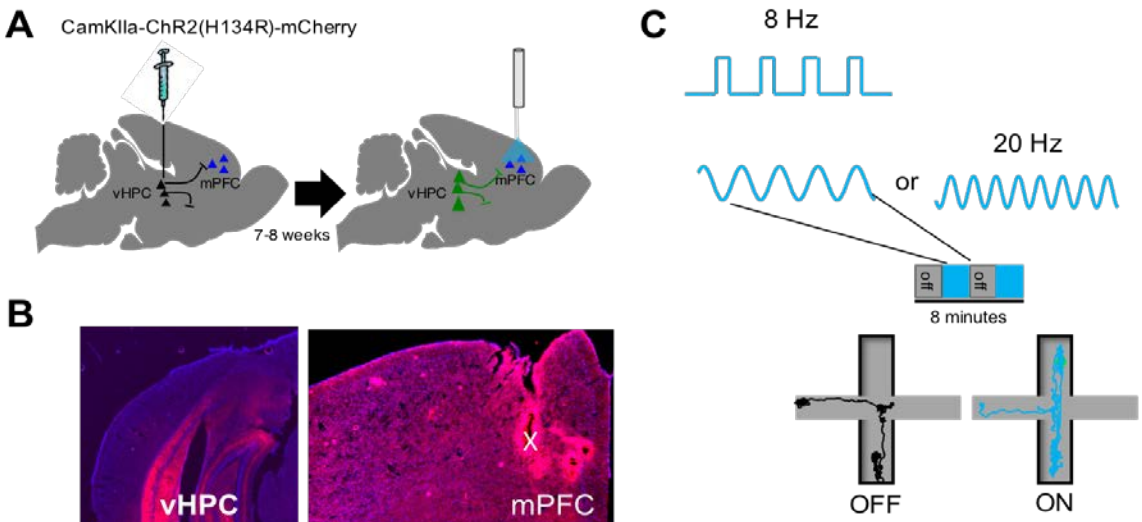

Figure 1: Experimental Protocol. (**A**) Schematic of viral injection and terminal illumination. (**B**) Coronal views of opsin fluorescence in vHPC somata (left) and terminals within the mPFC (right). White x indicates lesion location. (**C**) Illumination protocol and paths for an example mouse during laser off and on in the EPM.

5.2 Results

CamKIIa-ChR2(h134R)-mCherry was injected bilaterally in the vHPC and optical fibers implanted in the mPFC. Seven weeks after the injection we observed robust expression of ChR2 in mPFC terminals (Figure 1A-B). Mice were tested in the elevated plus maze (EPM) alternating the light off and on every two minutes (Figure 1C).

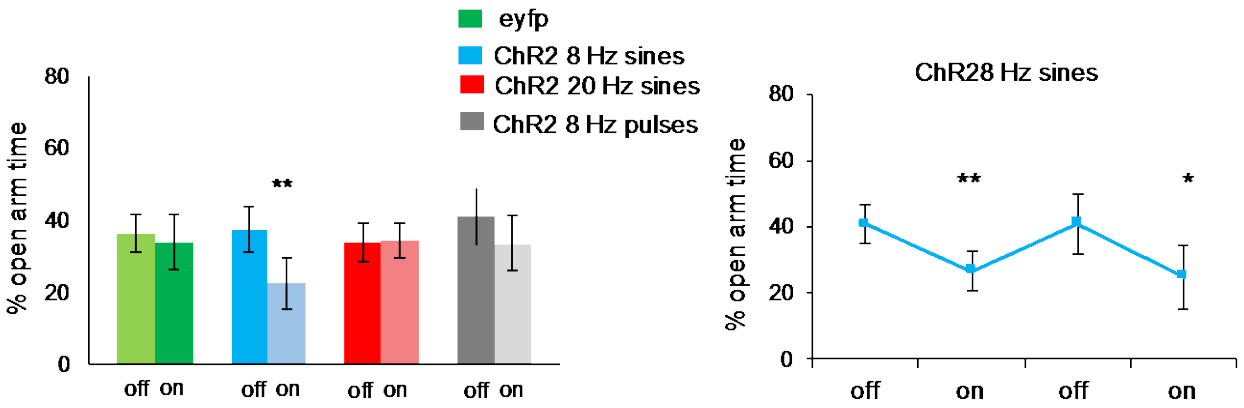

Figure 2: vHPC-mPFC stimulation with 8 Hz sinusoidal light increased avoidance behavior (**A**) Average % time spent in open arms across light off and on conditions (**p<0.01). (**B**) Percent open arm time for ChR2-injected mice during stimulation with 8 Hz sinusoids (n=12)

Stimulating the vHPC-mPFC pathway with a sinusoidal light pattern at 8 Hz significantly increased avoidance behavior in the EPM, while stimulating with brief pulses of light at 8 Hz or sinusoidal light at 20 Hz had no effect (Figure 2). These experiments demonstrate that the anxiogenic effect of vHPC terminal stimulation is frequency- (8 Hz but not 20 Hz) and pattern- (sinusoids but not pulses) specific. This result was surprising, as pulses of light are the most common light pattern used to stimulate neurons and terminals optogenetically and are thought to be most efficacious at activating neurons.

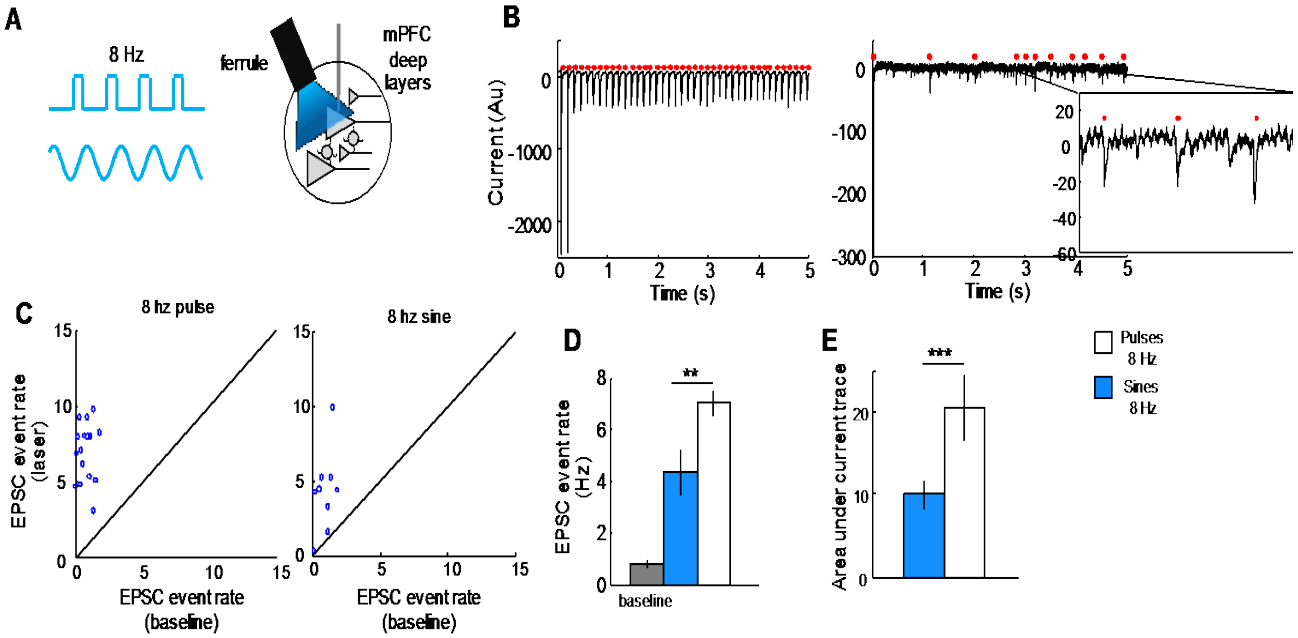

Figure 3: mPFC pyramidal post-synaptic responses to vHPC stimulation is weaker with sinusoids. A. Diagram of experimental protocol to stimulate vHPC terminals in mPFC. B. Left, example trace of an mPFC pyramida neuron's response to 8 Hz pulses. Right, example trace of an mPFC pyramida neuron's response to 8 Hz sinusoids. In red, EPSC events determined by 4 standard deviations from baseline. C. EPSC event rates for all recorded cells (two trials per recorded cell) during baseline and during laser. D. Average event rate during pulses and sinusoids at 8 Hz (Wilcoxon test $p<0.01$). E. Area under the laser induced-current trace for 8 Hz pulses and sinusoids (Wilcoxon test $p<0.01$).

To understand how pulses and sinusoidal light modulate mPFC neurons differentially, mPFC pyramidal neurons were recorded using *in vitro* slice whole-cell electrophysiology while stimulating vHPC terminals with the same sinusoidal or pulsatile patterns (Figure 3A). mPFC pyramidal neurons were held at -70 mV in voltage clamp, and light was delivered via a 200 um optical fiber placed adjacent to the 40x field of view. 8 Hz pulses evoked large, stimulus-locked post-synaptic excitatory currents, which were not seen with either the 8 or 20 Hz sin stimulation. Although robust stimulus-locked currents were only seen with 8 Hz pulsatile stimulation, 8 Hz sinusoidal stimulation did result in a significant increase in spontaneous-like EPSCs (Figure 3B-C). The mean rate of EPSCs during sinusoidal stimulation was lower than for pulsatile stimulation (Figure 3D).

Moreover, the EPSCs that occurred during sinusoids were smaller in size than pulse-evoked excitatory events (Figure 3E).

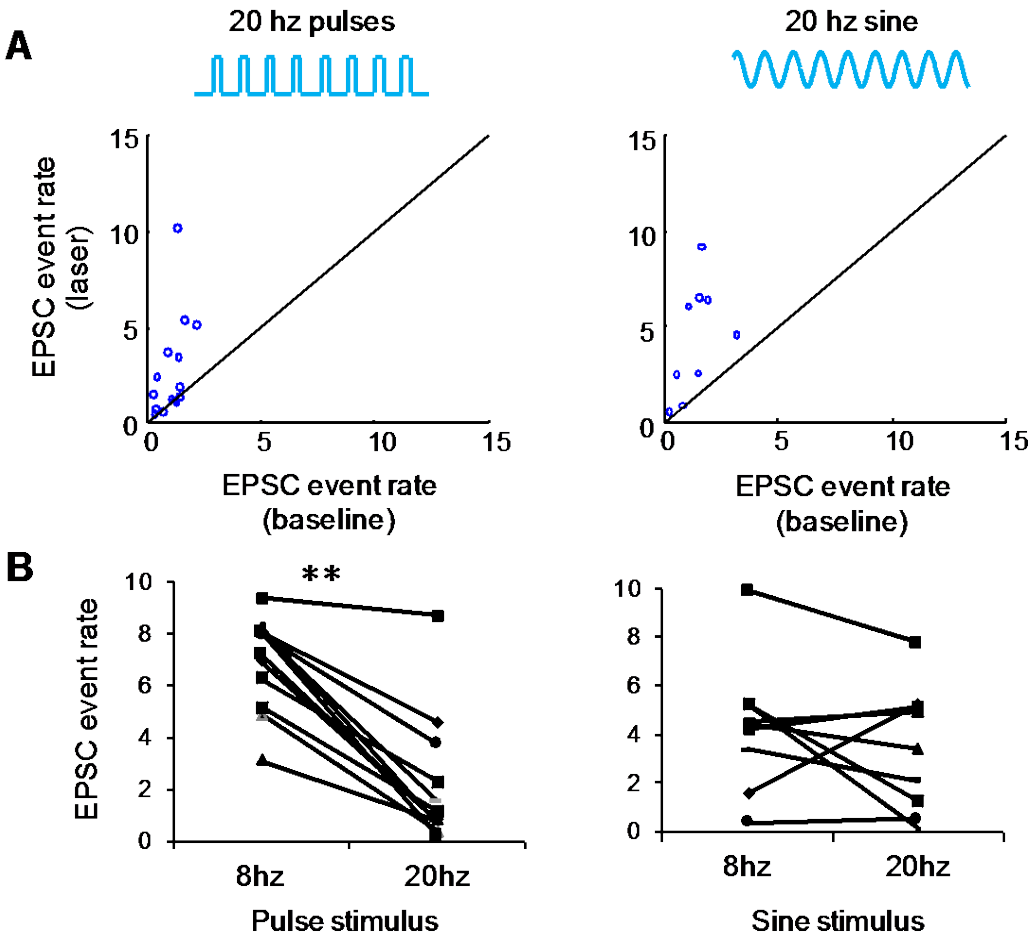

Figure 4: mPFC pyramidal post-synaptic responses to pulsatile stimulation are frequency dependent. A. Left, EPSC event rate for all recorded cells during baseline 20 Hz pulses. Right, EPSC event rate for all recorded cells during baseline and 20 Hz sinusoids. B. Left, Same cell comparison of event rate for pulses at 8 vs 20 Hz (paired t-test p<0.01), and for sinusoids at different frequencies (right).

To explore possible frequency-dependent effects, responses to 8 Hz and 20 Hz stimulation EPSCs event rate were compared within the same neuron. First, we calculated significant EPSCs event rate during baseline (prior to light onset) and during 20 Hz pulses or sinusoids (Figure 4A). The average EPSCs event rate during 20 Hz

pulses was weaker than 8 Hz pulsatile stimulation (Figure 4B). During sinusoidal there was no significant difference in the EPSCs event rate for 8 Hz vs 20 Hz, although 5 out of 9 cells decreased event rate during 20 Hz sinusoids compared to 8 Hz sinusoids (Figure 4B). Next, we quantified how locked to the stimulus the EPSC responses were, by calculating phase-locking strength of a cell's significant events to the optical stimulus. If the events are occurring a preferred phase of the optical stimulus (e.g. peak of pulse or peak of sine) then the cell events will be significantly phase-locked by a Rayleigh test. EPSCs evoked by pulses were more likely to be stimulus-locked, while EPSCs during sinusoidal stimulation were not phase-locked to the stimulus regardless of the frequency (Figure 5). Surprisingly, events evoked by 8 Hz pulses were significantly phase-locked in all recorded neurons, but only 30 % of the neurons had significantly phase-locked events during 20 Hz pulses. The postsynaptic response to 20 Hz pulses have low fidelity, as neurons had EPSCs event rates much lower than 20 Hz (see individual cells in Figure 4A), but 30% of cell's had significantly phase-locked events during 20 Hz pulses (Figure 5). These results suggest that while EPSCs that occur during pulsatile stimulation are stimulus-locked, while EPSCs

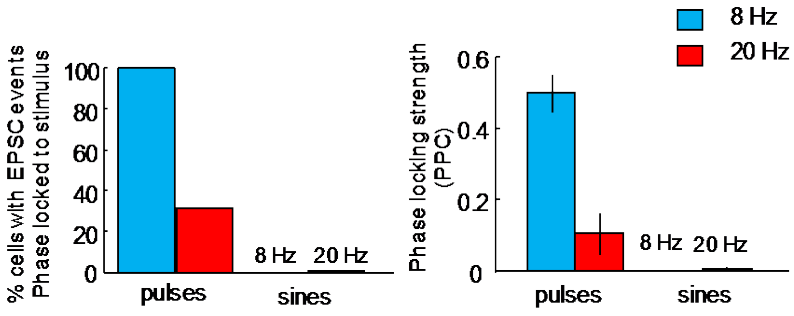

Figure 5: EPSCs evoked by pulses are phase locked to the stimulus. Left, percent of cells with significantly phase locked EPSCs across frequencies and stimulation pattern. Right, pairwise phase consistency for EPSCs across frequencies and stimulation pattern.

events that occur during sinusoidal stimulation do not occurred phase-locked manner suggesting that they occur in a more spontaneous manner.

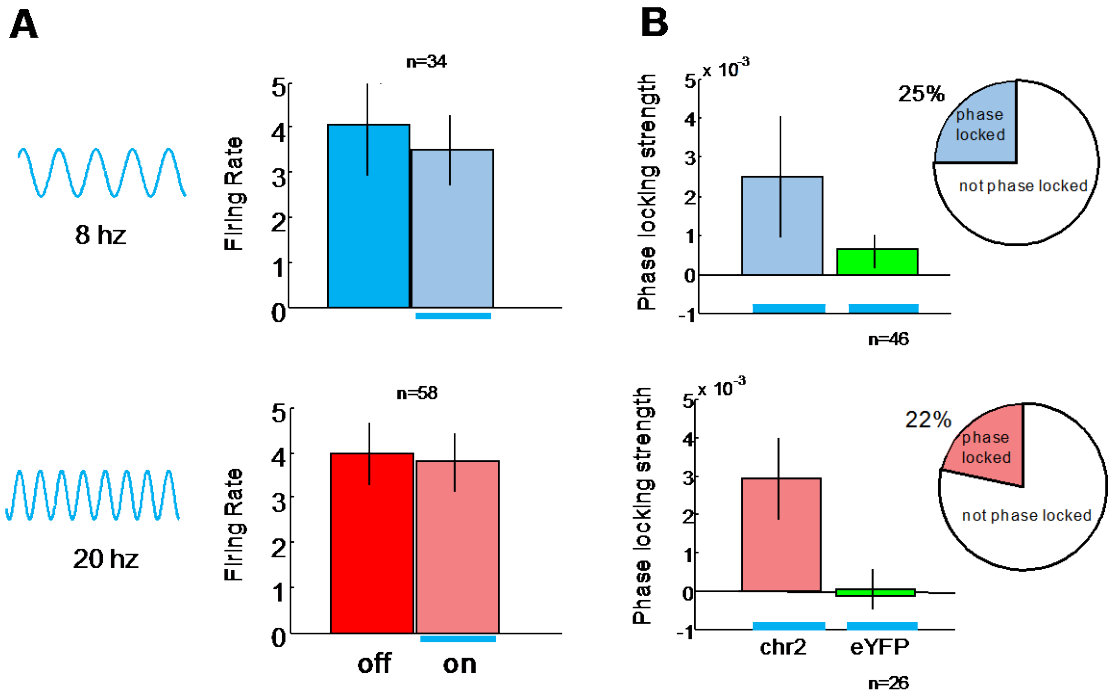

Figure 6: mPFC single unit phase locking to the optical stimulus during terminal stimulation of vHPC A. Overall firing rate for light off vs on periods of sinusoidal stimulation at 8 Hz (top) or 20 Hz (bottom) does not significantly change firing rate in mPFC single units. B. Pairwise phase consistency of single units to the stimulus at 8 Hz (top) vs 20 Hz (bottom), significant phase locking is seen in 25 and 22% of the single units respectively.

Next, to investigate if sinusoidal stimulation is sufficient to enhance rhythmic activity *in vivo*, single units from mPFC were recorded during sinusoidal vHPC terminal stimulation at 8 and 20 Hz. *In vivo*, sinusoidal stimulation of vHPC terminals increased phase-locking of mPFC single units to the optical stimulation pattern without changing overall firing rates. Firing rate was compared during light off and on epochs (2 minute epochs for 8 minutes) for sinusoidal stimulation at 8 Hz and 20 Hz, there was no difference in overall firing rate for both frequencies (Figure 6A). On the other hand, there was significant phase-locking to the sinusoidal stimulus at both frequencies (Figure 6B).

These results demonstrate that sinusoidal stimulation can successfully bias spiking to occur rhytmically in vivo.

5.3 Discussion:

In this study, we combined optogenetic stimulation with *in vivo* single unit recording and *in vitro* whole cell recording to compare how different patterns of vHPC terminal stimulation affect mPFC activity and anxiety-like behavior. The results suggest that sinusoidal stimulation at a theta frequency increases spontaneous excitatory events in mPFC and increases theta-frequency oscillatory intracellular activity in the membrane. These postsynaptic changes induced by vHPC terminal stimulation, might in turn account for the enhancement in phase locking to 8 Hz of single units *in vivo* as well as an increase in anxiety-related behavior. Moreover, they suggest that theta-frequency components of neural activity play a privileged role in vHPC-mPFC communication and hippocampal-dependent forms of anxiety.

Theta-frequency sinusoidal stimulation is sufficient to for anxiety-like behavior

Terminal stimulation of vHPC-mPFC pathway increased avoidance behavior in the EPM, only when stimulated at 8 Hz in a sinusoidal pattern, but not at 20 Hz. This result is consistent with our vHPC-mPFC inhibition experiments showing that inhibiting this pathway decreases avoidance behavior and decreases vHPC-mPFC theta synchrony and not synchrony occurring in other frequencies (see chapters 2 & 4). The frequency specificity observed in the current behavior experiment is also consistent with work showing that during anxiety assays there is an increase in theta synchrony between

vHPC-mPFC (Adhikari et al. 2011). One possible mechanism for this enhancement in anxiety behavior is that the optical stimulation facilitates vHPC-mPFC information transfer. The stimulation might enhance vHPC input that signals aversion by increasing oscillatory activity in the membrane of mPFC neurons, which in turn might bring the membrane closer to firing threshold in a rhythmic manner such that the cell is more likely to fire in response to naturally occurring vHPC input. Behaviorally, the increase in avoidance behavior can be explain by the following models 1) the existing aversive information is enhanced by 8 Hz sinusoidal stimulation or 2) the stimulation is aversive itself, causing the animals to seek refuge in the closed arms. Our experiment in the EPM does not distinguish between these two models. Ongoing experiments stimulating vHPC-mPFC with a sinusoidal 8 Hz and addressing if stimulation elicits conditioned place aversion will allow determining if there is evidence for model 2). Moreover, it is still unclear what the 8 Hz sinusoidal stimulation does to the representation of aversion firing patterns in mPFC single units. Once we know which model explains the increase in avoidance behavior and what the stimulation does to the mPFC representation of aversion (arm-type specific firing in EPM) we will have a better understanding of the mechanism of this frequency- and pattern-specific effect.

Although 8 Hz pulsatile stimulation of vHPC-mPFC caused strong evoked excitation of mPFC neurons, it did not affect avoidance behavior, at least as measured in time spent in open arms. It is possible that 8 Hz pulses affected other behavioral measurements that we did not quantify. Ongoing analyses are considering risk assessment behaviors (head dips, body stretches) during 8 Hz pulsatile stimulation. One prediction is that the

strong evoked excitation of 8 Hz pulses can interrupt ongoing vHPC information and decreased anxiety-like behavior modestly.

Reconciling in vivo and in vitro results

Surprisingly, when stimulating vHPC terminals *in vitro* there was no detected significant phase locking of EPSCs events to the sinusoidal stimulation. The lack of phase locking in the *in vitro* EPSCs suggests that the excitatory events are spontaneous or too sparse to detect phase locking. One possibly mechanism for the increase in spontaneous asynchronous activity, as ChR2 conducts Ca^{2+} (Nagel et al. 2003), is an accumulation of Ca^{2+} in the terminals resulting in an increase probability of vesicle release in vHPC terminals. On the other hand, during pulsatile stimulation all EPSCs were strongly phase-locked to the stimulus demonstrating that they were evoked by the pulses rather than being spontaneous and asynchronous.

However, *in vivo* mPFC spiking was significantly phase-locked to the 8 Hz sinusoidal stimulation. Considering the in vitro findings, a possible explanation for the phase locking observed *in vivo* is that the sinusoidal stimulus causes an increase in oscillatory depolarization of the membrane at 8 Hz. This oscillatory depolarization increases probability of the postsynaptic cell firing, and therefore the spikes are phase-locked to the optical sinusoid stimulus. It is therefore possible that the sinusoidal stimulus entrains spiking activity *in vivo* via fluctuations of the cellular membrane.

Lessons from frequency differences in postsynaptic response

Surprisingly, the postsynaptic response to pulsatile stimulation of terminals was frequency dependent. Stimulating vHPC terminals with 20 Hz pulses evoked fewer EPSCs than 8 Hz pulses (Figure 4B). This effect was unlikely to be due to the kinetics of ChR2 as hypothalamic cells expressing ChR2 can follow 20 Hz pulsatile stimulation *in vitro* with near 100% efficacy (Adamantidis et al. 2007). This frequency dependency can arise at the pre-synaptic terminal if 20 Hz is less efficient than 8 Hz at inducing the release of vesicles at 20 Hz, or post-synaptically, if mPFC neurons cannot follow vHPC input at 20 Hz. Both mechanisms, however, are consistent with the vHPC-mPFC pathway having biophysical frequency limits that are independent of the opsin kinetics. The frequency preference for 8 Hz is consistent with in vivo studies showing that HPC cells fire close to 8 Hz during a spatial navigation task (Harvey et al. 2009). This efficacy of specific frequencies could be true in other pathways. Scientists who use optogenetics should use a frequency and pattern of stimulation that best fits what their pathway of interest does under physiological conditions.

In vivo, the sinusoidal stimulation at 8 Hz was sufficient that entrain mPFC spiking to 8 Hz. How is this increase in rhythmic spike activity occurring during 8 Hz sinusoidal stimulation? One possibility is that this rhythmic activity is generated by presynaptic release of neurotransmitter in a rhythmic manner that produces currents below the threshold of what we consider events in this study, therefore causing oscillatory activity in the postsynaptic membrane. Another possibility is that interneuron activation could mediate this effect. *In vitro*, it has been demonstrated that the firing of a single interneuron is sufficient to entrain the cell membrane of a pyramidal CA1 cell to oscillate

at theta (Cobb et al. 1995). Moreover, *in vivo* evidence suggests that CA1 LFP theta oscillations may be entrained by interneurons spiking at specific theta phases (Klausberger et al. 2003). vHPC projects to both mPFC interneurons and pyramidal neurons, so it is possible that the increase in oscillatory intracellular activity in pyramidal mPFC neurons is achieved via interneuron activation by the optical stimulus. Alternatively, rhythmic changes in the extracellular field that occur by influx of positive ions in the terminals during the sinusoidal stimulation could cause the postsynaptic membrane to oscillate.

Altogether, these results reinforce that theta-range frequencies, can maximize information transfer between vHPC and mPFC. Past in vivo studies that show task related changes in theta synchrony between vHPC and mPFC together with the current findings support this hypothesis (Adhikari et al. 2010; Lesting et al. 2011).

5.4 Methods

Surgical Procedures: For the EPM experiments, 45 mice were bilaterally infected with either AAV5 CamKIIa-hChR2(H134R)-mCherry or AAV5 CamKIIa–eYFP into the vHPC under isoflurane anesthesia. 200 nl of 10 12 vg/ml virus was pressure-injected through a glass micropipette. In each hemisphere, five injections were done at -3.10 and at -3.30 AP levels for a total of 10 injections per hemisphere. At each AP level, the five injection sites were ±2.90, -4.0; ±3.30, -3.60; ±3.30 -1.7; ±3.70, -3.2; ±3.70, -2.5 (ML and DV, respectively). Coordinates are in mm relative to Bregma (AP, ML) or brain surface (DV). All viruses were obtained from the University of North Carolina Vector core. Virus was infused at a rate of 200 nl/min. 6–8 weeks after viral infection, a subset

of mice for the EPM experiment, were implanted with electrodes and optical fibers in a second surgery, also under isoflurane anesthesia. Stereo-optrodes were implanted in the mPFC (AP -1.60 ML ±0.4 DV -1.25). Each stereo-optrode was comprised of a 230 um optical fiber glued to a bundle of 14 tungsten wire (13 mM diameter) stereotrodes placed 400–500 mm below the end of the optical fiber. 75 mM diameter tungsten wire LFP electrodes were implanted in the BLA (AP -1.80, ML ±3.16, DV -4.10) and the CA1 region of the vHPC (AP -3.30, ML ±3.30, DV -3.60). A reference screw was implanted in the skull over the frontal cortex and a ground screw in the skull over the cerebellum.

Behavioral procedure: EPM behavioral protocol: Behavior 5–7 days after electrode microdrive implantation, mice were food restricted to 80% of pre-operative weight and habituated to the opto/electrical tether in a small dark wooden box (20x3x30 cm) as they foraged for food pellets. On the fifth day of habituation, after 1 hr rest, mice were placed in the EPM under 250-300 lux illumination. Five mice were excluded from behavioral analysis for never visiting the open arms throughout the duration of the experiment. Behavior in the EPM was hand scored by a blinded scorer to ensure consistency of analysis. A mouse was said to be inside an open or closed arm if all four paws were inside the arm. The LED (465 nm; PlexBright LD-1 Single Channel LED Driver from Plexon) output was controlled with an Arduino device and custom made code and sent to the LED via the analog channel of the LED Driver to deliver pulses or sinusoids of 465 nm light at ~8 mW (measured at the tip of the optical patch cord fiber) every 2 min for 8 minutes.

In vivo electrophysiology: Data were acquired using a Digital Lynx system (Neuralynx). LFPs were referenced to a screw located in the skull over the frontal cortex/olfactory bulb, band-pass filtered (1–1,000 Hz), and acquired at 2 kHz. The Arduino signal that controlled the LED was recorded as a proxy for the optical stimulation signal by copying the output of the Arduino into a channel of the Neuralynx system. Unit recordings were band-pass filtered at 600–6,000 Hz and acquired at 32 kHz; spikes were detected by thresholding and sorted off-line. Initial automated spike sorting was done based on peak, energy and principal component analysis, using Klustakwik (Ken Harris, UCL) instantiated in SpikeSort3D (Neuralynx); clusters were subsequently manually confirmed. Phase locking to the Arduino sinusoidal stimulus was calculated using the phase component of a Hilbert transform of the sinusoidal stimulus. A given unit was said to be significantly phase-locked if the distribution of the sinusoidal phases where the spikes occurred was not uniform as assessed with Rayleigh's test for non-uniformity of circular data. Zero phase corresponds to the peak of the signal. Phase locking strength was quantified using pairwise phase consistency (PPC) (Vinck et al., 2010).

In vitro electrophysiology: Whole-cell current and voltage clamp recordings were performed in layer 5/6 pyramidal cells in the prelimbic (PrL) region of the mPFC. Recordings were obtained with a Multiclamp 700B amplifier (Molecular Devices, Sunnyvale, CA, USA) and digitized using a Digidata 1440A acquisition system (Molecular Devices) with Clampex 10 (Molecular Devices) and analyzed with pClamp 10 (Molecular Devices). Following decapitation, 300 μM slices containing mPFC were incubated in artificial cerebral spinal fluid containing (in mM) 126 NaCl, 2.5 KCl, 2.0

MgCl 2, 1.25 NaH 2PO4, 2.0 CaCl2, 26.2 NaHCO3 and 10.0 D- glucose, bubbled with oxygen, at 32˚C for 30 min before being returned to room temperature for at least 30 min prior to use. During recording, slices were perfused in artificial cerebral spinal fluid (with drugs added as detailed below) at a rate of 5 ml min−1. Electrodes were pulled from 1.5 mM borosilicate-glass pipettes on a P-97 puller (Sutter Instruments, Novato, CA, USA). Electrode resistance was typically 3–5MΩ when filled with internal solution consisting of (in mM): 130 K-gluconate, 5 NaCl, 10 HEPES, 0.5 EGTA, 2 MgATP and 0.3 NaGTP (pH 7.3, 280 mOs). Pyramidal cells were visually identified based on their shape and prominent apical dendrite at × 40 magnification under infrared and diffusion interference contrast microscopy using an inverted Olympus BX51W1 microscope (Olympus America, Center Valley, PA, USA) coupled to a Hamamatsu C8484 camera (Hamamatsu, Middlesex, NJ, USA).

Recordings were made in voltage clamp at aholding potential of -70 mV… and at the cell's natural resting membrane potential in current clamp. Optogenetic stimulation was done with a blue LED (465 nm; PlexBright LD-1 Single Channel LED Driver from Plexon) connected via patchcords to a rotary joint that was then connected via patchcords (200 µm, 0.22 NA) to the light fiber, which was placed just adjacent to the 40x field of view. Light pulses were 5 ms long and were delivered at 8 Hz or 20 Hz for 30 seconds, via pulsed or sinusoidal stimulation generated with an Arduino device and custom-made code and sent to the LED via the analog channel of the LED Driver. Recording analysis was performed with Matlab (Mathworks, Natick, MA). Events were

defined as excitatory currents that were >4 standards deviations away from the baseline mean (red dots in Figure 3B).

Chapter 6: Discussion

6.1 Summary of findings

The findings described in this thesis demonstrate that activity within the direct vHPC- to-mPFC pathway is necessary and sufficient for anxiety-related behavior. Also, they demonstrate that this pathway is necessary for vHPC-mPFC theta synchrony, and spatial representations of aversion in the mPFC. Intriguingly, optogenetic inhibition and excitation of vHPC terminals resulted in frequency-specific effects. Together, these findings suggest a model in which behaviorally relevant information about the spatial aversive structure of the environment from the vHPC is sent to the mPFC and utilized to guide avoidance behavior; theta-frequency synchrony appears to be important for this process. The implications of these findings and future directions, particularly in terms of the extended BLA-vHPC-mPFC circuit, are discussed below.

6.2 Implications for Theta Synchrony in the vHPC-mPFC-BLA Circuit

The BLA, vHPC, and mPFC comprise a tripartite circuit in which each element is important for anxiety-like behavior. Silencing or lesioning any of these three structures alters avoidance behavior in tests such as the EPM (Jinks and McGregor 1997;.Kjelstrup et al. 2002; Shah and Treit 2003; Bannerman et al. 2003). Similarly, optogenetically manipulating BLA inputs into the vHPC (Felix-Ortiz et al. 2013) or the mPFC (Felix-Ortiz et al. 2016) alters anxiety. However, these structures are intimately interconnected (Hoover and Vertes 2007; Pikkarainen et al. 1999), as evidenced by the remarkable degree of synchrony that arises during fear and anxiety behaviors (Adhikari et al. 2010; Lesting et al. 2011; Likhtik et al. 2014; Seidenbecher et al. 2003; Stujenske et al. 2014). Thus, manipulations of any one structure could alter activity patterns in any

other within the circuit; the specificity of such manipulations is questionable. I attempted to address this caveat by recording local field potentials (LFP) simultaneously from the three structures while inhibiting the vHPC terminals in mPFC. Inhibition of the vHPC terminals within the mPFC was relatively specific, disrupting synchrony in the theta frequency range between the vHPC and the mPFC with minimal effects on theta synchrony between the BLA and either structure.

Optogenetic stimulation of vHPC-mPFC at a theta range frequency (8 Hz), and not at 20 Hz, was sufficient to increased avoidance behavior. In vitro whole-cell recordings of mPFC suggest that vHPC terminal sinusoidal stimulation at a theta frequency increases spontaneous excitatory events in mPFC and increases theta-frequency oscillatory activity in the membrane. These postsynaptic changes induced by vHPC terminal stimulation, might in turn account for the enhance in theta-frequency spiking activity *in vivo* as well as the increase in anxiety-related behavior. Moreover, altogether these results suggest that theta-frequency components of neural activity play a privileged role in vHPC-mPFC communication and hippocampal-dependent forms of anxiety. Perhaps this privileged role of theta during aversive behaviors could extend to mPFC theta. A recent study showed that inhibiting PV-interneurons caused a reset in mPFC theta and increased mPFC theta power. This manipulation also increased fear behavior, even in the lack of fear stimuli (Courtin et al. 2013).

6.3 Implications for Resonance in the vHPC-prefrontal pathway

Three findings in this thesis suggest that the vHPC-mPFC pathway has resonance or preferred frequencies. The first finding is that, although ChR2 kinetics follow 20 Hz stimulation, optical stimulation of vHPC terminals with 20 Hz pulses failed to evoked EPSCs in mPFC pyramidal cells as well as 8 Hz pulses. This resonant frequency filtering could be occurring at the level of the vHPC terminal or at the level of the postsynaptic mPFC pyramidal cell, or perhaps both. The data in this thesis does not distinguish between these possibilities, but some past studies suggest, that at least HPC projecting pyramidal neurons do exhibit resonance. In vivo, dorsal HPC CA1 pyramidal cells fire at an average of ~7 Hz during a navigational task (Harvey et al. 2009), so perhaps their biophysical properties are such that they function better at theta-like frequencies. This finding could explain why optical stimulation with 20 Hz pulses failed to evoked EPSCs as well as 8 Hz pulses. Possibly, stimulating with 8 Hz pulses was more natural for the terminals, as they responded better to this frequency, compared to 20 Hz pulses.

The second finding is that stimulating vHPC terminals with 8 Hz sinusoids elicited oscillatory activity in the intracellular membrane, but 20 Hz sinusoids failed to do so. Theta frequency oscillations in the membrane potential of CA1 pyramidal cells increase in amplitude when the animal is inside the place field of the cell (Harvey et al. 2009). Moreover, by injecting electrical sinusoidal currents at various frequencies into CA1 neurons in vitro, many studies have demonstrated that the maximal (resonant) response of the CA1 membrane potential is theta frequency. Therefore, the resonant frequency was about the same as the natural oscillation frequency (Leung 1998; Hu, Vervaeke,

and Storm 2002). These findings may explain why 20 Hz sinusoids failed to evoke oscillatory membrane activity in mPFC neurons.

The third finding is that inhibition of the vHPC terminals in the mPFC decreased theta-frequency synchrony between vHPC and mPFC, but not synchrony in other frequencies. One possibility is that synchrony in other frequencies that were unaffected by the inhibition is mediated by multiple common inputs to mPFC and vHPC, or that they are noise, part of the resting state networks.

This special role of frequency specificity and cross-regional coupling of theta is best tested with a closed-loop stimulation design that enhances or disrupts synchrony with the same optogenetic stimulation. This approach would vary the timing of that stimulation based on the ongoing theta recorded, such that you have an internal control for total activity induced by ChR2. If the vHPC LFP is recorded and filtered for theta at real time, the phase information can be used to guide the stimulation and potentially enhance the synchrony between vHPC and its outputs. Phase in the HPC changes across layer and location, so LFP should be consistently recorded in the pyramidal layer with a high impedance electrode, such that it reflects best the extracellular field surrounding the projecting neurons. However, once the theta phase information is collected, it is not clear what ChR2 stimulation pattern or approach could enhance the synchrony between vHPC and mPFC. A recent study used a closed-loop approach to alter hippocampal outputs relative to ongoing theta rhythms on a trial-by-trial basis, providing within-animal controls for all stimulation conditions. Siegle and Wilson chose

to alter hippocampal outputs via timed ChR2 activation of parvalbumin-positive interneurons, at either the falling phase or rising phase of theta recorded in the LFP. Triggering inhibition at the peak of theta and the trough of theta had opposite behavioral effects during spatial working memory (Siegle and Wilson 2014). This study shows that the HPC theta timing during spatial working memory is behaviorally meaningful. However, in this study there were no measures of cross-regional synchrony. Unfortunately, no study has reported a close-looped stimulation paradigm that increases cross-regional coupling thus far. Here are some potential stimulation paradigms to try to increase theta coupling between mPFC and vHPC:

1. Stimulate vHPC terminals in mPFC with short pulses at the trough phase of vHPC theta. The trough would indicate when the vHPC cells are most likely firing, as the extracellular field is negative. If mPFC cells are uniformly phase locked to a specific phase of vHPC theta, then that phase can be the stimulated phase rather than the trough. This protocol may enhance the vHPC input to the mPFC and subsequently the theta activity in mPFC. But it could also be problematic, as ChR2 spikes generated at the terminals could cause collision with ongoing natural spikes and possible disrupt synchrony.

2. Stimulate PV interneurons in mPFC at the peak phase of vHPC theta. PV IN in mPFC have been shown to reset mPFC theta, so re-setting mPFC theta in a coordinated manner with vHPC theta could increase synchrony between the vHPC-mPFC. This approach takes into consideration the previous closed-loop

experiment (Siegle and Wilson 2014), and that interneuron inhibition to pyramidal cells in HPC has been shown to be sufficient to generate theta oscillations (Goutagny et al. 2009). The caveat of this approach is that it would cause stimulation of all mPFC PV interneurons, rather than the selected PV interneurons that are innervated by vHPC. Ideally, only the PV interneurons innervated by vHPC would express ChR2, and that would make this stimulation paradigm more specific to vHPC input and potentially more naturalistic to vHPC-mPFC theta generation. To this date no viral approach would accomplish this specificity, but most likely future technology will allow it.

3. Stimulate vHPC terminals in mPFC using the instantaneous amplitude of vHPC theta as an analog input to control the power of laser. This approach, rather than focusing on the phase, focuses on mimicking the amplitude of vHPC theta in mPFC, which could potentially enhance the power synchrony between vHPC and mPFC. This protocol would benefit from knowing what vHPC terminals do in response to a sinusoidal optical ChR2 input. Before employing this protocol, it would be best to record vHPC terminal output during a sinusoid optical stimulus.

6.4 Implications for the Origin of Spatial Representations of Aversion

Inhibition of the direct vHPC input ablated the representation of aversive and non-aversive context within the mPFC. This result is consistent with recent findings during a working memory task, in which the representation of goal location was disrupted by the same manipulation (Spellman et al. 2015). However, mPFC units encode valence;

neurons that fire in response to bright, enclosed arms also fire in response to open arms in the dark (Adhikari et al. 2011). Moreover, terminal inhibition altered additional behavioral measures of valence, independent of arm choice, suggesting that vHPC inputs are crucial not just for spatial representations but also for the anxiety valence. Whether this valence is constructed in the mPFC with the help of vHPC input or is present in the vHPC itself is unclear. A recent report demonstrates that mPFC-projecting vHPC neurons preferentially encode arm type in the EPM, while very few have well-defined place fields (Ciocchi et al. 2015). Evidence from human hippocampal imaging suggests that the anterior hippocampus (the human homolog of the vHPC) responds to negative valence (Gerdes et al. 2010; Sterpenich et al. 2014). These findings suggest the possibility that vHPC inputs indeed convey valence information to the mPFC. It is still unknown how 8 Hz sinusoidal stimulation of vHPC terminal affects the mPFC representation of aversion. Knowing how it affects mPFC representation will help interpret the increase in anxiety-like behavior observed with the stimulation.

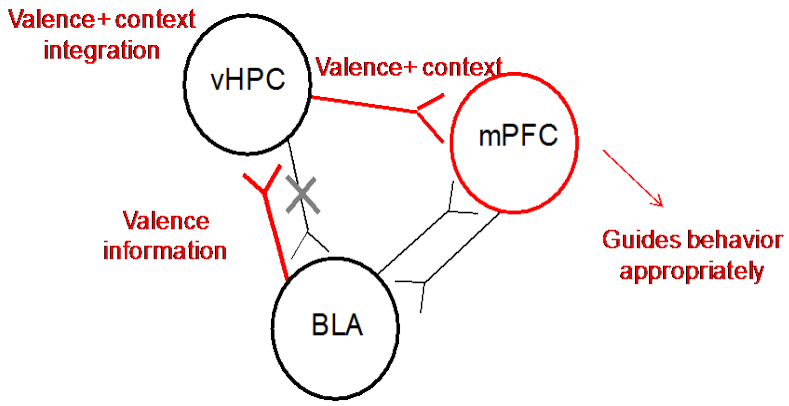

Figure 1: Working model that supports the findings in this thesis.

Where might the vHPC get information about valence? It could come from the BLA, given the demonstration that optogenetic inhibition of BLA terminals within the vHPC also disrupts anxiety-like avoidance behavior (Felix-Ortiz et al. 2013). However,

inhibition of the vHPC terminals in BLA did not disrupt anxiety-like behavior (Jimenez et al. personal communication). This suggests that the flow of necessary anxiety-relevant information goes from BLA to vHPC, and given the findings presented here, from vHPC to mPFC (Figure 1). BLA has been long implicated in valence representation, so it is reasonable to hypothesize that valence information is sent from BLA to vHPC and there it is integrated with contextual information, and relayed to mPFC. To directly test this hypothesis, I propose to inhibit the BLA projection to the vHPC while recording single units in the mPFC during the EPM and a non-aversive maze with two contexts as a negative control. If inhibition of the BLA-vHPC decreases arm-type representation during the EPM, but not the non-aversive maze, then it can be concluded that indeed valence information travels from the BLA to the vHPC, where it can be integrated with contextual information and then relayed to the mPFC.

6.5 Conclusion

A long literature links theta-frequency synchrony between the vHPC, mPFC, and BLA to both learned fear and innate anxiety (Adhikari et al., 2011; Lesting et al., 2011; Likhtik et al., 2014; Seidenbecher et al., 2003; Stujenske et al., 2014). Indeed, optogenetically enhancing theta-frequency oscillations within the mPFC increased anxiety-like behavior. Moreover, inhibition of the vHPC-to-mPFC pathway disrupted anxiety-like behavior and theta-frequency synchrony between the two structures without affecting synchrony at other frequencies. Interestingly, inhibition of this same vHPC-to- mPFC pathway during a working memory task had no effect on theta-frequency synchrony (Spellman et al., 2015); instead, low gamma (30–70 Hz) synchrony was specifically disrupted. These

contrasting findings demonstrate the surprising result that a specific anatomical pathway can mediate synchrony at different frequencies depending on behavioral state.

References:

Adamantidis, Antoine R., Feng Zhang, Alexander M. Aravanis, Karl Deisseroth, and Luis De Lecea. 2007. “Neural Substrates of Awakening Probed with Optogenetic Control of Hypocretin Neurons.” *Nature* 450 (7168): 420–424.

Adhikari, Avishek, Talia N. Lerner, Joel Finkelstein, Sally Pak, Joshua H. Jennings, Thomas J. Davidson, Emily Ferenczi, et al. 2015. “Basomedial Amygdala Mediates Top-down Control of Anxiety and Fear.” *Nature*. http://www.nature.com/nature/journal/vaop/ncurrent/full/nature15698.html.

Adhikari, Avishek, Mihir A. Topiwala, and Joshua A. Gordon. 2010. “Synchronized Activity between the Ventral Hippocampus and the Medial Prefrontal Cortex during Anxiety.” *Neuron* 65 (2): 257–69. doi:10.1016/j.neuron.2009.12.002.

Adhikari, Avishek, Mihir A. Topiwala, and Joshua A. Gordon. 2011. “Single Units in the Medial Prefrontal Cortex with Anxiety-Related Firing Patterns Are Preferentially Influenced by Ventral Hippocampal Activity.” *Neuron* 71 (5): 898–910. doi:10.1016/j.neuron.2011.07.027.

Aftanas, Ljubomir I., Sergey V. Pavlov, Natalia V. Reva, and Anton A. Varlamov. 2003. “Trait Anxiety Impact on the EEG Theta Band Power Changes during Appraisal of Threatening and Pleasant Visual Stimuli.” *International Journal of Psychophysiology* 50 (3): 205–212.

Anagnostaras, Stephan G., Greg D. Gale, Michael S. Fanselow, and others. 2001. “Hippocampus and Contextual Fear Conditioning: Recent Controversies and Advances.” *Hippocampus* 11 (1): 8–17.

Anagnostaras, Stephan G., Stephen Maren, and Michael S. Fanselow. 1999. "Temporally Graded Retrograde Amnesia of Contextual Fear after Hippocampal Damage in Rats: Within-Subjects Examination." *The Journal of Neuroscience* 19 (3): 1106–1114.

Anastassiou, Costas A., Rodrigo Perin, Henry Markram, and Christof Koch. 2011. "Ephaptic Coupling of Cortical Neurons." *Nature Neuroscience* 14 (2): 217–223.

Anthony, Todd E., Nick Dee, Amy Bernard, Walter Lerchner, Nathaniel Heintz, and David J. Anderson. 2014. "Control of Stress-Induced Persistent Anxiety by an Extra-Amygdala Septohypothalamic Circuit." *Cell* 156 (3): 522–536.

Bandettini, Peter A. 2009. "Seven Topics in Functional Magnetic Resonance Imaging." *Journal of Integrative Neuroscience* 8 (3): 371–403.

Bandler, Richard, and Pascal Carrive. 1988. "Integrated Defence Reaction Elicited by Excitatory Amino Acid Microinjection in the Midbrain Periaqueductal Grey Region of the Unrestrained Cat." *Brain Research* 439 (1): 95–106.

Bandler, Richard, and Michael T. Shipley. 1994. "Columnar Organization in the Midbrain Periaqueductal Gray: Modules for Emotional Expression?" *Trends in Neurosciences* 17 (9): 379–389.

Bannerman, D. M, M Grubb, R. M. J Deacon, B. K Yee, J Feldon, and J. N. P Rawlins. 2003. "Ventral Hippocampal Lesions Affect Anxiety but Not Spatial Learning." *Behavioural Brain Research* 139 (1–2): 197–213. doi:10.1016/S0166-4328(02)00268-1.

Bannerman, D. M, J. N. P Rawlins, S. B McHugh, R. M. J Deacon, B. K Yee, T Bast, W. -N Zhang, H. H. J Pothuizen, and J Feldon. 2004. "Regional Dissociations within

the Hippocampus—memory and Anxiety." *Neuroscience & Biobehavioral Reviews*, Festschrift in Honour of Jeffrey Gray - Issue 1: Anxiety and Neuroticism, 28 (3): 273–83. doi:10.1016/j.neubiorev.2004.03.004.

Behbehani, Michael M. 1995. "Functional Characteristics of the Midbrain Periaqueductal Gray." *Progress in Neurobiology* 46 (6): 575–605.

Beyeler, Anna, Praneeth Namburi, Gordon F. Glober, Clémence Simonnet, Gwendolyn G. Calhoon, Garrett F. Conyers, Robert Luck, Craig P. Wildes, and Kay M. Tye. 2016. "Divergent Routing of Positive and Negative Information from the Amygdala during Memory Retrieval." *Neuron* 90 (2): 348–361.

Blanchard, Robert J., and D. Caroline Blanchard. 1989. "Attack and Defense in Rodents as Ethoexperimental Models for the Study of Emotion." *Progress in Neuro-Psychopharmacology and Biological Psychiatry* 13, Supplement 1: S3–14. doi:10.1016/0278-5846(89)90105-X.

Blundell, Jacqueline, Robert Adamec, and Paul Burton. 2005. "Role of NMDA Receptors in the Syndrome of Behavioral Changes Produced by Predator Stress." *Physiology & Behavior* 86 (1–2): 233–43. doi:10.1016/j.physbeh.2005.07.012.

Brady, Joseph V., and Walle JH Nauta. 1953. "Subcortical Mechanisms in Emotional Behavior: Affective Changes Following Septal Forebrain Lesions in the Albino Rat." *Journal of Comparative and Physiological Psychology* 46 (5): 339.

Bravo-Rivera, Christian, Ciorana Roman-Ortiz, Edith Brignoni-Perez, Francisco Sotres-Bayon, and Gregory J. Quirk. 2014. "Neural Structures Mediating Expression and

Extinction of Platform-Mediated Avoidance." *The Journal of Neuroscience* 34 (29): 9736–9742.

Bremner, J. Douglas, Bernet Elzinga, Christian Schmahl, and Eric Vermetten. 2007. "Structural and Functional Plasticity of the Human Brain in Posttraumatic Stress Disorder." In *Progress in Brain Research*, edited by Melly S. Oitzl and Eric Vermetten E. Ronald De Kloet, 167:171–86. Stress Hormones and Post Traumatic Stress Disorder Basic Studies and Clinical Perspectives. Elsevier. http://www.sciencedirect.com/science/article/pii/S0079612307670125.

Bremner, J. Douglas, Lawrence H Staib, Danny Kaloupek, Steven M Southwick, Robert Soufer, and Dennis S Charney. 1999. "Neural Correlates of Exposure to Traumatic Pictures and Sound in Vietnam Combat Veterans with and without Posttraumatic Stress Disorder: A Positron Emission Tomography Study." *Biological Psychiatry* 45 (7): 806–16. doi:10.1016/S0006-3223(98)00297-2.

Burgos-Robles, Anthony, Ivan Vidal-Gonzalez, and Gregory J. Quirk. 2009. "Sustained Conditioned Responses in Prelimbic Prefrontal Neurons Are Correlated with Fear Expression and Extinction Failure." *The Journal of Neuroscience* 29 (26): 8474–8482.

Burgos-Robles, Anthony, Ivan Vidal-Gonzalez, Edwin Santini, and Gregory J. Quirk. 2007. "Consolidation of Fear Extinction Requires NMDA Receptor-Dependent Bursting in the Ventromedial Prefrontal Cortex." *Neuron* 53 (6): 871–880.

Buzsáki, György. 2002. "Theta Oscillations in the Hippocampus." *Neuron* 33 (3): 325–340.

Buzsáki, György, and Andreas Draguhn. 2004. “Neuronal Oscillations in Cortical Networks.” *Science* 304 (5679): 1926–1929.

Buzsáki, György, and Brendon O. Watson. 2012. “Brain Rhythms and Neural Syntax: Implications for Efficient Coding of Cognitive Content and Neuropsychiatric Disease.” *Dialogues Clin Neurosci* 14 (4): 345–367.

Calandreau, Ludovic, Robert Jaffard, and Aline Desmedt. 2007. “Dissociated Roles for the Lateral and Medial Septum in Elemental and Contextual Fear Conditioning.” *Learning & Memory* 14 (6): 422–429.

Calhoon, Gwendolyn G., and Kay M. Tye. 2015. “Resolving the Neural Circuits of Anxiety.” *Nature Neuroscience* 18 (10): 1394–1404. doi:10.1038/nn.4101.

Canon, W. B. 1915. “Bodily Changes in Pain.” *Hunger, Fear and Rage*.

Carr, David B., and Susan R. Sesack. 1996. “Hippocampal Afferents to the Rat Prefrontal Cortex: Synaptic Targets and Relation to Dopamine Terminals.” *Journal of Comparative Neurology* 369 (1): 1–15.

Cheriyan, John, Mahesh K. Kaushik, Ashley N. Ferreira, and Patrick L. Sheets. 2016. “Specific Targeting of the Basolateral Amygdala to Projectionally Defined Pyramidal Neurons in Prelimbic and Infralimbic Cortex.” *Eneuro* 3 (2): ENEURO–0002.

Ciocchi, S., J. Passecker, H. Malagon-Vina, N. Mikus, and T. Klausberger. 2015. “Brain Computation. Selective Information Routing by Ventral Hippocampal CA1 Projection Neurons.” *Science (New York, N.Y.)* 348 (6234): 560–63. doi:10.1126/science.aaa3245.

Cobb, S. R., E. H. Buhl, K. Halasy, O. Paulsen, and P. Somogyi. 1995. “Synchronization of Neuronal Activity in Hippocampus by Individual GABAergic Interneurons.” http://www.nature.com/nature/journal/v378/n6552/abs/378075a0.html.

Colgin, Laura Lee. 2013. “Mechanisms and Functions of Theta Rhythms.” *Annual Review of Neuroscience* 36: 295–312.

Comte, Magali, Aïda Cancel, Jennifer T. Coull, Daniele Schön, Emmanuelle Reynaud, Sarah Boukezzi, Pierre-François Rousseau, et al. 2015. “Effect of Trait Anxiety on Prefrontal Control Mechanisms during Emotional Conflict.” *Human Brain Mapping* 36 (6): 2207–2214.

Courtin, Julien, Fabrice Chaudun, Rober R. Rozeske, Nikolaos Karalis, Cecilia Gonzalez-Campo, Helene Wurtz, Azzedine Adbi, Jerome Baufreton, Thomas C.M. Bienvenu, and Ceyril Herry. 2014. “Prefrontal Parvalbumin Interneurons Shape Neuronal Activity to Drive Fear Expression” 505 (January): 92–96.

Cullinan, William E., James P. Herman, and Stanley J. Watson. 1993. “Ventral Subicular Interaction with the Hypothalamic Paraventricular Nucleus: Evidence for a Relay in the Bed Nucleus of the Stria Terminalis.” *Journal of Comparative Neurology* 332 (1): 1–20.

Davis, Michael, and Changjun Shi. 2000. “The Amygdala.” *Current Biology* 10 (4): R131. doi:10.1016/S0960-9822(00)00345-6.

Davis, Michael, David L. Walker, and Younglim Lee. 1997. “Roles of the Amygdala and Bed Nucleus of the Stria Terminalis in Fear and Anxiety Measured with the Acoustic Startle Reflex.” *Annals of the New York Academy of Sciences* 821 (1): 305–31. doi:10.1111/j.1749-6632.1997.tb48289.x.

Davis, Michael, David L. Walker, Leigh Miles, and Christian Grillon. 2010. “Phasic vs Sustained Fear in Rats and Humans: Role of the Extended Amygdala in Fear vs Anxiety.” *Neuropsychopharmacology: Official Publication of the American College of Neuropsychopharmacology* 35 (1): 105–35. doi:10.1038/npp.2009.109.

Diorio, Diane, Victor Viau, and Michael J. Meaney. 1993. “The Role of the Medial Prefrontal Cortex (Cingulate Gyrus) in the Regulation of Hypothalamic-Pituitary-Adrenal Responses to Stress.” *The Journal of Neuroscience* 13 (9): 3839–3847.

Domschke, Katharina, Miriam Braun, Patricia Ohrmann, Thomas Suslow, Harald Kugel, Jochen Bauer, Christa Hohoff, et al. 2006. “Association of the Functional −1019C/G 5-HT1A Polymorphism with Prefrontal Cortex and Amygdala Activation Measured with 3 T fMRI in Panic Disorder.” *The International Journal of Neuropsychopharmacology* 9 (3): 349–355. doi:10.1017/S1461145705005869.

Dong, Hong-Wei, and Larry W. Swanson. 2004. “Organization of Axonal Projections from the Anterolateral Area of the Bed Nuclei of the Stria Terminalis.” *Journal of Comparative Neurology* 468 (2): 277–298.

Duvarci, Sevil, Elizabeth P. Bauer, and Denis Paré. 2009. “The Bed Nucleus of the Stria Terminalis Mediates Inter-Individual Variations in Anxiety and Fear.” *The Journal of Neuroscience* 29 (33): 10357–10361.

Etkin, Amit, Kristen C. Klemenhagen, Joshua T. Dudman, Michael T. Rogan, René Hen, Eric R. Kandel, and Joy Hirsch. 2004. “Individual Differences in Trait Anxiety Predict the Response of the Basolateral Amygdala to Unconsciously Processed Fearful Faces.” *Neuron* 44 (6): 1043–55. doi:10.1016/j.neuron.2004.12.006.

Fakra E, Hyde LW, Gorka A, and et al. 2009. “EFfects of htr1a c(−1019)g on Amygdala Reactivity and Trait Anxiety.” *Archives of General Psychiatry* 66 (1): 33–40. doi:10.1001/archpsyc.66.1.33.

Fanselow, Michael S., and Hong-Wei Dong. 2010. “Are the Dorsal and Ventral Hippocampus Functionally Distinct Structures?” *Neuron* 65 (1): 7–19.

Felix-Ortiz, A. C., A. Burgos-Robles, N. D. Bhagat, C. A. Leppla, and K. M. Tye. 2016. “Bidirectional Modulation of Anxiety-Related and Social Behaviors by Amygdala Projections to the Medial Prefrontal Cortex.” *Neuroscience* 321 (May): 197–209. doi:10.1016/j.neuroscience.2015.07.041.

Felix-Ortiz, Ada C., Anna Beyeler, Changwoo Seo, Christopher A. Leppla, Craig P. Wildes, and Kay M. Tye. 2013. “BLA to vHPC Inputs Modulate Anxiety-Related Behaviors.” *Neuron* 79 (4): 658–64. doi:10.1016/j.neuron.2013.06.016.

Fendt, M., and M. S. Fanselow. 1999. “The Neuroanatomical and Neurochemical Basis of Conditioned Fear.” *Neuroscience & Biobehavioral Reviews* 23 (5): 743–60. doi:10.1016/S0149-7634(99)00016-0.

Gabbott, Paul, Anthony Headlam, and Sarah Busby. 2002. “Morphological Evidence That CA1 Hippocampal Afferents Monosynaptically Innervate PV-Containing Neurons and NADPH-Diaphorase Reactive Cells in the Medial Prefrontal Cortex (Areas 25/32) of the Rat.” *Brain Research* 946 (2): 314–322.

Gerdes, Antje B. M., Matthias J. Wieser, Andreas Mühlberger, Peter Weyers, Georg W. Alpers, Michael M. Plichta, Felix Breuer, and Paul Pauli. 2010. “Brain Activations to Emotional Pictures Are Differentially Associated with Valence and Arousal

Ratings.” *Frontiers in Human Neuroscience* 4: 175. doi:10.3389/fnhum.2010.00175.

Gordon, Joshua A., Clay O. Lacefield, Clifford G. Kentros, and Rene Hen. 2005. “State-Dependent Alterations in Hippocampal Oscillations in Serotonin 1A Receptor-Deficient Mice.” *The Journal of Neuroscience* 25 (28): 6509–6519.

Gotsick, James E., and Roger C. Marshall. 1972. “Time Course of the Septal Rage Syndrome.” *Physiology & Behavior* 9 (4): 685–687.

Goutagny, Romain, Jesse Jackson, and Sylvain Williams. 2009. “Self-Generated Theta Oscillations in the Hippocampus.” *Nature Neuroscience* 12 (12): 1491–1493.

Gray, Thackery S., and Debra J. Magnuson. 1992. “Peptide Immunoreactive Neurons in the Amygdala and the Bed Nucleus of the Stria Terminalis Project to the Midbrain Central Gray in the Rat.” *Peptides* 13 (3): 451–460.

Greenberg, Paul E., Tamar Sisitsky, Ronald C. Kessler, Stan N. Finkelstein, Ernst R. Berndt, Jonathan RT Davidson, and Abby J. Fyer. 1999. “The Economic Burden of Anxiety Disorders in the 1990s.” *The Journal of Clinical Psychiatry* 60 (7): 1–478.

Gross, Cornelius T., and Newton Sabino Canteras. 2012. “The Many Paths to Fear.” *Nature Reviews Neuroscience* 13 (9): 651–58. doi:10.1038/nrn3301.

Harris, Alexander Z., and Joshua A. Gordon. 2015. “Long-Range Neural Synchrony in Behavior.” *Annual Review of Neuroscience* 38 (July): 171–94. doi:10.1146/annurev-neuro-071714-034111.

Harvey, Christopher D., Forrest Collman, Daniel A. Dombeck, and David W. Tank. 2009. “Intracellular Dynamics of Hippocampal Place Cells during Virtual Navigation.” *Nature* 461 (7266): 941–946.

Hettema, John M., Michael C. Neale, and Kenneth S. Kendler. 2001. “A Review and Meta-Analysis of the Genetic Epidemiology of Anxiety Disorders.” *American Journal of Psychiatry* 158 (10): 1568–78. doi:10.1176/appi.ajp.158.10.1568.

Hofmann, Stefan G., and Jasper A. J. Smits. 2008. “COGNITIVE-BEHAVIORAL THERAPY FOR ADULT ANXIETY DISORDERS: A META-ANALYSIS OF RANDOMIZED PLACEBO-CONTROLLED TRIALS.” *The Journal of Clinical Psychiatry* 69 (4): 621–32.

Hoover, Walter B., and Robert P. Vertes. 2007. “Anatomical Analysis of Afferent Projections to the Medial Prefrontal Cortex in the Rat.” *Brain Structure & Function* 212 (2): 149–79. doi:10.1007/s00429-007-0150-4.

Hou, Cailan, Jun Liu, Kun Wang, Lingjiang Li, Meng Liang, Zhong He, Yong Liu, Yan Zhang, Weihui Li, and Tianzi Jiang. 2007. “Brain Responses to Symptom Provocation and Trauma-Related Short-Term Memory Recall in Coal Mining Accident Survivors with Acute Severe PTSD.” *Brain Research* 1144 (May): 165–74. doi:10.1016/j.brainres.2007.01.089.

Hu, Hua, Koen Vervaeke, and Johan F. Storm. 2002. “Two Forms of Electrical Resonance at Theta Frequencies, Generated by M-Current, H-Current and Persistent Na+ Current in Rat Hippocampal Pyramidal Cells.” *The Journal of Physiology* 545 (3): 783–805.

Hunsaker, Michael R., and Raymond P. Kesner. 2008. “Dissociations across the Dorsal–ventral Axis of CA3 and CA1 for Encoding and Retrieval of Contextual and Auditory-Cued Fear.” *Neurobiology of Learning and Memory* 89 (1): 61–69. doi:10.1016/j.nlm.2007.08.016.

Javanmard, Mahan, Jakov Shlik, Sidney H Kennedy, Franco J Vaccarino, Sylvain Houle, and Jacques Bradwejn. 1999. “Neuroanatomic Correlates of CCK-4-Induced Panic Attacks in Healthy Humans: A Comparison of Two Time Points.” *Biological Psychiatry* 45 (7): 872–82. doi:10.1016/S0006-3223(98)00348-5.

Jay, T. M., and M. P. Witter. 1991. “Distribution of Hippocampal CA1 and Subicular Efferents in the Prefrontal Cortex of the Rat Studied by Means of Anterograde Transport of Phaseolus Vulgaris-Leucoagglutinin.” *The Journal of Comparative Neurology* 313 (4): 574–86. doi:10.1002/cne.903130404.

Jay, Thérèse M., Anne-Marie Thierry, Leif Wiklund, and Jacques Glowinski. 1992. “Excitatory Amino Acid Pathway from the Hippocampus to the Prefrontal Cortex. Contribution of AMPA Receptors in Hippocampo-Prefrontal Cortex Transmission.” *European Journal of Neuroscience* 4 (12): 1285–1295.

Jenck, François, Jean-Luc Moreau, and James R. Martin. 1995. “Dorsal Periaqueductal Gray-Induced Aversion as a Simulation of Panic Anxiety: Elements of Face and Predictive Validity.” *Psychiatry Research* 57 (2): 181–191.

Jinks, Anthony L, and Iain S McGregor. 1997. “Modulation of Anxiety-Related Behaviours Following Lesions of the Prelimbic or Infralimbic Cortex in the Rat” 772: 181–90.

Jones, Matthew W., and Matthew A. Wilson. 2005. “Theta Rhythms Coordinate Hippocampal–prefrontal Interactions in a Spatial Memory Task.” *PLoS Biol* 3 (12): e402.

Kapp, Bruce S., Robert C. Frysinger, Michela Gallagher, and James R. Haselton. 1979. “Amygdala Central Nucleus Lesions: Effect on Heart Rate Conditioning in the Rabbit.” *Physiology & Behavior* 23 (6): 1109–17. doi:10.1016/0031-9384(79)90304-4.

Karalis, Nikolaos, Cyril Dejean, Fabrice Chaudun, Suzana Khoder, Robert R. Rozeske, Hélène Wurtz, Sophie Bagur, et al. 2016. “4-Hz Oscillations Synchronize Prefrontal-Amygdala Circuits during Fear Behavior.” *Nature Neuroscience* 19 (4): 605–12. doi:10.1038/nn.4251.

Kessler RC, Berglund P, Demler O, Jin R, Merikangas KR, and Walters EE. 2005. “Lifetime Prevalence and Age-of-Onset Distributions of Dsm-Iv Disorders in the National Comorbidity Survey Replication.” *Archives of General Psychiatry* 62 (6): 593–602. doi:10.1001/archpsyc.62.6.593.

Kheirbek, Mazen A., Liam J. Drew, Nesha S. Burghardt, Daniel O. Costantini, Lindsay Tannenholz, Susanne E. Ahmari, Hongkui Zeng, André A. Fenton, and René Hen. 2013. “Differential Control of Learning and Anxiety along the Dorsoventral Axis of the Dentate Gyrus.” *Neuron* 77 (5): 955–68. doi:10.1016/j.neuron.2012.12.038.

Kim, Jeansok J., and Michael S. Fanselow. 1992. “Modality-Specific Retrograde Amnesia of Fear.” *Science* 256 (5057): 675–677.

Kim, Sung-Yon, Avishek Adhikari, Soo Yeun Lee, James H. Marshel, Christina K. Kim, Caitlin S. Mallory, Maisie Lo, et al. 2013. “Diverging Neural Pathways Assemble a Behavioural State from Separable Features in Anxiety.” *Nature* 496 (7444): 219–223.

Kjelstrup, Kirsten Brun, Trygve Solstad, Vegard Heimly Brun, Torkel Hafting, Stefan Leutgeb, Menno P. Witter, Edvard I. Moser, and May-Britt Moser. 2008. “Finite Scale of Spatial Representation in the Hippocampus.” *Science* 321 (5885): 140–143.

Kjelstrup, Kirsten G., Frode A. Tuvnes, Hill-Aina Steffenach, Robert Murison, Edvard I. Moser, and May-Britt Moser. 2002. “Reduced Fear Expression after Lesions of the Ventral Hippocampus.” *Proceedings of the National Academy of Sciences of the United States of America* 99 (16): 10825–30. doi:10.1073/pnas.152112399.

Klausberger, Thomas, Peter J. Magill, László F. Márton, J. David B. Roberts, Philip M. Cobden, György Buzsáki, and Peter Somogyi. 2003. “Brain-State-and Cell-Type-Specific Firing of Hippocampal Interneurons in Vivo.” *Nature* 421 (6925): 844–848.

Kupfer, David J, Ellen Frank, and Mary L Phillips. 2012. “Major Depressive Disorder: New Clinical, Neurobiological, and Treatment Perspectives.” *The Lancet* 379 (9820): 1045–55. doi:10.1016/S0140-6736(11)60602-8.

Lacerda-Pinheiro, Sally França, Roberto Flávio Fontenelle Pinheiro Junior, Marcos Antonio Pereira de Lima, Claúdio Gleidiston Lima da Silva, Maria do Socorro Vieira dos Santos, Antonio Gilvan Teixeira Júnior, Pedro Neto Lima de Oliveira, Karla Denise Barros Ribeiro, Modesto Leite Rolim-Neto, and Bianca Alves Vieira

Bianco. 2014. “Are There Depression and Anxiety Genetic Markers and Mutations? A Systematic Review.” *Journal of Affective Disorders* 168: 387–398.

Lanius, Ruth A, Peter C Williamson, Kristine Boksman, Maria Densmore, Madhulika Gupta, Richard W. J Neufeld, Joseph S Gati, and Ravi S Menon. 2002. “Brain Activation during Script-Driven Imagery Induced Dissociative Responses in PTSD: A Functional Magnetic Resonance Imaging Investigation.” *Biological Psychiatry* 52 (4): 305–11. doi:10.1016/S0006-3223(02)01367-7.

Lee, Younglim, and Michael Davis. 1997. “Role of the Hippocampus, the Bed Nucleus of the Stria Terminalis, and the Amygdala in the Excitatory Effect of Corticotropin-Releasing Hormone on the Acoustic Startle Reflex.” *The Journal of Neuroscience* 17 (16): 6434–6446.

Lesting, Jörg, Rajeevan T. Narayanan, Christian Kluge, Susan Sangha, Thomas Seidenbecher, and Hans-Christian Pape. 2011. “Patterns of Coupled Theta Activity in Amygdala-Hippocampal-Prefrontal Cortical Circuits during Fear Extinction.” *PloS One* 6 (6): e21714. doi:10.1371/journal.pone.0021714.

Leung, L. Stan. 1998. “Generation of Theta and Gamma Rhythms in the Hippocampus.” *Neuroscience & Biobehavioral Reviews* 22 (2): 275–290.

Likhtik, Ekaterina, Joseph M. Stujenske, Mihir A. Topiwala, Alexander Z. Harris, and Joshua A. Gordon. 2014. “Prefrontal Entrainment of Amygdala Activity Signals Safety in Learned Fear and Innate Anxiety.” *Nature Neuroscience* 17 (1): 106–13. doi:10.1038/nn.3582.

Lister, Richard G. 1987. “The Use of a plus-Maze to Measure Anxiety in the Mouse.” *Psychopharmacology* 92 (2): 180–85. doi:10.1007/BF00177912.

Lovett-Barron, Matthew, Patrick Kaifosh, Mazen A. Kheirbek, Nathan Danielson, Jeffrey D. Zaremba, Thomas R. Reardon, Gergely F. Turi, René Hen, Boris V. Zemelman, and Attila Losonczy. 2014. “Dendritic Inhibition in the Hippocampus Supports Fear Learning.” *Science (New York, N.Y.)* 343 (6173): 857–63. doi:10.1126/science.1247485.

Maren, Stephen. 1999. “Neurotoxic or Electrolytic Lesions of the Ventral Subiculum Produce Deficits in the Acquisition and Expression of Pavlovian Fear Conditioning in Rats.” *Behavioral Neuroscience* 113 (2): 283.

Maren, Stephen, and William G. Holt. 2004. “Hippocampus and Pavlovian Fear Conditioning in Rats: Muscimol Infusions into the Ventral, but Not Dorsal, Hippocampus Impair the Acquisition of Conditional Freezing to an Auditory Conditional Stimulus.” *Behavioral Neuroscience* 118 (1): 97–110. doi:10.1037/0735-7044.118.1.97.

Maren, Stephen, and Gregory J. Quirk. 2004. “Neuronal Signalling of Fear Memory.” *Nature Reviews Neuroscience* 5 (11): 844–52. doi:10.1038/nrn1535.

Markus, Etan J., Carol A. Barnes, Bruce L. McNaughton, Victoria L. Gladden, and William E. Skaggs. 1994. “Spatial Information Content and Reliability of Hippocampal CA1 Neurons: Effects of Visual Input.” *Hippocampus* 4 (4): 410–421.

McNaughton, N., and E. M. Sedgwick. 1978. “Reticular Stimulation and Hippocampal Theta Rhythm in Rats: Effects of Drugs.” *Neuroscience* 3 (7): 629–632.

Menard, Janet, and Dallas Treit. 1996. “Lateral and Medial Septal Lesions Reduce Anxiety in the plus-Maze and Probe-Burying Tests.” *Physiology & Behavior* 60 (3): 845–853.

Milad, Mohammed R., and Gregory J. Quirk. 2012. “Fear Extinction as a Model for Translational Neuroscience: Ten Years of Progress.” *Annual Review of Psychology* 63: 129–151.

Mizumori, S. J. Y., C. A. Barnes, and B. L. McNaughton. 1990. “Behavioral Correlates of Theta-on and Theta-off Cells Recorded from Hippocampal Formation of Mature Young and Aged Rats.” *Experimental Brain Research* 80 (2): 365–373.

Moser, May-Britt, and Edvard I. Moser. 1998. “Functional Differentiation in the Hippocampus.” *Hippocampus* 8 (6): 608–19. doi:10.1002/(SICI)1098-1063(1998)8:6<608::AID-HIPO3>3.0.CO;2-7.

Nagel, Georg, Tanjef Szellas, Wolfram Huhn, Suneel Kateriya, Nona Adeishvili, Peter Berthold, Doris Ollig, Peter Hegemann, and Ernst Bamberg. 2003. “Channelrhodopsin-2, a Directly Light-Gated Cation-Selective Membrane Channel.” *Proceedings of the National Academy of Sciences* 100 (24): 13940–13945.

Nashold Jr, Blaine S., William P. Wilson, and D. Graham Slaughter. 1969. “Sensations Evoked by Stimulation in the Midbrain of Man.” *Journal of Neurosurgery* 30 (1): 14–24.

Nauta, Walle JH. 1971. “The Problem of the Frontal Lobe: A Reinterpretation.” *Journal of Psychiatric Research* 8 (3): 167–187.

Padilla-Coreano, Nancy, Scott S. Bolkan, Georgia M. Pierce, Dakota R. Blackman, William D. Hardin, Alvaro L. Garcia-Garcia, Timothy J. Spellman, and Joshua A. Gordon. 2016. “Direct Ventral Hippocampal-Prefrontal Input Is Required for Anxiety-Related Neural Activity and Behavior.” *Neuron* 89 (4): 857–866.

Pellow, Sharon, Philippe Chopin, Sandra E. File, and Mike Briley. 1985. “Validation of Open : Closed Arm Entries in an Elevated plus-Maze as a Measure of Anxiety in the Rat.” *Journal of Neuroscience Methods* 14 (3): 149–67. doi:10.1016/0165-0270(85)90031-7.

Peters, Jamie, Peter W. Kalivas, and Gregory J. Quirk. 2009. “Extinction Circuits for Fear and Addiction Overlap in Prefrontal Cortex.” *Learning & Memory* 16 (5): 279–288.

Petsche, H., Ch Stumpf, and G. Gogolak. 1962. “The Significance of the Rabbit’s Septum as a Relay Station between the Midbrain and the Hippocampus I. The Control of Hippocampus Arousal Activity by the Septum Cells.” *Electroencephalography and Clinical Neurophysiology* 14 (2): 202–211.

Pikkarainen, Maria, Seppo Rönkkö, Vesa Savander, Ricardo Insausti, and Asla Pitkänen. 1999. “Projections from the Lateral, Basal, and Accessory Basal Nuclei of the Amygdala to the Hippocampal Formation in Rat.” *The Journal of Comparative Neurology* 403 (2): 229–60. doi:10.1002/(SICI)1096-9861(19990111)403:2<229::AID-CNE7>3.0.CO;2-P.

Pillay, Srinivasan S., Jadwiga Rogowska, Staci A. Gruber, Norah Simpson, and Deborah A. Yurgelun-Todd. 2007. “Recognition of Happy Facial Affect in Panic

Disorder: An fMRI Study." *Journal of Anxiety Disorders* 21 (3): 381–93. doi:10.1016/j.janxdis.2006.04.001.

Richmond, A.M., B. K Yee, B. Pouzet, L. Veenman, J. N. P, J. Feldon, and D. M Bannerman. 1999. "Dissociating Context and Space within the Hippocampus: Effects of Complete, Dorsal, and Ventral Excitotoxic Hippocampal Lesions on Conditioned Freezing and Spatial Learning." *Behavioral Neuroscience* 113 (6): 1189–1203. doi:10.1037/0735-7044.113.6.1189.

Risold, P. Y., and L. W. Swanson. 1996. "Structural Evidence for Functional Domains in the Rat Hippocampus." *Science* 272 (5267): 1484–86. doi:10.1126/science.272.5267.1484.

Robinson, Jennifer, Frédéric Manseau, Guillaume Ducharme, Bénédicte Amilhon, Erika Vigneault, Salah El Mestikawy, and Sylvain Williams. 2016. "Optogenetic Activation of Septal Glutamatergic Neurons Drive Hippocampal Theta Rhythms." *The Journal of Neuroscience* 36 (10): 3016–3023.

Rodgers, R. J., B.J. Cao, and A. Holmes. 1997. "Animal Models of Anxiety: An Ethological Perspective." *Brazilian Journal of Medical and Biological Research* 30 (3): 289–304. doi:10.1590/S0100-879X1997000300002.

Royer, Sébastien, Anton Sirota, Jagdish Patel, and György Buzsáki. 2010. "Distinct Representations and Theta Dynamics in Dorsal and Ventral Hippocampus." *The Journal of Neuroscience* 30 (5): 1777–1787.

Satpute, Ajay B., Jeanette A. Mumford, Bruce D. Naliboff, and Russell A. Poldrack. 2012. "Human Anterior and Posterior Hippocampus Respond Distinctly to State and Trait Anxiety." *Emotion* 12 (1): 58–68. doi:10.1037/a0026517.

Schunck, Thérèse, Gilles Erb, Alexandre Mathis, Christian Gilles, Izzie Jacques Namer, Yann Hode, Agnès Demaziere, Rémy Luthringer, and Jean-Paul Macher. 2006. "Functional Magnetic Resonance Imaging Characterization of CCK-4-Induced Panic Attack and Subsequent Anticipatory Anxiety." *NeuroImage* 31 (3): 1197–1208. doi:10.1016/j.neuroimage.2006.01.035.

Seidenbecher, Thomas, T. Rao Laxmi, and Hans-Christian Pape. 2003. "Amygdalar and Hippocampal Theta Rhythm Synchronization During Fear Memory Retrieval" 301 (5634): 846–50.

Shah, Akeel A, and Dallas Treit. 2003. "Excitotoxic Lesions of the Medial Prefrontal Cortex Attenuate Fear Responses in the Elevated-plus Maze, Social Interaction and Shock Probe Burying Tests." *Brain Research* 969 (1–2): 183–94. doi:10.1016/S0006-8993(03)02299-6.

Sheehan, Teige P., R. Andrew Chambers, and David S. Russell. 2004. "Regulation of Affect by the Lateral Septum: Implications for Neuropsychiatry." *Brain Research Reviews* 46 (1): 71–117.

Shin, Lisa M., and Israel Liberzon. 2009. "The Neurocircuitry of Fear, Stress, and Anxiety Disorders." *Neuropsychopharmacology* 35 (1): 169–91. doi:10.1038/npp.2009.83.

Shin, Lisa M, Paul J Whalen, Roger K Pitman, George Bush, Michael L Macklin, Natasha B Lasko, Scott P Orr, Sean C McInerney, and Scott L Rauch. 2001. "An fMRI Study of Anterior Cingulate Function in Posttraumatic Stress Disorder." *Biological Psychiatry* 50 (12): 932–42. doi:10.1016/S0006-3223(01)01215-X.

Siapas, Athanassios G., Evgueniy V. Lubenov, and Matthew A. Wilson. 2005. "Prefrontal Phase Locking to Hippocampal Theta Oscillations." *Neuron* 46 (1): 141–51. doi:10.1016/j.neuron.2005.02.028.

Siegle, Joshua H., and Matthew A. Wilson. 2014. "Enhancement of Encoding and Retrieval Functions through Theta Phase-Specific Manipulation of Hippocampus." *eLife* 3: e03061.

Sierra-Mercado, Demetrio, Nancy Padilla-Coreano, and Gregory J. Quirk. 2011. "Dissociable Roles of Prelimbic and Infralimbic Cortices, Ventral Hippocampus, and Basolateral Amygdala in the Expression and Extinction of Conditioned Fear." *Neuropsychopharmacology: Official Publication of the American College of Neuropsychopharmacology* 36 (2): 529–38. doi:10.1038/npp.2010.184.

Smith, G. Elliot. 1910. "The Arris and Gale Lectures ON SOME PROBLEMS RELATING TO THE EVOLUTION OF THE BRAIN." *The Lancet* 175 (4508): 221–227.

Sotres-Bayon, Francisco, and Gregory J. Quirk. 2010. "Prefrontal Control of Fear: More than Just Extinction." *Current Opinion in Neurobiology* 20 (2): 231–235.

Sotres-Bayon, Francisco, Demetrio Sierra-Mercado, Enmanuelle Pardilla-Delgado, and Gregory J. Quirk. 2012. "Gating of Fear in Prelimbic Cortex by Hippocampal and Amygdala Inputs." *Neuron* 76 (4): 804–12. doi:10.1016/j.neuron.2012.09.028.

Spellman, Timothy, Mattia Rigotti, Susanne E. Ahmari, Stefano Fusi, Joseph A. Gogos, and Joshua A. Gordon. 2015. "Hippocampal-Prefrontal Input Supports Spatial Encoding in Working Memory." *Nature* 522 (7556): 309–14. doi:10.1038/nature14445.

Steimer, Thierry. 2002. “The Biology of Fear- and Anxiety-Related Behaviors.” *Dialogues in Clinical Neuroscience* 4 (3): 231–49.

Stein, Murray B., Alan N. Simmons, Justin S. Feinstein, and Martin P. Paulus. 2007. “Increased Amygdala and Insula Activation during Emotion Processing in Anxiety-Prone Subjects.” *American Journal of Psychiatry*. http://ajp.psychiatryonline.org/doi/pdf/10.1176/ajp.2007.164.2.318.

Sterpenich, Virginie, Sophie Schwartz, Pierre Maquet, and Martin Desseilles. 2014. “Ability to Maintain Internal Arousal and Motivation Modulates Brain Responses to Emotions.” *PloS One* 9 (12): e112999. doi:10.1371/journal.pone.0112999.

Stujenske, Joseph M., Ekaterina Likhtik, Mihir A. Topiwala, and Joshua A. Gordon. 2014. “Fear and Safety Engage Competing Patterns of Theta-Gamma Coupling in the Basolateral Amygdala.” *Neuron* 83 (4): 919–33. doi:10.1016/j.neuron.2014.07.026.

Treit, Dallas, Harinder Aujla, and Janet Menard. 1998. “Does the Bed Nucleus of the Stria Terminalis Mediate Fear Behaviors?” *Behavioral Neuroscience* 112 (2): 379.

Treit, Dallas, and Janet Menard. 1997. “Dissociations among the Anxiolytic Effects of Septal, Hippocampal, and Amygdaloid Lesions.” *Behavioral Neuroscience* 111 (3): 653–58. doi:10.1037/0735-7044.111.3.653.

Treit, Dallas, Christine Pesold, and Susan Rotzinger. 1993. “Dissociating the Anti-Fear Effects of Septal and Amygdaloid Lesions Using Two Pharmacologically Validated Models of Rat Anxiety.” *Behavioral Neuroscience* 107 (5): 770.

Trent, Natalie L., and Janet L. Menard. 2010. “The Ventral Hippocampus and the Lateral Septum Work in Tandem to Regulate Rats’ Open-Arm Exploration in the Elevated plus-Maze.” *Physiology & Behavior* 101 (1): 141–152.

Tye, Kay M., Rohit Prakash, Sung-Yon Kim, Lief E. Fenno, Logan Grosenick, Hosniya Zarabi, Kimberly R. Thompson, Viviana Gradinaru, Charu Ramakrishnan, and Karl Deisseroth. 2011. “Amygdala Circuitry Mediating Reversible and Bidirectional Control of Anxiety.” *Nature* 471 (7338): 358–62. doi:10.1038/nature09820.

van den Heuvel OA, Veltman DJ, Groenewegen HJ, and et al. 2005. “DIsorder-Specific Neuroanatomical Correlates of Attentional Bias in Obsessive-Compulsive Disorder, Panic Disorder, and Hypochondriasis.” *Archives of General Psychiatry* 62 (8): 922–33. doi:10.1001/archpsyc.62.8.922.

Vanderwolf, Case H. 1969. “Hippocampal Electrical Activity and Voluntary Movement in the Rat.” *Electroencephalography and Clinical Neurophysiology* 26 (4): 407–418.

Walker, David L., and Michael Davis. 1997. “Double Dissociation between the Involvement of the Bed Nucleus of the Stria Terminalis and the Central Nucleus of the Amygdala in Startle Increases Produced by Conditioned versus Unconditioned Fear.” *The Journal of Neuroscience* 17 (23): 9375–9383.

Walkup, John T., Anne Marie Albano, John Piacentini, Boris Birmaher, Scott N. Compton, Joel T. Sherrill, Golda S. Ginsburg, et al. 2008. “Cognitive Behavioral Therapy, Sertraline, or a Combination in Childhood Anxiety.” *New England Journal of Medicine* 359 (26): 2753–66. doi:10.1056/NEJMoa0804633.

Walsh, Roger N., and Robert A. Cummins. 1976. “The Open-Field Test: A Critical Review.” *Psychological Bulletin* 83 (3): 482–504. doi:10.1037/0033-2909.83.3.482.

Willner, Paul. 1986. “Validation Criteria for Animal Models of Human Mental Disorders: Learned Helplessness as a Paradigm Case.” *Progress in Neuro-Psychopharmacology and Biological Psychiatry* 10 (6): 677–90. doi:10.1016/0278-5846(86)90051-5.

Yang, Pinchen, Ming-Ting Wu, Chia-Chuang Hsu, and Jhy-Horng Ker. 2004. “Evidence of Early Neurobiological Alternations in Adolescents with Posttraumatic Stress Disorder: A Functional MRI Study.” *Neuroscience Letters* 370 (1): 13–18. doi:10.1016/j.neulet.2004.07.033.